Two Odorant-Binding Protein Genes in Mosquitoes: Comparative Genomics, Expression, and Function

Meryem Senay Sengul

Dissertation submitted to the faculty of the Virginia Polytechnic Institute and State University in partial fulfillment of the requirements for the degree of

Doctor of Philosophy
In
Biochemistry

Dr. Zhijian J. Tu, Chairman
Dr. Glenda E. Gillaspy
Dr. Timothy J. Larson
Dr. John M. McDowell
Dr. Edward J. Smith

February 1st, 2008
Blacksburg, VA

Keywords: odorant-binding protein genes, olfaction, mosquito, gene expression, gene knockdown, Sindbis virus

Two Odorant-Binding Protein Genes in Mosquitoes: Comparative Genomics, Expression, and Function

Meryem Senay Sengul

Abstract

Insect **O**dorant-**B**inding **P**roteins (OBPs) are small, water-soluble molecules that solubilize hydrophobic odorant molecules in the sensillum lymph and transport them to their cognate receptors in the olfactory receptor neurons. With the availability of the genome sequence of the African malaria mosquito, *Anopheles gambiae*, there has been a profound interest in the characterization and functional analyses of *Obp* genes in order to understand the molecular basis of mosquito host-seeking behavior. However, no direct evidence has been found for specific functions of any mosquito OBPs.

In this study, I describe the comparative genomics and expression analyses on two mosquito *Obp* genes (*Obp1* and *Obp7*) as well as efforts to determine their functions. Both of these *Obp* genes were identified in *Anopheles stephensi* and only *Obp7* gene was identified in *Anopheles quadriannulatus* by screening bacterial artificial chromosome (BAC) libraries of these species. Comparative analyses revealed several interesting features including segments of conserved non-coding sequences (CNSs) that contain potential regulatory elements relevant to olfactory tissue development and blood-feeding.

The expression profiles of these genes were examined in detail in the Asian malaria mosquito *An. stephensi*. *Obp1* and *Obp7* transcripts were significantly higher in females than male mosquitoes and they were predominantly found in the antenna, which is the primary olfactory organ of mosquitoes. Twenty-four hours after a blood meal, mRNA levels of these two genes were significantly reduced in the maxillary palp and proboscis, referred to as secondary olfactory organs of mosquitoes. These findings collectively

indicate that *Obp1* and *Obp7* genes in *An. stephensi* likely function in female olfactory response and may be involved in behaviors related to blood-feeding.

To investigate the function of these *Obp* genes more directly, a Sindbis virus based expression system is established to knockdown the two *Obp* gene orthologs in *Aedes aegypti*. The effective knockdown of *Obp1* and *Obp7* genes (8 and 100-fold, respectively) is accomplished in female mosquito olfactory tissues. The potential for a systematic analysis of the molecular players involved in mosquito olfaction using this newly developed technique is discussed. Such analysis will provide the foundation for interfering with mosquito host-seeking behavior for the prevention of disease transmission.

Dedication

To the memory of my uncle, Osman Sengul (1938-2007),
whose courage and insight shaped my future goals of becoming a
scientist during my childhood, and in doing so helped me follow the steps
of a scientist and produce this dissertation.

Acknowledgements

I would like to thank to my advisor, Zhijian Jake Tu, for having led me into a fascinating area of research apart from the studies in his laboratory. Everything has a reason in life and changing my initial dissertation project at the end of my third year gave me the chance to be involved in this challenging and exciting field. It brought lots of stress while going through this, of course, and I know that I would not be successful without his support and motivation when I needed the most. I learnt from him that science requires patience and in order to be productive, not to let anything interfere with my goals. I appreciate the times we spent on scientific discussions as well as showing his friendship outside the work. Thank you for being a good advisor and a friend.

My sincere thanks to my committee members Dr. Timothy Larson, Dr. Glenda Gillaspy, Dr. John McDowell, and Dr. Ed Smith for their constructive input, ideas and insightful comments. My special thanks to Dr. Timothy Larson for his help and encouragement to pursue a degree at Virginia Tech. Also I would like to thank Dr. Ed Smith for bringing joy and a different taste to our discussions.

Thanks to other members of the faculty, especially Drs. Kevin M. Myles, Zachary N. Adelman, Thomas W. Keenan, Peter Kennelly, and William E. Newton. My special thanks to former department head, Dr. John L. Hess for his support.

Thanks to all my lab mates, especially Jim Biedler and Monica Alvarez for their friendship, support and humor. It was so much fun to share the laboratory with them during the last few years. Also my special thanks to Yumin Qi for all the help he provided since I joined the Tu laboratory. I benefited from his experiences a lot during my study. Many thanks to Randy Saunders for supplying the mosquitoes whenever I needed them and for his patience.

Last, but not the least, I would like to thank my parents, Recep Sengul, Raife Sengul; my sisters, Sencan Sengul and Tulay Sengul; and my beloved husband Sinan Demirak for believing in me and for their endless support, love, and patience.

Table of Contents

List of Figures

Chapter 1

Chapter 2

Chapter 3

Chapter 4

List of Tables

Chapter 2

Chapter 3

Chapter 4

List of Abbreviations

Aaeg	*Aedes aegypti*
Aaeg-Obp1	*Aedes aegypti Obp1* gene
Aaeg-Obp7	*Aedes aegypti Obp7* gene
Aaeg-Rps7	*Aedes aegypti ribosomal protein S7* gene
ABPX	Antennal binding proteins
Ae	*Aedes*
Agam	*Anopheles gambiae*
Agam-Obp1	*Anopheles gambiae Obp1* gene
Agam-Obp7	*Anopheles gambiae Obp7* gene
Aqua	*Anopheles quadriannulatus*
Aqua-Obp7	*Anopheles quadriannulatus Obp7* gene
ASP1	Antennal specific protein-1
Aste	*Anopheles stephensi*
Aste-Obp1	*Anopheles stephensi Obp1* gene
Aste-Obp7	*Anopheles stephensi Obp7* gene
Aste-Rps4	*Anopheles stephensi ribosomal protein S4* gene
An	*Anopheles*
BAC	Bacterial artificial chromosome
bp	base pair(s)
BHK-21	Baby hamster kidney cells
cAMP	cyclic adenosine 3', 5'-monophosphate
CNS	Central nervous system
CNSs	Conserved non-coding sequences
CO_2	Carbon dioxide
Cx	*Culex*
DAG	1,2-diacylglycerol
d_S	The Jukes-Cantor correction for multiple hits of ps
dsRNA	double-stranded RNA
dsSIN	double subgenomic Sindbis

d_N	The Jukes-Cantor correction for multiple hits of pn
d_N/d_S	The ratio of non-synonymous to synonymous substitutions
FISH	Fluorescent *in situ* hybridization
GOBPs	General odorant-binding proteins
GPCRs	G-protein coupled receptors
GRs	Gustatory receptors
GRNs	Gustatory receptor neurons
GTP	Guanosine 5'-triphosphate
IP_3	Inositol 1,4,5-triphosphate
kb	kilo base
NCR	Noncoding region
NMR	Nuclear magnetic resonance
OBPs	Odorant-binding proteins
Obp	*Odorant-binding protein* gene
ODEs	Odorant-degrading enzymes
ORs	Odorant receptors
Or	*Odorant receptor* gene
ORFs	Open reading frames
ORNs	Olfactory receptor neurons
PBPs	Pheromone-binding proteins
p.i.	post virus-inoculation
PLC	Phospholipase C
ps	The proportion of observed synonymous substitutions
pn	The proportion of observed non-synonymous substitutions
qRT-PCR	quantitative Real-time PCR
RACE	Rapid amplification of cDNA ends
RNAi	RNA interference
RT-PCR	Reverse transcription-polymerase chain reaction
SE	Sensilla esterase
SIN	Sindbis
$TCID_{50}$	Tissue culture infectious dose 50%

TFBSs	Transcription factor binding sites
UTRs	Untranslated regions
VA	11-*cis* vaccenyl acetate

Chapter 1

Introduction

1.1 Insect olfaction

1.1.1 Introduction

Insects have a negative impact on human health as disease vectors affecting millions of people around the world and on agriculture causing crop damage and loss (Hill, 1997). Their impact can be attributed in part to their chemosensory systems that detect and discriminate a wide range of chemical cues in their environment, which serve as signals that affect behaviors important for their survival and reproduction as well as behaviors that are relevant to disease transmission and crop damage.

The cellular and molecular characterization of olfactory processes in insects has revealed common organization of vertebrate and insect olfactory systems (Hildebrand and Shepherd, 1997). Indeed, insects provide good models for basic studies of olfaction, based largely on the studies in *Drosophila*. They exhibit olfaction-mediated behaviors controlled by an olfactory system that is significantly simpler than that of vertebrates. Genetic manipulation of their genomes and the use of robust molecular techniques help gain insights into the molecular and physiological aspects of insect olfactory systems. A significant amount of research has been conducted on various insect species to elucidate the molecular players and chemical ligands involved in odor perception and processing. In this chapter, I provide a review of the current literature on the behavioral and molecular aspects of insect olfaction and highlight relevant information on mosquito olfaction. I also provide the significance and overall plan of my dissertation research.

1.1.2 Molecular basis of insect olfaction

Insects possess two major chemosensory systems, which are olfaction (the sense of smell) and gustation (the sense of taste) (Stocker, 1994). Olfaction involves the

detection of volatile chemicals by the specialized hair structures, the sensilla (Fig. 1.1), in the antenna, the primary olfactory organ in insects. The antennal sensilla are of different shapes, which include long, thick walled hairs (sensilla trichodea), short, thin-walled pegs with branched dendrites (sensilla basiconica) and grooved pit pegs with a double wall and spoke channels (sensilla coeloconica) (Steinbrecht, 1996). Despite their different morphology, they all contain numerous pores in the sensillar wall that permit entry of odorants (including pheromones) to the sensillum lymph to access the chemosensory neurons (Steinbrecht, 1997) (Fig. 1.1). The maxillary palp is a secondary olfactory organ in insects and it contains only one class of sensilla, the basiconic sensilla.

Gustation, on the other hand, includes the detection of non-volatile chemicals by the taste sensilla. They have a single pore at the tip (Steinbrecht, 1984) and are proposed to make a direct physical contact with their ligands. Chemosensory neurons of the gustatory sensilla may be stimulated by nutrients, water, salts, and feeding stimulants or deterrents (Vogt, 2005). Gustatory sensilla are mainly found in the maxillary palp and proboscis and other parts of the insect body, such as legs and wings. The functional role of the maxillary palp and proboscis is not restricted to gustatory perception in insects. For example, maxillary palp has been found to express different odorant receptors (ORs) in olfactory receptor neurons (ORNs) that converge upon distinct glomeruli in the antennal lobe, while it is innervated with gustatory neurons that target the suboesophageal ganglion, which is the primary target area for gustatory receptor neurons (GRNs) (reviewed in Vosshall and Stocker, 2007). Additionally, while proboscis includes a diversity of gustatory neurons, a recent finding has shown an expression of an *Or* gene in the labellum (Kwon et al., 2006), which suggests that it may be involved in olfaction.

Insect olfactory systems can be divided into two groups: the pheromone olfactory system and the general olfactory system (Pelosi and Maida, 1995). The former includes the detection of pheromone signals (i.e. sex pheromones), which are produced by individuals of one species and detected by the members of the same species. The latter detects general odorants, such as plant volatiles. Despite the ligand specificity, the underlying mechanisms for the detection of odorant/pheromone molecules in the two

chemosensory systems are similar. The molecular characterization of the genes involved in olfactory processes in insects has been of great value unraveling the molecular biology of insect olfaction. Insect sensillum lymph (Fig. 1.1) contains different families of odorant-binding proteins (OBPs) that are thought to bind pheromone/odorant molecules and transport them to ORs (Ziegelberger, 1996). Once the ligand is detected by its cognate OR of the ORNs, a G-protein coupled signaling pathway is initiated (Krieger and Breer, 2003) that causes changes in the membrane potential and stimulation of neurons to elicit the biologically relevant behavior of the olfactory stimuli in an insect. Following the activation of the ORs, odorants need to be removed from the vicinity of the ORs to inhibit further stimulation of the ORNs. The degradation of odorants is thought to be carried out by enzymes in the sensillum lymph, referred to as odorant-degrading enzymes (ODEs) (Vogt and Riddiford, 1981). The molecular basis of insect odorant detection and processing will be discussed in detail in the following sections.

1.2 Mosquitoes and their olfaction

There are approximately 3,500 mosquito species that belong to the family Culicidae in the order Diptera (Clements, 2000). They are classified into two major subfamilies: Anophelinae (i.e. *Anopheles gambiae*) and Culicinae (i.e. *Aedes aegypti*) (Harbach and Kitching, 1998). Anophelinae mosquitoes include the primary vectors of malaria, caused by the parasites of the genus *Plasmodium*. Approximately, 40% of the world's population is at risk of malaria (http://www.who.int). More than 500 million people become severely ill with malaria and about one million people die every year, mostly children and pregnant women. The burden of the disease affects mostly developing countries, such as regions in sub-Saharan Africa.

Culicinae mosquitoes are also major vectors of human diseases such as yellow fever, dengue and dengue haemorrhagic fever, caused by viral pathogens in the *flavivirus* group. It is estimated that 200,000 people are affected by yellow fever per year, of which 30,000 die (http://www.who.int). The impact of dengue fever is increasing dramatically in the recent years with an estimated report of 50 million cases per year affecting

predominantly tropical and sub-tropical regions around the world (http://www.who.int). Unfortunately, the disease is spreading to new areas around the world due to expanding geographic distribution of dengue viruses and their mosquito vectors.

Extensive research and hundreds of millions of dollars have been spent over the past few decades to develop effective control strategies to prevent or reduce the transmission of mosquito-borne diseases. Despite the advances in medicine and research, the progress and the control have been slow due to resistance to both antimalarial drugs and insecticides. Novel tools are desperately needed to combat mosquito-borne infectious diseases. Identification of novel targets and development of effective vaccines are needed that affect the parasite transmission by the mosquitoes. Current efforts also include the genetic manipulation of mosquito genomes generating a refractory phenotype. Although it is theoretically feasible, replacing a wild population of mosquitoes with the genetically modified, transgenic mosquitoes may encounter technical and social problems. Those efforts mentioned above mainly target the mosquito-pathogen interactions to interfere with the disease transmission. Alternatively, control strategies to reduce the mosquito-host interaction would also be promising. The knowledge on mosquito behavior that causes host-selection and localization and a better understanding of the molecular basis of the mosquito olfactory system will ultimately aid in the development of novel, more effective control products to prevent mosquito-borne diseases.

In Culicidae, the *An. gambiae* and *Ae. aegypti* genomes have been annotated (Holt et al., 2002; Nene et al., 2007) and there are few studies describing the genes involved in mosquito olfaction (e.g. Hill et al., 2002; Xu et al., 2003; Justice et al., 2003; Li et al., 2005; Biessmann et al., 2005; Bohbot et al., 2007). Such information will reveal potential targets to interfere with mosquito olfactory behavior. It is possible that novel repellents can be developed that interfere with the host-seeking behaviors of mosquitoes. Current developments on novel drug design and genetic-control strategies will lead to more efficient and novel tools in the battle against mosquito-borne disease transmission.

1.2.1 Olfaction-mediated behaviors in mosquitoes

Mosquito behavior results from the interaction between its genome and its environment and is mediated by both internal and external factors, the latter of which include temperature, humidity, visual objects, auditory stimuli and chemical cues (Takken and Knols, 1999). Among those, olfactory cues are undoubtedly the most important external stimuli that affect mosquito behaviors crucial for their survival and reproduction (Takken and Knols, 1999). These behaviors include host-seeking (human or animal) for a blood meal, looking for suitable oviposition sites to lay their eggs, and sugar feeding as the energy source (Takken and Knols, 1999). Many behavioral studies have focused mainly on the highly anthropophilic (i.e. tendency to feed on humans) mosquito species such as *An. gambiae* and *Ae. aegypti*. These studies were corroborated with the electrophysiological recordings of the stimulated olfactory organs (antennae and/or maxillary palps) of mosquitoes to determine the chemical nature of host odors as being either potential attractants or repellents. Olfactory cues and their importance in mosquito behavior are discussed below.

1.2.1.1 Host-seeking behavior

Only female mosquitoes are obligatory blood feeders; blood is required for successful egg production. To ingest a blood meal, female mosquitoes must undergo a series of behaviors that will enable them to find an appropriate host. Host localization for a blood meal is influenced by the physiological state of the mosquitoes and to a large extent by the olfactory cues (Takken and Knols, 1999). Odors obtained from sweat, blood, breath or specific body regions (i.e. arm, palm, foot emanations) have been recognized as potential sources of olfactory cues for mosquito host-seeking behavior. Volatile compounds emitted from human breath like acetone and carbon dioxide (henceforth CO_2), and other compounds that are present in skin emanations, such as lactic acid, ammonia, carboxylic acids and octenol, are well known as mosquito host attractants (Kline et al., 1990; Braks and Takken, 1999; Dekker et al., 2005).

Among them, CO_2 has been determined as the most universal attractant, although it elicits different responds in different mosquito species. It is present in the expired

breath of vertebrates and attracts female mosquitoes to their hosts for blood-feeding (Gillies, 1980). Behavioral studies in the laboratory using skin emanations and human breath have identified CO_2 as a significant attractant for *Ae. aegypti* mosquitoes (Grant and O'Connell, 1996; Dekker et al., 2005) whereas its effect is much less clear for *Anopheles* species. It is found that CO_2 alone does not show a significant effect on *An. gambiae*, but it attracts *An. stephensi* mosquitoes (Takken et al., 1997). CO_2 has also been shown to act as a synergistic attractant in combination with other odor stimuli. For example, acetone causes a significant response in the behavior of *An. gambiae* when CO_2 is present (Takken et al., 1997).

Lactic acid, a major constitute of the human sweat, is an attractant for *Ae, aegypti* (Geier et al., 1996). Previously, Acree et al. (1968) have found that L-lactic acid is an attractant for *Ae. aegypti* only in the presence of CO_2 but a recent study indicates its attraction alone as well as its effect in the attractiveness of CO_2 in a synergistic manner (Geier et al., 1996).

Electrophysiological studies performed on *An. gambiae* mosquitoes showed that they give strong responses to lactic acid, 1-octen-3-ol, carboxylic acids and ammonia (Cork and Park, 1996). Behavioral responses to these compounds have also been determined (Dekker et al., 2002; Kline et al., 1990; Takken and Kline, 1989; Knols et al., 1997; Braks and Takken, 1999; Braks et al., 2001). In contrast, *An. quadriannulatus*, which exhibits a zoophilic behavior (i.e. preference to non-human vertebrate host, such as cattle), shows differences in their responses to these compounds. It is found that *An. quadriannulatus* is repelled by human emanations, while CO_2 and cattle odor attract this species (Dekker and Takken, 1998). Accordingly, the differences in response to host volatiles would support the observation that these species show either a zoophilic or an anthropophilic behavior mediated by odor stimuli. Efforts to reduce the disease transmission by producing host attractants for anthropophilic species may be highly influenced by the determination of the chemical nature of the host compounds that elicit behavioral and physiological responses in the mosquitoes.

1.2.1.2 Sugar feeding behavior

Mosquitoes use plant nectar as the sugar resources for metabolic processes and energy source for flight (Foster, 1995). They ingest plant sugars as floral, extrafloral nectar, and honeydew. While male mosquitoes solely depend on plants for their food source, female mosquitoes use nectar as an energy source to fly towards their potential hosts for a blood meal (Takken and Knols, 1999). The preference for sugar feeding and blood-feeding in females solely depends on the choice for survival (i.e. energy source) and reproduction (i.e. egg development). Other factors, such as differences in age, size, and energy reserves affect their preferences to sugar feeding behavior (Takken and Knols, 1999). For example, due to lack of sufficient energy reservoir, newly emerged, small female mosquitoes of *An. gambiae* feed on plants to obtain more energy compared to larger mosquitoes (Takken et al., 1998).

It is believed that mosquitoes locate plants by the odors emitted from the host plants. Plant odors are found to constitute cyclic and bicyclic monoterpenes. Thujone, a terpene that is present in essential plant oils, has been found to attract *Culex pipiens* mosquitoes to locate host plants. Green plant volatiles, fatty acids, and a variety of plant volatiles have also been found to attract various mosquito species (reviewed in Takken and Knols, 1999).

Although sugar feeding is a characteristic activity of young female mosquitoes, changes in physiological condition of adult females may also affect their sugar feeding behavior. It is found that females of *Culex tarsalis* feed on nectar within a few hours of oviposition (Reisen et al., 1986b). Ingested sugar also plays a role in the development of anautogenous females (i.e. absolute requirement for a blood meal for egg maturation), such that they feed on sugars more frequently than autogenous females (i.e. blood meal is not required for egg maturation) and prefer a blood meal and plant sugar source equally (Bowen and Romo, 1995a). In wild populations of *Ae. aegypti*, it has been proposed that human blood is the primary energy source, but where there is a shortage of human, plant sugars are used for survival (Day and Van Handel, 1986).

1.2.1.3 Oviposition behavior

For generation of new offspring, female mosquitoes have to return to an aquatic habitat when ready to lay eggs. The change of their preferences from a terrestrial habitat to an aquatic environment is mediated by both visual and chemical cues (Beehler et al., 1992). Oviposition attractants are produced by bacterial or fungal breakdown products in aquatic sites as well as oviposition pheromones from mosquitoes (Bentley and Day, 1989) that allow the female mosquitoes to lay their eggs in suitable sites for larval development. The oviposition pheromone, erythro-6-acetoxy-5-hexadecanolide, is the only known pheromone that was identified from the deposited egg rafts of *Cx. quinquefasciatus* in water and is found to attract a number of *Culex* species (reviewed in Takken and Knols, 1999). Also gravid *Culex molestus* mosquitoes were found to be attracted to chemical compounds produced by the bacterium *Pseudomonas vesicularis* (Dhileepan, 1997). At least five other compounds have also been isolated from hay fusions, which include phenol, 4-methylphenol, 4-ethylphenol, indole and 3-methylindole, that *Cx. quinquefasciatus* mosquitoes respond (Millar et al., 1992). Other mosquitoes, such as *Ae. aegypti* and *Ae. albopictus*, also show differential response to these compounds (reviewed in Takken and Knols, 1999). It has been also determined that these compounds were acting independent of the pheromone erythro-6-acetoxy-5-hexadecanolide, indicating no synergistic effects of the pheromone with these volatiles (Millar et al., 1994). Once the female mosquitoes locate suitable oviposition sites to lay their eggs, closer-range stimuli (i.e., temperature, light, and water salinity) will induce their oviposition behavior (Zahiri 1997; Mokany and Shine, 2003).

1.3 Peripheral events in insect olfaction

In recent years, the knowledge on olfaction in insects has been accumulated significantly by using biochemical, molecular and genomic approaches. Odorant and pheromone perception in insects occurs through a series of events, in which several proteins are found to mediate these events. At the beginning of the eighties, the first OBP of insects was identified in the giant moth *Antheraea polyphemus* (Vogt and Riddiford, 1981). About 10 years later, the discovery of ORs in a vertebrate system (Buck and Axel,

1991) was the milestone for a better understanding of the peripheral events in olfactory systems. With the availability of the first insect genome, *Drosophila*, the insect counterparts of vertebrate ORs have been identified (Clyne et al., 1999; Vosshall et al., 1999). Subsequent genome sequences as well as molecular cloning techniques have identified the molecular players in the olfactory sensillum lymph, which include OBPs, ORs, and ODEs that are involved in odor perception, processing and degradation in insect olfactory systems.

1.3.1 Odorant-binding proteins (OBPs)

1.3.1.1 Classification

The majority of early studies to identify insect OBP sequences have been performed in Lepidoptera (moths and butterflies; Vogt and Riddiford, 1981; Vogt et al., 1989). More recently, cDNA sequences and genes encoding OBPs have also been obtained from various insect orders such as Hymenoptera (bees, wasps, and ants; Danty et al., 1999), Diptera (flies and mosquitoes; Pikielny et al., 1994; Galindo and Smith, 2001; Graham and Davies, 2002; Biessmann et al., 2002; Xu et al., 2003), Coleoptera (beetles; Wojtasek et al., 1998; Wojtasek and Leal, 1999), and Hemiptera (true bugs; Vogt et al., 1999). Identification and distribution of OBPs among various insect orders (more than 40 insect species) support the fact that OBPs are common elements of insect olfactory systems.

The first insect OBP was identified from the male antennae of the *Antheraea polyphemus*, using the radioactively labeled pheromone (E, Z)-6,11-hexadecadienyl acetate as a probe in ligand-binding experiments (Vogt and Riddiford, 1981). This protein was named pheromone-binding protein (PBP), and a great number of proteins similar in their amino acid sequences to PBPs were identified in several insect species. Later, identification and cloning of general odorant-binding proteins (GOBPs) have been described that showed differential expression pattern from PBPs (Vogt et al., 1991a) and distinct binding properties to different classes of odorant molecules. More recently, a group of antennal specific genes have been cloned in *Bombyx mori* (Krieger et al., 1996)

and in other Lepidopteran species (reviewed in Pelosi, 1998), with low similarity to PBPs and GOBPs, thus, have been named as antennal binding proteins (ABPX). As a result, on the basis of their amino acid sequences, OBPs have been classified into three groups in insects: PBPs, GOBPs and ABPX.

Comparison of insect OBPs revealed common structural properties such that they are small (15-17kDa), water-soluble, extracellular proteins with a signal peptide sequence at the N-terminal. However, they appear to be highly divergent among the insect orders. For example, the OBPs of *Drosophila* share as low as 15% identity with OBPs of Lepidoptera (reviewed in Pelosi et al., 2006). The amino acid similarities among *Drosophila* OBPs range from 9.2 to 62.6% (Galindo and Smith, 2001). In the genome of the malaria vector, *Anopheles gambiae*, OBPs range from 5 to 100% amino acid identity (Xu et al., 2003). Despite the low sequence similarity among different insect OBPs, most of them have, in common, a pattern of six cysteines, whose relative positions are conserved. This has been accepted as the hallmark feature of "classical OBPs" in insects.

In *Drosophila*, fifty-one *Obp* genes have been identified, thirty-nine of which encode the classical OBPs with the six cysteine motif (Galindo and Smith, 2001; Hekmat-Scafe et al., 2002; Graham and Davies, 2002). In *An. gambiae*, twenty-nine of the fifty-seven *Obp* genes encode the classical OBPs (Xu et al., 2003). Both in *D. melanogaster* and *An. gambiae*, a different class of *Obp* genes was identified, which exhibits additional cysteines in addition to the conserved pattern of six cysteines (Hekmat-Scafe et al., 2002; Xu et al., 2003). These genes were categorized as the "Plus-C subfamily" of OBPs. Interestingly, it was found that *An. gambiae* contain sixteen *Obp* genes, referred to as "Atypical OBPs", which have an extended C-terminal region with several conserved cysteine residues (Xu et al., 2003). Their orthologs have not been identified in *Drosophila*. It is possible that this gene cluster arose after the divergence of mosquitoes and flies and may indicate a mosquito-specific function.

1.3.1.2 Expression of OBPs

The discovery of the first insect OBP in moth antennae (Vogt and Riddiford, 1981) has provided another field of study towards understanding the physiological function of the OBPs at the subcellular level. Using polyclonal antibody against the moth PBP, it was shown that it is located exclusively in the sensillum lymph of male antennae (Vogt et al., 1989). Immunocytochemical studies have also shown that two - trichogen and tormogen - of the three accessory cells (Fig. 1.1) at the base of the sensillum were labeled, demonstrating that the protein was concentrated in the extracellular compartment of the lymph, but was absent in the cytoplasm of the dendrites (Steinbrecht et al., 1992). These findings support the idea that OBPs are produced in the accessory cells and secreted into the sensillum lymph surrounding the outer dendritic segment.

It was found that there are morphologically different types of olfactory sensilla in the antenna; sensilla trichodea, sensilla basiconica and sensilla coeloconica (Steinbrecht, 1996; reviewed in Stocker, 1994). Immunocytochemical localization of OBPs has indicated a general rule in Lepidoptera such that pheromone-sensitive sensilla trichodea express PBPs (Steinbrecht et al., 1992), whereas sensilla basiconica mainly express GOBPs (Laue et al., 1994) and no co-localization of PBPs and GOBPs in the same sensillum is observed (Steinbrecht et al., 1995). Differential expression of OBPs was also found in Diptera (Hekmat-Scafe et al., 1997; Park et al., 2000). Apart from the observations in Lepidoptera, co-localization of closely related OBPs (i.e. OS-E and OS-F) in the same sensilla was detected in *Drosophila* (Hekmat-Scafe et al., 1997). This finding has shown that more than one OBP can be expressed in an individual sensillum.
As found in moths, PBPs were thought to be male antennae specific; however, they are also found in female antenna of the cockroach *Leucophae maderae* (Riviere et al., 2003).

In *D. melanogaster* and *An. gambiae*, expression of OBPs in different tissues has been determined using OBP promoter constructs, *in situ* hybridization and non-quantitative reverse transcription-polymerase chain reaction (RT-PCR). In *Drosophila*, temporal and spatial expression patterns of putative *Obp* genes have been elucidated using OBP promoter-driven expression of the LacZ reporter gene, where 9 *Obp* genes

were expressed only in the olfactory sensilla (antenna and maxillary palp), 7 *Obp* genes were exclusively expressed in gustatory tissues (wings, legs and labellum), and another 9 *Obp* genes were expressed in both gustatory and olfactory tissues (Galindo and Smith, 2001). *In situ* hybridization of *Drosophila* OBPs has also indicated that they are expressed in olfactory and/or gustatory tissues (Hekmat-Scafe et al., 2002).

The expression of OBPs in *An. gambiae* is also consistent with observation in *Drosophila*. Using non-quantitative RT-PCR, it is found that 11 *Obp* genes are expressed only, or mainly in olfactory tissues of *An. gambiae* (Li et al., 2005). Further investigation of the *Obp* gene transcripts has been performed by RT-PCR and/or microarray (Biessmann et al., 2005). These results showed that 18 *Obp* genes were expressed in olfactory tissues only, and 16 *Obp* genes were expressed both in olfactory and gustatory organs.

These findings indicate that *Obp* genes are differentially expressed in chemosensory tissues of insects. There is a considerable overlapping expression of *Obp* genes in olfactory and gustatory tissues, which may indicate that these genes may be involved, not only, in olfaction but also for both types of chemoreception. It is also possible that both olfactory and gustatory tissues have some common functions. It should be noted that it is the type of sensilla where an olfactory function can be attributed to an OBP (or OR) in a chemosensory tissue. Therefore, it is the type of the sensilla, where an OBP is expressed, that indicates their possible roles in olfaction or gustation (reviewed in Pelosi et al., 2006). Thus, it is reasonable to speculate that *Obp* genes expressed in different chemosensory tissues may share similar biological functions. In fact, some receptor genes classified as gustatory receptors (GRs) in *Drosophila* are expressed in the antennal neurons, indicating their involvement in olfactory perception (Scott et al., 2001).

1.3.1.3 Structural biology of OBPs

To date, the structures of only six insect OBPs have been resolved. The first OBP structure determined was the PBP from the moth *Bombyx mori* (Sandler et al., 2000). Later, the structures of a PBP from cockroach *Leucophae maderae* (Lartigue et al., 2003),

antennal specific protein-1 (ASP1) from the honeybee *Apis mellifera* (Lartigue et al., 2004), a PBP of the giant moth *Antheraea polyphemus* (Mohanty et al., 2004), the ethanol binding protein, LUSH from the fruit fly *Drosophila melanogaster* (Kruse et al., 2003), and an OBP from the mosquito *Anopheles gambiae* (Wogulis et al., 2006) have been determined.

The three-dimensional structure of the PBP from *B. mori* (*Bmor*PBP) has been determined to be complexed with its natural ligand, bombykol, by X-ray diffraction spectroscopy (Fig. 1.2; Sandler et al., 2000). The protein has six α-helices, named α1 to α6, linking α1 to α3, α3 to α6 and α5 to α6. This linkage stabilizes the protein structure by formation of three disulphide bonds between cysteine pairs, Cys19-Cys54, Cys50-Cys108 and Cys97-Cys117 (Fig. 1.3). Polar residues are found at the hydrophobic surface of the PBP that are probably involved in the solubilization of the protein in the aqueous sensillum lymph. The bombykol is bound to the binding pocket formed by the helices α1, α4, α5 and α6, and interacts with the residues located in the binding pocket. These residues are Met5, Phe12, Phe36, Trp37, Ile52, Ser56, Phe76, Val94, Glu98, Ala115, and Phe118 and are highly conserved among lepidopteran OBPs. Residues Met61, Leu62, Ile91 and Val114 are found to be specific to *Bmor*PBP and are likely involved in the ligand binding specificity. Further studies calculating the intermolecular forces involved in the formation of the bombykol-*Bmor*PBP complex have indicated that bombykol is attracted to the binding pocket by the residues located in the pocket, and not caused by the hydrophobic interactions (Klusak et al., 2003).

Solution nuclear magnetic resonance (NMR) studies suggest that the binding of the bombykol to the *Bmor*PBP and release from the binding cavity involve the conformational changes of the *Bmor*PBP in a pH-dependent manner (i.e. from *Bmor*PBP^{B} to *Bmor*PBP^{A}) (Horst et al., 2001; Lee et al., 2002). It has been shown that bombykol-*Bmor*PBP is stable at pH 7.5, but unstable at pH 5.5. The proposed mechanism of how *Bmor*PBP functions involves the binding of the bombykol to *Bmor*PBP^{B} at the cuticular pore (or pore tubules, structures for the transport of pheromone molecules from the sensillum surface to the receptors of the olfactory neurons), conformational change from

*Bmor*PBP^{B} to *Bmor*PBP^{A} at an acidic pH at the site of the cytoplasmic membrane, and opening up the binding pocket, thus releasing the bombykol to the its cognate receptor at the membrane.

The PBP of the *L. maderae* (*Lma*PBP) also consists of six α-helices, named A to F, forming three disulfide bridges linking helix A to C, helix C to F and helix E to F (Lartigue et al., 2003). *Lma*PBP binds to the components of the pheromonal blend 3-hydroxy-butan-2-one and butane-2,3-diol with high affinity (Lartigue et al., 2003; Riviere et al., 2003). The ligand binding pocket of *Lma*PBP is formed by the hydrophobic side chains of the six α-helices (Leu residues at positions 36, 45, 49, and 54, Ala46, Val89, Ile107, and Phe110), but also contains polar non-charged residues (Tyr5, Tyr75, and Thr111). Interestingly, this protein does not show a pH-dependent pheromone binding and release mechanism as proposed for *Bmor*PBP. The lack of C-terminus region of *Lma*PBP precludes the formation of a seventh α-helix that will push the ligand out of the binding cavity. Moreover, *Lma*PBP exhibits a hydrophilic pocket compared to that of *Bmor*PBP. In its three-dimensional structure bound to its natural ligand 3-hydroxy-butan-2-one, the binding cavity of *Lma*PBP remains open and no conformational changes can be observed (Lartigue et al., 2003) suggestive of a different ligand binging and release mechanism.

The tertiary structure of ASP1 from *A. mellifera* (*Amel*ASP1) consists of six α-helices, named A to F, and three disulfide bridges are formed by connecting helix A to C, helix C to F and helix E to F (Lartigue et al., 2004). *Amel*ASP1 binds to the major components of the queen pheromone 9-keto-2(E)-decenoic acid and 9-hydroxy-2(E)-decenoic acid (Danty et al., 1999). The α-helices forms the ligand binding pocket, forming a hydrophobic cavity containing Val13, Met49, Leu residues at 53 and 74, Met86, and Tyr102. Polar residues (Glu8, Asp16 and Ser57) and hydrophobic residues (Trp4, Pro residues at 6, 7, and 75, Leu residues at 12 and 73) are located at the opening of the cavity. In contrast to *Bmor*PBP and *Lma*PBP, the C-terminus of *Amel*ASP1 folds back into the binding cavity without forming an α-helix.

The PBP from *A. polyphemus* (*Apol*PBP) is the first PBP structure that has an acetate binding function with its ability to bind the pheromone (E,Z)-6,11-hexadecadienyl acetate (Vogt and Riddiford, 1981). The structure of the *Apol*PBP has been determined by NMR spectroscopy (Mohanty et al., 2004). Nine α-helices, α1a, α1b, α1c, α2, α3a, α3b, α4, α5 and α6, are arranged in a globular shape. Three disulfide bridges are formed by connecting helices α2 to α3b, α3a to α5, and α5 to α6. These α-helices constitute the hydrophobic ligand binding site. α3a is separated from α3b by Asn53 that interacts with the acetate group of the pheromone molecule. The terminal polar group of the ligand is recognized by the residues 53 to 61 of the *Apol*PBP, which play an important role in the ligand specificity. Two forms of the *Apol*PBP have been proposed which is induced by pH-dependent conformational change of the protein. At pH 6.3, it is found as a complex with its ligand (Mohanty et al., 2004). At the acidic pH 5.2, the protein undergoes a conformational change, where the protonation of the His69, His70 and His95 causes a reorientation of the helices (α1, α3, and α4) and release of the pheromone molecule (Zubkov et al., 2005).

In *D. melanogaster*, the structure of an OBP, LUSH, has been determined by X-ray crystallography (Kruse et al., 2003). LUSH is believed to be involved in the detection of alcohols, and *lush* mutants have been reported to lack the avoidance behavior to high concentrations of alcohol (Kim et al., 1998; Kim and Smith, 2001). The three-dimensional structure of LUSH consists of 6 α-helices, named α1 to α6 that occupy a hydrophobic cavity. Helices are linked as α1 to α3, α3 to α6 and α5 to α6 to form the three disulfide bridges. The structure was complexed with different alcohols (i.e. ethanol, n-propanol and n-butanol) that occupy the binding cavity. The alcohol-binding pocket of LUSH is formed by helix α3, helix α6 and the C-terminus (Fig. 1.4). Within the binding pocket, Ser52, Thr57, Phe64, Phe113 and Trp123 form the edges at the opening of the pocket and nonpolar groups of Val106, Thr109 and Ala110 are located at the bottom of the pocket. The hydroxyl group of the alcohol makes hydrogen bonds with Thr48, Thr57 and Ser52 (Fig. 1.4). LUSH has the same structure at acidic and neutral pH and still binds to alcohols at pH 4.6. This indicates that the conformational change in LUSH is

independent of the pH factor and may suggest a different ligand binding and release mechanism than what is observed in *Bmor*PBP.

A recent study has revealed that LUSH does not bind ethanol but some phthalates that are repellents for flies (Zhou et al., 2004). The authors also propose a conformational change for the protein as reported for *Bmor*PBP, with the unique finding that the C-terminus of the protein is displaced after the ligand enters the binding site. LUSH is also involved in the perception of an aggregation pheromone (see below).

Agam-OBP1 is the only known mosquito OBP with a defined structure in *An. gambiae* (Wogulis et al., 2006). *Agam*-OBP1 also contains six α-helices that form a hydrophobic binding pocket. Within the binding pocket are Tyr10, Ser79, His111, Trp114, Phe123 and Val125. The opening of this binding pocket is formed by the residues Leu15, Ala18, Leu22, Ala62, Val64, and Leu73. It has been determined that the *Agam*-OBP1 undergoes a pH-dependent conformational change. At lower pH, the short C-terminus of *Agam*-OBP1 does not form a helix that would displace the ligand but move away from it leaving the binding pocket exposed to the solvent, thus decreasing the binding affinity of the protein to the ligand. The crystal structure of *Agam*-OBP1 has been determined as a dimer. It was proposed that the long, hydrophobic tunnel that goes through the dimer interface allows the passage of the ligand through the protein.

1.3.1.4 Functions of OBPs

Despite a wealth of biochemical and structural information, the exact physiological function of OBPs remains elusive. Their presence and abundance in the olfactory sensillum lymph strongly suggests that OBPs are the first molecular component of insect olfactory transduction. It now appears that they serve as a solubilizer and carrier for the hydrophobic odorants, deactivators of the stimulus and play an important role in odor discrimination.

Before the odorant molecules can reach the ORs, they have to pass through an aqueous sensillum lymph. Because of the hydrophobic nature of odorant molecules, it is

very likely that OBPs bind and solubilize these molecules and carry them in such an aqueous environment. Indeed, binding of odorants to OBPs has been demonstrated in moths. PBP in moth has been shown to bind the pheromone and act as a solubilizer, suggesting the formation of a pheromone-PBP complex (Vogt and Riddiford, 1986; Du and Prestwich, 1995). Electrophysiological recordings from the antennae of *A. polyphemus* suggested that the pheromone alone did not activate the ORNs, but when the pheromone was incubated with PBPs, it stimulated the ORs to elicit a respond (Pophof, 2002). Another study also indicated that the response of the receptor cell to the pheromone is significantly increased when the PBP was added (Van den Berg and Ziegelberger, 1991). It has been suggested that *A. polyphemus* PBPs occur in two forms, which exhibit different binding properties to its ligand (Ziegelberger, 1995). The pheromone is initially bound by the reduced form of the PBP (PBP_{red}) and it is the pheromone-PBP_{red} complex that interacts with the receptor proteins. This interaction and the delivery of the pheromone to the receptor involves a conformational change of the PBP to an oxidized form (PBP_{ox}) serving as deactivator for the pheromone (Ziegelberger, 1995), thus preventing receptor overloading. As a result, these two states of the PBP with different affinities to the ligand indicate PBP acting as a carrier and as a deactivator for the pheromone molecules. Structural studies of OBPs have also identified the evidence for the pH-dependent conformational changes in PBPs (i.e. *Bmor*PBP) suggesting the pheromone binding and release by these proteins.

It is also possible that the binding of the pheromone by the PBP might prevent the degradation of the stimulus before it reaches the ORs to elicit a response. In fact, higher concentrations of PBPs have shown to protect the pheromone from ODEs *in vitro* (Vogt and Riddiford, 1986). Also the structure of a pheromone-PBP complex showed that the ligand is completely hidden in the binding cavity of the PBP (Sandler et al., 2000), thus preventing its accessibility to ODEs.

Despite the findings that ORs can be directly stimulated by the odorants or pheromones, a recent study in *Drosophila* indicates that OBPs are required in the perception of a chemical ligand and signal transduction. It has been found that a

Drosophila mutant for an OBP (LUSH) showed defects in perception of the aggregation pheromone, 11-*cis* vaccenyl acetate (VA) (Xu et al., 2005). However, the expression of the *lush* transgene in the mutants restored the LUSH expression, indicating that LUSH is required to bind the VA and, in turn, stimulate the VA-sensitive neurons to elicit a pheromone-induced behavior.

The identification of a large number of different OBPs expressed in different subsets of sensilla types suggests some odorant binding specificity of these proteins. It is possible that chemical ligands bind with different affinities to OBPs. In fact, binding studies have shown that PBPs have a range of affinities toward different pheromone compounds. For example, in the honeybee PBPs, ASP1 binds specifically to the pheromonal components 9-keto-2(E)-decenoic acid and 9-hydroxy-2(E)-decenoic acid, whereas ASP2 does not bind them (Danty et al., 1999). Moreover, PBPs of *A. polyphemus*, *Apol*PBP1 and *Apol*PBP3, bind the pheromone (6E, Z11)-hexadecadienyl acetate ((6E, Z11)-16:OAc) but not (6E, Z11)-hexadecadienal ((6E, Z11)-16:A1). Besides, *Apol*PBP3 has a higher affinity for (6E, Z11)-16:OAc (Maida et al., 2003). Specific ligand binding has also been demonstrated for the GOBP of *M. sexta* (Feng and Prestwich, 1997) and *M. brassicae* (Jacquin-Joly et al., 2000). The former is able to bind (E6, Z11)-16:DZa, while the latter binds Z11-hexadecen-1-ol (Z11-16:OH) and is unable to bind other pheromone components. These results indicate that OBPs discriminate between chemical ligands and are involved in the initial steps of odor coding in insect olfactory system.

1.3.2 Odorant receptors (ORs)

A major breakthrough in understanding the molecular basis of odorant perception and processing came from the characterization of the first candidate *Or* genes from rat olfactory epithelium (Buck and Axel, 1991), a discovery that has been recognized by the 2004 Nobel Prize in Medicine and Physiology. However, the identification of ORs in insects was unsuccessful using similar cloning approaches. The sequencing of the *D. melanogaster* genome (Adam et al., 2000) has allowed screening for the similar G-protein coupled receptors (GPCRs) using a computational algorithm (Clyne et al., 1999).

Subsequent studies using a variety of approaches have identified a large family of candidate ORs in *D. melanogaster* (Gao and Chess, 1999; Vosshall et al., 1999). Later, ORs have been identified in different insect species, such as *B. mori* (Sakuari et al., 2004), *H. virescens* (Krieger et al., 2002), *A. mellifera* (Robertson and Wanner, 2006). Similar approaches have also revealed candidate *Or* genes in the *An. gambiae* genome (Fox et al., 2001; Hill et al., 2002) and more recently in the genome of *Ae. aegypti* (Bohbot et al., 2007).

Or genes in vertebrates encode a family of GPCRs, characterized by the presence of seven transmembrane segments spanning the plasma membrane of the ORN dendrites with an extracellular N-terminus (Buck and Axel, 1991). In insects, however, a different membrane topology was observed, with the N-terminus of the receptors located intracellularly (reviewed in Benton, 2006). Thus, it is still debated whether insect ORs are true GPCRs.

Vertebrate ORs comprise a large family, approximately ~400 genes in humans (Malnic et al., 2004), as many as 1200 genes in mice (Godfrey et al., 2004) and down to 100 genes in catfish (Ngai et al., 1993). On the contrary, insect genomes contain relatively small number of *Or* genes; 60 genes (encoding 62 proteins) in *D. melanogaster*, 79 genes in *An. gambiae* and 131 genes in *Ae. aegypti* that are expressed in subsets of ORNs of the antenna and maxillary palp (Clyne et al., 1999; Vosshall et al., 1999; Robertson et al., 2003; Hill et al., 2002; Bohbot et al., 2007). Several *Or* genes are found as clusters in these genome. A comparison of the *Or* genes in *Drosophila* and *An. gambiae* revealed little or no sequence similarity with each other. For example, *An. gambiae* contains 27 ORs that do not have their orthologs in the *Drosophila*, suggesting an expansion of this gene family in the mosquito (Hill et al., 2002). This would indicate that the ligands recognized by its cognate OR would define the host-preference of the mosquitoes.

Despite a high level of divergence among ORs, there is one member of the *Or* gene family, *Or83b*, that is structurally and functionally conserved among different insect

species (Vosshall et al., 2000; Krieger et al., 2003; Pitts et al., 2004), which may reflect an important function of this gene in insect olfaction. *Or83b* is co-expressed with the conventional receptor gene in nearly all ORNs (Larsson et al., 2004). It does not appear to function directly in odor recognition, but act as a co-receptor in olfactory signaling (Benton et al., 2006). In fact, *Or83b* deletion mutants in *Drosophila* showed that the conventional ORs were not localized correctly along the dendritic portion of ORNs but to the cell bodies. The absence of ORs in the ORNs resulted in the lack of odor perception and olfactory-mediated behavior in mutant flies. These results indicate that *Or83b* is essential for proper localization of ORs to the dendrites of ORNs and their interaction with cognate ligands (Larsson et al., 2004). In addition to assisting the localization of ORs to the plasma membrane, they may also be involved in odorant binding and signal transduction (reviewed in de Bruyne and Warr, 2006).

Molecular studies also provide invaluable information on how distinct odorants are recognized by different classes of ORNs. One neuron-one receptor rule has been proposed for vertebrate olfactory systems (Ressler et al., 1993; Vassar et al., 1993; Hildebrand and Shepherd, 1997), such that each class of ORN expresses a unique OR for odor discrimination. There is evidence consistent with one receptor-one neuron rule in *Drosophila* as well (Vosshall et al., 2000). Authors have determined that individual ORNs are functionally distinct, expressing only a single receptor gene. However, it should be noted that these studies might not be conclusive due to large number of receptor genes and neurons in olfactory systems. Interestingly, co-expression of two ORs, *Or33c* and *Or85e*, are found in the pb2A neurons in *Drosophila* (Goldman et al., 2005). The significance of this finding has been highlighted by the fact that these genes are not the products of a recent duplication event. Moreover, the expression of both *Or* genes is conserved in evolution (Goldman et al., 2005). In conclusion, exceptions to the one receptor-one neuron rule has been described in the olfactory system of the fruit fly and this may provide another dimension for the odor coding dynamics of ORNs.

1.3.3 Odorant-degrading enzymes (ODEs)

It is important that odorant molecules are deactivated after they stimulate the ORNs. The process of pheromone degradation has been studied since the identification of the pheromone in *B. mori* (Butenandt et al., 1959). Studies have been performed where the radiolabeled bombykol was observed for its degradation in the male antenna of *B. mori* (Kasang and Kaissling, 1972; Kasang et al., 1989). However, their results did not indicate any enzymatic activity for the pheromone degradation. The antennal specific sensilla esterase (SE) has been identified in the antenna of *A. polyphemus* and referred to as the first pheromone degrading enzyme in insects (Vogt and Riddiford, 1981). It has been found to attack the acetate component of the pheromone for degradation. Similarly, antennal specific aldehyde oxidases that degrade aldehyde components of the pheromones have been identified (Rybczynski et al., 1989, 1990).

1.4 Olfactory signal transduction

Once the receptor has bound an odorant molecule, a cascade of events occurs that transforms the stimulus to an action potential of the ORN. In insects, ORs are thought to transduce the odor signal by coupling it to downstream effectors through heterotrimeric guanosine 5'-triphosphate (GTP) binding proteins and intracellular second messengers, although the precise mechanism remains unclear (reviewed in Rutzler and Zwiebel, 2005). Experimental evidence indicates the formation of inositol 1,4,5-triphosphate (IP_3) and 1,2-diacylglycerol (DAG) by activation of phospholipaseC (PLC) upon stimulation of ORNs with odorants. Stimulation of the antennal preparations from cockroaches resulted a rapid rise in IP_3 (Breer et al., 1990), which is assumed to be mediated by a receptor activated G-protein (Boekhoff et al., 1990a, b). Also, immunological studies showed the presence of PLC in homogenates of sensilla from the silkmoth (Maida et al., 2000; Krieger and Breer, 2003). The Gα subunits, Go and Gq, have been cloned from various insects, including moths, cockroaches and flies (Breer et al., 1988; Boekhoff et al., 1990b; Raming et al., 1990; Talluri et al., 1995). Furthermore, immunohistological studies localized the Gq-like proteins in the dendrites of the olfactory neurons from *B. mori* and *A. polyphemus* (Laue et al., 1997). An essential role of PLC has been established by *Drosophila* mutants, in which they were impaired in odor detection

(Riesgo-Escovar et al., 1995). Also an IP_3-dependent influx of the Ca^{++} ions was observed in the olfactory neurons of the moth *M. sexta* (Stengl, 1994). Another product of the IP_3 pathway, DAG, is found to elicit action potentials in the neurons of the moth *B. mori* (Pophof and van der Goes van Naters, 2002). The role of cyclic adenosine 3', 5'-monophosphate (cAMP) in insect olfactory transduction has been investigated in a few studies, but no increase in cAMP was determined upon stimulation of the neurons with odorant molecules (Ziegelberger et al., 1990; Boekhoff et al., 1993). However, in lobster, odorant compounds differentially stimulate two second messenger cascades, either cAMP or IP_3 cascades (Michel and Ache, 1992).

These findings, taken together, suggest a canonical model of G-protein coupled IP_3 pathway for insect olfactory transduction. Binding of the pheromone or an odorant molecule to the OR activates the G-protein, which in turn activate PLC that leads to the production of IP_3 and/or cAMP and depolarization of the plasma membrane (Hildebrand and Shepherd, 1997). These processes convert the chemical signals into neuronal activity in the insect nervous system to elicit appropriate behavioral responses.

1.5 Odor coding in insects

The olfactory system of insects allows the detection and discrimination of a large number of odorants in the environment. Despite the detailed analyses of *Or* gene expression, until recently little was known about the function of ORs in insect olfactory organs. Its simple olfactory system organization and easy genetic manipulation has led most of the work elucidating the molecular basis of odor coding on the fruit fly *D. melanogaster*.

Drosophila has two pairs of olfactory organs, the antennae and the maxillary palps. Each antenna contains approximately 1200 ORNs, whereas each maxillary palp contains about 120 ORNs (Stocker, 1994). Upon odor stimulation, the ORNs of these olfactory organs generate action potentials to elicit an olfactory response. Extensive electrophysiological measurements of the antennal sensilla identified 18 functional

classes of ORNs organized within 8 functional types of sensilla (de Bruyne et al., 2001; Hallem et al., 2004b). These studies revealed different odorants elicit responses from different subsets of ORNs. Moreover, these ORNs show remarkable diversity of responses, which can be either excitatory or inhibitory (de Bruyne et al., 2001).

More recently, a systematic approach has been used to characterize the molecular basis of odor coding in the entire olfactory organ of the *D. melanogaster* (Hallem and Carlson, 2004). Previously, it has been found that *Or22a* and *Or22b* genes were co-expressed in the ab3A antennal neurons and the deletion mutants that lack these genes lost the odorant response in the ab3A neurons (Dobritsa et al., 2003). This mutant ab3A neuron was then used to determine the function of the antennal repertoire of *Or* genes in *Drosophila* by expressing them in an *in vivo* expression system: the "empty neuron" system. This expression system involves that the receptor gene is introduced into mutant ab3A neuron using the GAL4/UAS system. *Or22a*-GAL4 is used to drive the expression from a UAS-OR construct. Subsequently, the odor response spectrum is determined by single-unit electrophysiology. By using this approach, a large number of odorants can be rapidly screened for the odor response spectrum of the ORN. Additionally, the empty neuron system can be efficiently used to perform functional analysis in other insect species. To illustrate, two ORs from *An. gambiae*, *AgOr1* and *AgOr2*, were expressed in the empty neuron system of the *Drosophila* and *AgOr1* has been shown to elicit an electrophysiological response to the components of human sweat (Hallem et al., 2004a). A recent work also showed the complete olfactory sensory map of the *An. gambiae* maxillary palp (Lu et al., 2007). These studies collectively facilitate the understanding of the molecular basis of how the olfactory cues are coded in the olfactory systems of mosquitoes and the link between odor recognition and behavior.

1.6 Odor processing in olfactory organs

Studies of molecular and cellular organization of insect central olfactory systems give insights about how the odors are processed in the central nervous system (CNS), thus help the knowledge on the olfaction-mediated behavior in insects. The action

potentials generated in response to the olfactory stimulus via signaling transduction pathway is directed along the ORN axons and are projected directly in the antennal lobe of the brain (Anton and Hansson, 1996; Hildebrand and Shepherd, 1997), the primary olfactory processing center in insects. In the antennal lobe, ORNs synapse onto second-order projection neurons and terminate in globular-shaped structures called the glomeruli (Hildebrand and Shepherd, 1997). These structures provide the sites of synaptic connections between ORN axons and interneurons of the CNS (Tolbert and Hildebrand, 1981). The glomeruli also contain local interneurons that provide a means of information transfer between individual glomerulus.

In insects, the number of glomeruli varies from species to species. In *D. melanogaster*, 43 morphologically distinct glomeruli have been identified (Laissue et al., 1999). In other insects species, such as locust, as many as 1000 glomeruli have been described (Ernst et al., 1977). More recently, approximately 60 glomeruli were found in *An. gambiae* (Ghaninia et al., 2007). Studies from several insect systems suggests that glomeruli constitute the functional units of peripheral olfactory systems such that ORNs expressing a certain type of OR terminate in the same glomerulus (Gao et al., 2000). Thus, convergent wiring of the neurons expressing the same OR in response to the same odorant may provide the basis for the olfactory processing in the CNS. Genetic labeling of the projection neuron axons has revealed axon branching patterns within the mushroom body and the lateral horn of the brain (Lee et al., 1999). Consistent with this finding, the spatial pattern of the odor-evoked activity has been determined in these structures (Wang et al., 2001), thus, suggesting the integration of olfactory information from multiple antennal lobe glomeruli to the higher brain centers (Wong et al., 2002; Marin et al., 2002).

1.7 Research significance and objectives

As described above, significant amount of information is available on the molecular and structural aspects of the key players of chemoreception from several insect species. There are several studies describing the genes involved in mosquito olfaction

(e.g., Hill et al., 2002; Xu et al., 2003; Justice et al., 2003; Biessmann et al., 2005; Bohbot et al., 2007), facilitated by the availability of the *Anopheles gambiae* and *Aedes aegypti* genome assemblies (Holt et al., 2002; Nene et al., 2007). Genomic comparison between closely-related as well as distant mosquito species will provide a great amount of information that will reveal conserved elements involved in olfactory gene regulation as well as genomic divergence that underline the behavioral and physiological differences among them. In this aspect, it is important to establish approaches that will enable us to identify olfactory genes in a variety of mosquitoes and determine their biological functions.

In this study, I focused on the odorant-binding proteins (OBPs), which are likely key players in mosquito olfaction (Biessmann et al., 2002; Justice et al., 2003; Xu et al., 2003). *Anopheles stephensi* was selected as the mosquito species to study in this research because it is the primary malaria vector in Asia and these mosquitoes are accessible in our departmental insectaries. Moreover, the availability of genetic tools makes it a good model mosquito species to work with in the laboratory. *Anopheles quadrianulatus* was also included in this study because it is a zoophilic species within the *Anopheles gambiae* species complex. These two species together with the reference species *Anopheles gambiae* make a good set for comparative genomics analysis. In addition, a rapid method to knockdown OBP genes was established in *Aedes aegypti*, which has the potential to significantly improve the ability to study the function of olfactory genes in mosquitoes.
The Specific Aims of this research were:

Specific Aim 1. Identify two *Obp* genes (*Obp1* and *Obp7*) in *Anopheles stephensi* and *Anopheles quadriannulatus* for comparative genomics analysis. Multi-species comparison of targeted *Obp* genes was performed to 1) examine *Obp* gene organization and possible events of gene expansion or loss, 2) identify conserved non-coding sequences that are potential regulatory elements of selected *Obp* genes, and 3) study the potential adaptive evolution of these genes.

Specific Aim 2. Study the expression profile of *Obp1* and *Obp7* genes in *Anopheles stephensi,* which will provide clues to their function. This was investigated by 1) examining the expression of these genes in early developmental stages and in olfactory and gustatory tissues in early and late adult stages as well as blood-fed females, 2) characterizing the structure of these *Obp* genes by RT-PCR and RACE, 3) determining the relative amount of *Obp* gene expression in olfactory and gustatory tissues by quantitative real-time PCR.

Specific Aim 3. Examine the expression profile of *Obp1* and *Obp7* genes in *Aedes aegypti* and establish a method to study the function of these genes in this mosquito species. The mRNA levels of these genes were determined in female chemosensory tissues. A double subgenomic Sindbis (dsSIN) virus expression system was used to knockdown *Obp1* and *Obp7* gene expression in olfactory organs of *Aedes aegypti*.

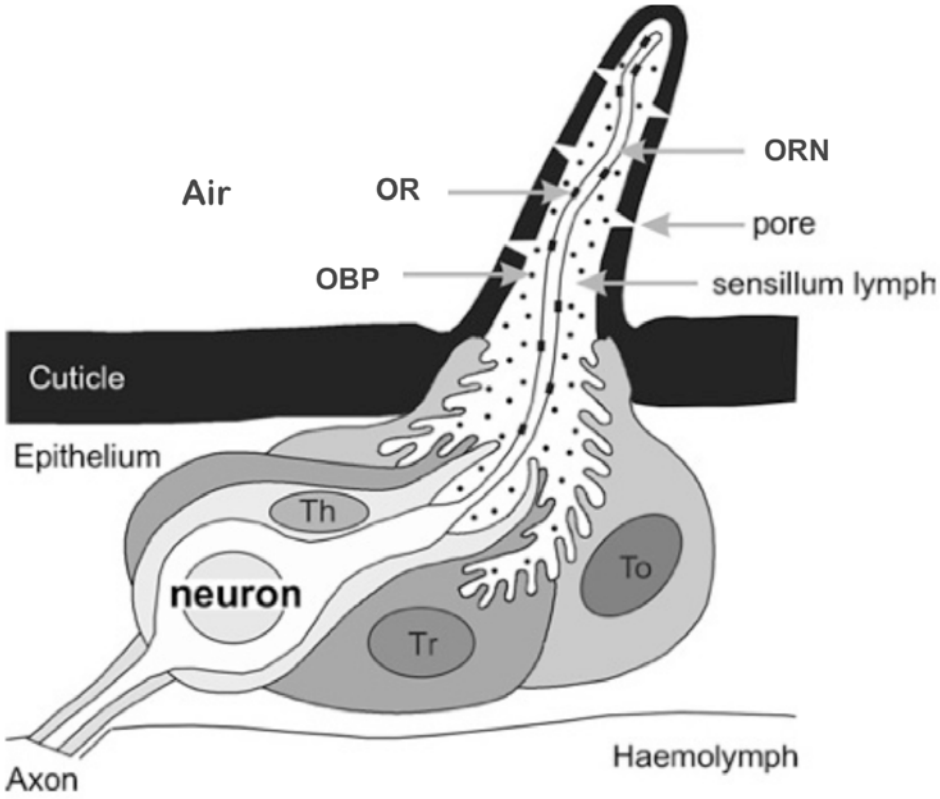

Figure 1.1 Schematic drawing of an insect olfactory sensillum. It is a cuticular structure that has many pores on the surface that allows the passage of the odorant molecules. It contains three accessory cells: Tormogen (To), thecogen (Th) and trichogen (Tr) cells. In the sensillum lymph are olfactory receptor neurons (ORNs), that contains membrane bound odorant receptors (ORs), and odorant-binding proteins (OBPs) (Modified from Jacquin-Joly and Merlin, 2004) [1].

[1]Reprinted, with kind permission from Springer Science and Business Media, Journal of Chemical Ecology, Volume 30, 2004, pp. 2359-2397, Insect Olfactory Receptors: Contributions of Molecular Biology to Chemical Ecology, Jacquin-Joly, E. and Merlin, C., Figure 1 © 2004 Springer Science+Business Media, Inc.

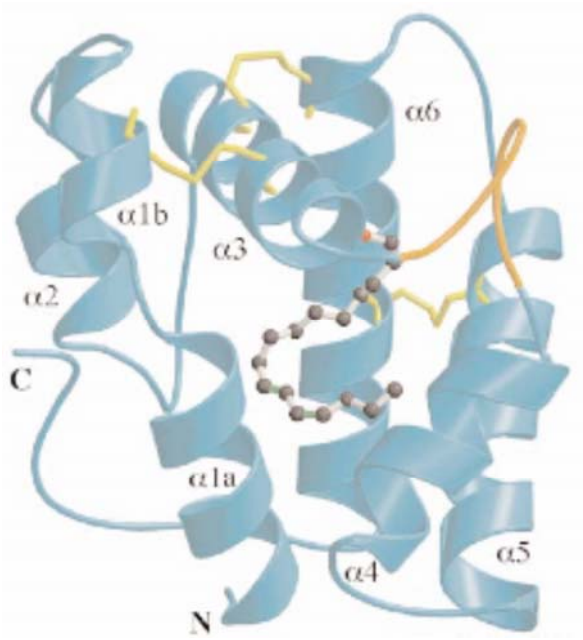

Figure 1.2 Structure of the PBP in *B. mori* (*Bmor*PBP). The 3-D structure of *Bmor*PBP with the ligand, bombykol, shown in a ball-and-stick representation. Six α-helices are shown and the disulfide bridges are indicated in yellow (From Sandler et al., 2000)[2].

[2] Reprinted from Chemistry & Biology, Volume 7, Sandler, B.H., Nikonova, L., Leal, W.S., and Clardy J., Sexual attraction in the silkworm moth: structure of the pheromone-binding-protein-bombykol complex, pp. 143-151, Copyright 2000, with permission from Elsevier Limited.

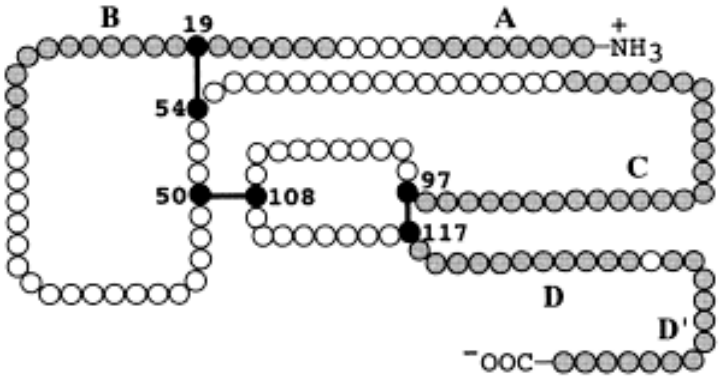

Figure 1.3 Schematic diagram of the three disulfide bonds in *Bmor*PBP. α-helices are indicated as A, B, C, D, and D' and in gray. Six cysteines are shown in black and the disulfide linkages between cysteine residues are shown in lines (From Leal et al., 1999)[3].

[3]Reprinted from FEBS Letters, Volume 464, Leal, W.S., Nikonova, L., and Peng, G., Disulfide structure of the pheromone binding protein from the silkworm moth, *Bombyx mori*, pp. 85-90, Copyright 1999, with permission from Elsevier Limited.

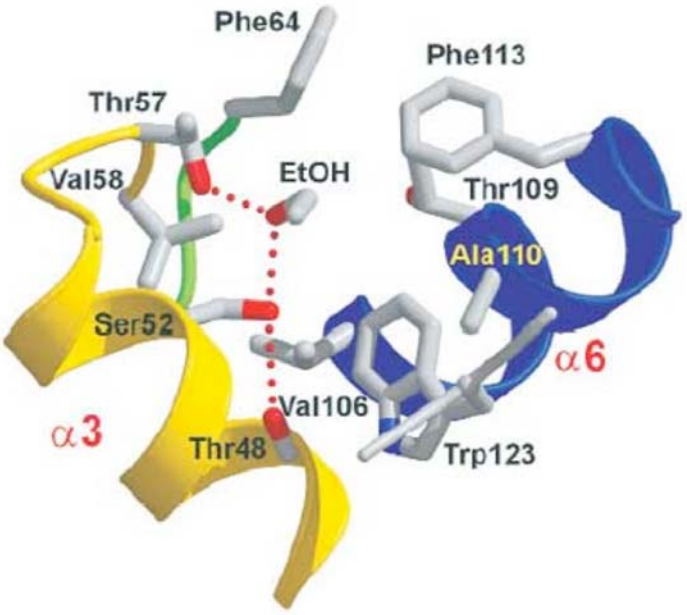

Figure 1.4 Structure of the alcohol-binding pocket of LUSH. The formation of the alcohol-binding pocket is established by the interactions of the residues in helix α3, helix α6 and the C-terminal strand. Hydrogen bond formation between ethanol and Thr48, Thr57, and Ser52 are shown in red (From Kruse et al., 2003)[4].

[4] Reprinted by permission from Macmillan Publishers Ltd: Nature Structural & Molecular Biology, advance online publication, 27 July 2003 (doi: 10.1038/nsb960).

Chapter 2

Characterization and expression of the odorant-binding protein 7 gene in *Anopheles stephensi* and comparative analysis among five mosquito species

Submitted for Publication in: *Insect Molecular Biology*

2.1 Abstract

Odorant-binding proteins (OBPs) are important molecular players in insect olfaction, which has a great influence on the host-seeking behavior of mosquitoes and other disease vectors. *Anopheles gambiae Obp7* gene (*Agam-Obp7*) is highly expressed in the adult female antenna, indicative of possible importance in female olfactory response. Here we report the cloning, sequencing, chromosomal mapping, and transcript analysis of *Aste-Obp7,* the *Obp7* gene from the Asian malaria mosquito *Anopheles stephensi*. Quantitative real-time PCR showed that in adult female mosquitoes, *Aste-Obp7* was expressed abundantly in the antenna, much less in pooled maxillary palp and proboscis, and at the lowest level in the legs. *Aste-Obp7* level in the female antenna was significantly higher than in male antenna and it slightly increased 24 h after a blood meal. The same pattern holds for leg samples as well. *Aste-Obp7* level dropped more than 10-fold in the female maxillary palp and proboscis after a blood meal, although it was still significantly higher than in the males. Together, the above expression profiles suggest that *Aste-Obp7* likely functions in female olfaction and may possibly be involved in behavior related to blood-feeding. We also characterized the *Obp7* gene from *Anopheles quadriannulatus*. Comparison of *Anopheles Obp7* genes revealed conserved non-coding sequences that contain potential regulatory elements. The coding sequence and gene structure of *Obp7* as well as local synteny of surrounding genes are conserved among the three *Anopheles* species and two divergent mosquitoes, *Aedes aegypti* and *Culex pipiens quinquefasciatus*. OBP7 protein phylogeny is congruent with the mosquito phylogeny and there is evidence of purifying selection acting on the mosquito *Obp7* gene.

Comparative genomics analysis will improve our understanding of the evolution and regulation of genes involved in mosquito olfaction.

2.2 Introduction

Insects developed two major chemosensory systems to detect chemical signals in the environment, namely olfaction (smell) and gustation (taste) (Stocker, 1994). Odorants are detected by specialized hair-like structures or "sensilla" found in the chemosensory organs and they contain numerous pores to allow odorants to enter the sensillum lymph and stimulate the olfactory receptor neurons (ORNs) (Steinbrecht, 1996, 1997). Olfaction has a great influence on the host-seeking behavior of disease vectors such as mosquitoes (Takken and Knols, 1999), thus directly affects the transmission of vector-borne infectious diseases such as malaria and dengue fever.

Odor-baited trapping systems have been used to study behavioral responses of mosquitoes toward chemical cues (Cork, 1996; Kline et al., 1990*;* Takken and Knols, 1999). For example, 1-octen-3-ol, in the presence of carbon dioxide (CO_2) and L-lactic acid, are found to be attractants to several mosquito species (Takken and Kline 1989; Geier et al., 1996; Takken et al., 1997). Electroantennogram (EAG) studies, which measure the response of ORNs to odorant stimulation in the antenna, suggest that CO_2 and L-lactic acid are attractants to the African malaria mosquito, *Anopheles gambiae* (Cork and Park, 1996).

Molecular studies have revealed key players involved in odorant perception. One important family of proteins present in the sensillum lymph is odorant-binding proteins (OBPs) (Pelosi and Maida, 1995). The first insect OBP was discovered in the male antenna of the giant moth, *Antheraea polyphemus* (Vogt and Riddiford, 1981). OBPs have now been identified in numerous insect species through molecular cloning and whole genome analyses. Insect OBPs are classified as pheromone binding proteins and general odorant-binding proteins (Vogt et al., 1991a,b) according to whether they bind pheromones or general odorant molecules. In general, OBPs are small, water-soluble

proteins secreted into the sensillum lymph by the surrounding accessory cells (Vogt and Riddiford, 1981; Steinbrecht et al., 1992; Pelosi, 1994). The hallmark feature of insect OBPs is characterized by the presence of six conserved cysteines. The precise physiological function of OBPs still remains unclear. They are believed to bind the hydrophobic odorants and transport them to the membrane bound odorant receptors (ORs) in the ORNs (Vogt et al., 1985; Vogt and Riddiford, 1986; Pelosi and Maida, 1995). They may also protect the odorants from odorant-degrading enzymes (ODEs) in the sensillum lymph (Vogt and Riddiford, 1981; Vogt et al., 1999).

In *Drosophila*, fifty-one *Obp* genes have been identified by whole genome sequence analyses (Hekmat-Scafe et al., 2002). Subsequent homology-based searches of the *An. gambiae* genome revealed fifty-seven *Obp* genes (Vogt, 2002; Xu et al., 2003). The *An. gambiae Obp7* (*Agam-Obp7*) is one of the *Obp* genes highly expressed in the female antenna. A recent study also showed an approximately 10-fold higher expression of *Agam-Obp7* in female antenna than in male antenna, suggesting that it may be important in female olfactory response (Biessmann et al., 2005). *Agam-Obp7* was also shown to be expressed in female maxillary palp and headless body samples by means of non-quantitative methods (Biessmann et al., 2005), indicating a broader odorant perception role of this gene.

Here we report detailed characterization and expression profile of the *Obp7* gene (*Aste-Obp7*) in the Asian malaria mosquito *Anopheles stephensi,* a species in the same subgenus as *An. gambiae*. Quantitative analyses of the *Aste-Obp7* expression profile suggests that it is likely important in female olfaction and it may be involved in blood-feeding. We also characterized the *Obp7* gene from *Anopheles quadriannulatus*, a species in the *An. gambiae* species complex. Comparative analyses of the three *Anopheles Obp7* genes revealed conserved non-coding sequences that contain potential regulatory elements. Further comparisons with two distantly related mosquitoes, *Aedes aegypti* and *Culex pipiens quinquefasciatus* revealed a number of conserved features. We discuss the applications of comparative genomics targeting olfactory genes in mosquitoes of various behavior phenotypes and evolutionary relationships.

2.3 Materials and methods

Mosquitoes and dissections

Anopheles stephensi Indian strain were reared at 27°C with 75% relative humidity and maintained in the insectary of the Department of Biochemistry at Virginia Tech. Generation time is about 2-3 weeks under our conditions. Larvae and pupae were frozen and stored at –80°C until use. Adults used for dissections were either 1 day or 5-6 days after emergence. The tissues were dissected on ice from live mosquitoes that were kept at 4°C for 10 minutes. Female mosquitoes were blood-fed on anaesthetized mice for approximately 20 minutes and dissected 24 h after blood-feeding.

Construction of Bacterial Artificial Chromosome (BAC) library

BAC libraries for *An. stephensi* and *An. quadriannulatus* were constructed by Amplicon Express (Pullman, WA) as described in Tao et al., 2002. Larvae were used as a starting material for each library construction. The average insert size was 125 kb and 123 kb for *An. stephensi* and *An. quadriannulatus* libraries, respectively. DNA from BAC clones were spotted on the filters, denatured, and irreversibly bound to the nylon membrane (Hybound-N+ Amersham Biosciences). Each filter contains 9,216 individual clones from the *An. quadriannulatus* library and 18,432 individual clones from the *An. stephensi* library. All clones were spotted in duplicate on the filter.

Generation of DIG-labeled, single-stranded DNA (ssDNA) probes and BAC library screening

The protein sequence alignment of *Agam*-OBP7 from *An. gambiae* (accession number: AY146742; Xu et al., 2003) and its fly ortholog, *Dmel*-OBP69a, from *D. melanogaster* (accession number: U05980; Pikielny et al., 1994) have been performed using Clustal X (1.8) (Thompson et al., 1997). This alignment was used to design degenerate primers, OBP7F1: 5'-GCNAARTGYTAYATHCAYTG-3' and OBP7R1: 5'-TARCAYTTNACNGTYTCRTANGC-3', from the highly conserved regions between the two species. The genomic DNAs were isolated from *An. stephensi* mosquitoes using DNAzol Genomic DNA Isolation Reagent (MRC, Inc.). Degenerate primers (mentioned

above) were used to amplify the region spanning the second intron of *Obp7* gene. The PCR products were cloned using pGEM-T-Easy vector systems (Promega, Madison, WI) and confirmed by sequencing (Virginia Bioinformatics Institute, Blacksburg, VA). The plasmid that contains *Obp7* gene sequence was used as a template in an asymmetric PCR using the primer, OBP7probe: 5'-ACACTTGTCCGGCGTTACTG-3', and DIG-dUTP labeling mixture (Roche Diagnostics, IN) to generate ssDNA probes. The DIG-labeled ssDNA probes were used to screen BAC libraries of *An. stephensi* and *An. quadriannulatus*. Hybridization was carried out at 55°C overnight. Two set of washes were performed at 55°C with 2X and 0.5X SSC. The positive clones were colorimetrically detected following the protocol of Boehringer Mannheim, Biochemicals (Indianapolis, IN).

BAC DNA sequencing

The positions of the positive clones were determined using the 384-well plate overlay. Single colony preps were made by dipping a sterile inoculating loop into stab (BACs are supplied as stabs in agar) and drawing parallel lines on the LB/chloramphenicol (12.5μg/ml) plates followed by incubation overnight at 37°C. One positive BAC clone per each screening was selected for BAC DNA isolation. Isolated DNA was checked by PCR before BAC sequencing (The Institute for Genomic Research, Rockville, MD).

Sequence analysis of BACs and identification of mosquito OBP7 orthologs

The sequenced BAC contigs from *An. stephensi* and *An. quadriannulatus* that had significant matches to the *Agam-Obp7* gene sequence and the nearby coding sequences were determined by using BLAST (Altschul et al., 1990). *Agam-Obp7* nucleotide and amino acid sequences were also used as a query to search against the *Cx. quinquefasciatus* trace file that has approximately 10X coverage with 5 million sequences and 4.6 billion bases (http://www.ncbi.nlm.nih.gov/). Blast hits were manually assembled using CAP3 program (Huang and Madan, 1999; http://pbil.univ-lyon1.fr/cap3.php) to construct genomic segments comprising both *Obp7* gene sequence and the flanking regions. The *Ae. aegypti* ortholog of OBP7, previously named AaegOBP2 (Ishida et al.,

2004), was obtained from NCBI database (AY189224). In this study, we named it as *Aaeg*-OBP7 (or *Aaeg-Obp7* for the gene) for consistency.

Chromosomal mapping of *Aste-Obp7* gene by fluorescent *in situ* hybridization (FISH)

MapOBP7L: 5'-CGGTTTACATTGTGCTTTCG-3' and MapOBP7R: 5'-GCGC GTTGAAGTAACATTTG-3' primer pair was used to amplify a 1,732 bp genomic sequence of *Aste-Obp7* gene. The PCR product was cloned using pGEM-T-Easy vector systems (Promega, Madison, VA) and confirmed by sequencing (Virginia Bioinformatics Institute, Blacksburg, VA). Probe was prepared from 1 μg DNA that was labeled with Cy5-AP3-dUTP (GE Healthcare, Little Chalfont, Buckinghamshire, UK) using Random Primers DNA Labeling System (Invitrogen, Carlsbad, CA). Ovaries from half-gravid females of *An. stephensi* mosquitoes were used for chromosome preparations that FISH analysis were performed as previously described (Sharakhova et al., 2006).

Expression analysis of *Aste-Obp7* by Reverse Transcription-Polymerase Chain Reaction (RT-PCR)

Total RNA was isolated from various *An. stephensi* developmental stages and dissected adult tissues using TRIzol reagent (Invitrogen, Carlsbad, CA). Following DNase treatment (Ambion, Inc., Austin, TX), samples were reverse transcribed using Superscript II reverse transcriptase (Invitrogen, Carlsbad, CA) at 42°C for 1.5 h followed by heat inactivation at 70°C for 15 minutes. All cDNA synthesis reactions were carried out in the absence of reverse transcriptase (-RT) in parallel as control for each sample. RT-PCR amplification of cDNAs were carried out using gene specific primers, RTOBP7L: 5'-CGGTTTACATTGTGCTTTCG-3' and RTOBP7R: 5'-GTACCCT CCTCGATCACGTC-3', that span the first intron sequence of *Aste-Obp7* gene to control for any genomic DNA contamination. Accordingly, PCR products with an expected size of 208 bp from cDNA amplification can be differentiated from genomic DNA amplification of a 1,509 bp product.

We were able to identify a ribosomal protein gene sequence from one product of a 5' RACE reaction in *An. stephensi*. We cloned a 1,668 bp region of this gene from *An. stephensi* and named it as ribosomal protein S4 gene, *Aste-Rps4*, because of its 97% amino acid identity (for a 562 bp *Aste-Rps4* cDNA sequence) to 40S ribosomal protein S4 in *An. gambiae* (accession number: XP_308886.3). *Aste-Rps4* gene is used as an internal control in the RT-PCR reactions to determine the integrity of cDNA templates. RT-PCR primer pairs; Rps4L: 5'-CACGAGGATGGATGTTGGAC-3' and Rps4R: 5'-ATCAGGCGGAAGTATTCACC-3' amplified a cDNA product of about 260 bp long, that can be differentiated from a gDNA amplification of about 1,368 bp in length.

The optimal annealing temperature for the RT-PCR was 60°C for both *Aste-Obp7* and *Aste-Rps4* genes. Both reactions were run for a total of 35 cycles. PCR products were analyzed by 2% agarose-gel electrophoresis.

Quantitative Real-time PCR (qRT-PCR)

For quantitative real-time PCR, total RNA from selected tissues were isolated from adult male and female mosquitoes as well as blood-fed females and used for cDNA synthesis as mentioned above. Our analyses included at least three biological replicates for all samples. The real-time PCR was performed using the TaqMan probe-based chemistry with an ABI Prism 7300 Sequence Detection System (SDS) (Applied Biosystems, Foster City, CA). For each 25 µl PCR reaction, 2 µl of cDNA was used with 9.25 µl nuclease-free water, 12.5 µl 2 X TaqMan Universal PCR Master Mix (Applied Biosystems, Foster City, CA), and 1.25 µl 20 X assay mix designed by ABI. The thermocycler program consisted of 50°C for 2 min, 95°C for 10 min, 40 cycles of 95°C for 15 sec and 60°C for 1 min. Since the relative mRNA amount of *Obp7* is being determined, parallel TaqMan assays were done for the ribosomal protein control gene, *Aste-Rps4,* as well. The assay mixture for *Obp7* gene and the control gene consists of 5'FAM, non-fluorescent quencher (NFQ) labeled probes and primer pairs as follows:

*Aste-Obp7*primerF: 5'-TGAAGGATGCGGTCAACCA-3'
*Aste-Obp7*primerR: 5'-AGGCGGTGTCACACTTGTC-3'

*Aste-Obp7*probe: 5'FAM-CAGCCACATCGTAACGC-NFQ
*Aste-Rps4*primerF: 5'-TTCGCACCGATCCGAACTAC-3'
*Aste-Rps4*primerR: 5'-GAAGTATTCACCGGTCTTGTGGAT-3'
*Aste-Rps4*probe: 5'FAM-TTGATCACATCCATGAAACC-NFQ

We used the ABI Assays-on-Demand setup for our TaqMan Gene Expression Assays. ABI does not recommend testing of amplification efficiency because their extensively tested assay design ensures near 100% (+/- 10%) efficiency and because commonly used testing methods tend to produce unreliable results (ABI Publication 127AP05-01). However, to be sure, we performed assay validation by checking the amplification curves (Bohbot and Vogt, 2005) and by using serial dilutions. All TaqMan PCR data were analyzed using SDS Software based on the comparative method ($\Delta\Delta C_T$) (Livak and Schmittgen, 2001). Briefly, for every sample, an amplification plot was generated showing the reporter dye fluorescence (ΔRn) at each PCR cycle. For each amplification, a threshold cycle (C_T) was calculated, representing the cycle number at which the fluorescence passes the threshold. Accordingly, relative amounts of *Obp7* and *Rps4* were determined as C_T values for each cDNA sample and the difference between these two values was obtained by subtraction, giving the ΔC_T value. Then, the ΔC_T value of each sample was normalized to that of the calibrator sample (See Fig. 2.5, Table 2.1, and Tables S2.1-S2.3 for specifications) resulting in the determination of $\Delta\Delta C_T$ value. And finally, $2^{-\Delta\Delta CT}$ values were calculated to estimate the fold changes in the mRNA levels of *Obp7* in different samples.

Statistical analysis

We used ΔC_T values for analysis of real-time PCR data. One-way ANOVA with Tukey's post test was performed using GraphPad Prism version 3.00 for Windows (GraphPad Software, San Diego, CA). Significance in comparisons is assumed if $P < 0.05$ is obtained in the appropriate test.

Rapid Amplification of cDNA Ends (RACE)

5' and 3' RACE were performed using the BD Smart RACE cDNA amplification kit (BD Biosciences Clontech, Palo Alto, CA) according to the manufacturers instructions. After the initial cDNA synthesis, PCR was performed using the adapter primer and the gene specific primers (5' RACE: 5'-CAGACAGTGGATGTAGCACTT GAC-3' and 3' RACE: 5'-CGTCAAGTGCTACATCCACTGTC-3'). The PCR products were cloned into pGEM-T-Easy vector (Promega, Madison, WI) and confirmed by sequencing (Virginia Bioinformatics Institute, Blacksburg, VA).

Sequence analyses of OBP7

The results from RT-PCR and RACE confirmed the *Obp7* gene structure in *An. stephensi*. The open reading frames (ORFs) of *Aqua-Obp7* were manually determined based on its similarity to *Agam-Obp7* coding regions. The peptide alignment of OBP7 orthologs was generated by using Clustal X (1.8) (Thompson et al., 1997). The following parameters were used for the alignment: pairwise gap penalty (open=35, extension=0.75), multiple gap penalty (open=15, extension=0.3). N-terminal signal peptide sequences of OBP7 were predicted by the SignalP V 3.0 program (Bendtsen et al., 2004; http://www.cbs.dtu.dk/services/SignalP/). Putative α-helical regions were predicted using Jpred (Cuff and Barton, 1999; http://www.compbio.dundee.ac.uk/~www-jpred/).

Multi-species comparison and transcription factor binding site (TFBS) predictions

The genome comparisons to identify conservation in coding and non-coding regions of *Obp7* from *An. stephensi, An. quadriannulatus* and *An. gambiae* were established by using MLAGAN (Multi-LAGAN) multiple alignment program (Brudno et al., 2003; http://genome.lbl.gov/vista/lagan/submit.shtml). The cut-off for sequence conservation is 75% over 100 bp. The *An. gambiae* genome annotation (Holt et al., 2002) is used to determine the coding regions in the alignment. The multi-species alignment was visualized by VISTA (Mayor et al., 2000), which gives a VISTA plot output calculating the percent identity over the window at each base pair. The X-axis shows the relative position of the *An. gambiae* genomic DNA, and the Y-axis shows the % identity

between *An. stephensi* and *An. gambiae* as well as *An. quadriannulatus* and *An. gambiae* sequences.

ConSite program (Sandelin et al., 2004; http://asp.ii.uib.no:8090/cgi-bin/CONSITE/consite/) is used to predict potential transcription factor binding sites for the 1 kb upstream sequence from the *Aste-Obp7* transcription start site. The cut-off for sequence conservation is 74%, and transcription factor score threshold is set to 80%.

Phylogenetic analysis of OBPs

In addition to *Aste*-OBP7, many OBPs from *An. gambiae, Ae. aegypti* and *D. melanogaster* were used in the phylogenetic analysis. The complete genome sequence for *Ae. aegypti* was not available at the time this work was initiated. Therefore, analyses were performed to search for selected *Obp* genes in *Ae. aegypti* using a database that comprise 36,203 sequences and 1,3 billion bases. Blast hits were manually identified and assembled for the coding regions of selected *Obp* genes. We named them such that they represented the ortholog of the corresponding OBPs in *An. gambiae*. Our results were subsequently confirmed with the current annotation of the *Ae. aegypti* genome (Nene et al., 2007). We determined one difference with the predicted peptide sequence of *Agam*-OBP19 ortholog in *Ae. aegypti*, which we named it as *Aaeg*-OBP19. The annotation of OBP19 in *Ae. aegypti* comprises the first peptides as "MEKTG". Our annotation included five more peptides upstream of this sequence in homology to *Agam*-OBP19. Moreover, we could not predict a signal peptide sequence for *Aaeg*-OBP19, which may suggest the presence of upstream sequences preceding the annotated transcription start site. Thus, we used our predicted peptide sequence of OBP19 in *Ae. aegypti.*

Selected OBP sequences with removed signal peptides were aligned using Clustal X (1.83) (Thompson et al., 1997) using the same parameters mentioned above. This alignment was used to perform phylogenetic analyses using PAUP* v4.0b10 (Swofford, 2002). Phylogenetic trees were constructed using the neighbor-joining, minimum evolution and maximum parsimony methods with bootstrap support of 1000 replicates.

The heuristic search was conducted using the tree bisection-reconnection (TBR) branch-swapping algorithm.

d_N and d_S calculations

Synonymous and nonsynonymous mutations were analyzed by the method of Nei and Gojobori, 1986. SNAP program (Synonymous/Nonsynonymous Analysis Program; http://www.hiv.lanl.gov/content/sequence/SNAP/SNAP.html) (Korber, 2000) was used to calculate d_N, d_S and to determine d_N/d_S ratios for mosquito OBP7 orthologs.

2.4 Results

Identification and chromosomal mapping of the *Obp7* gene in *An. stephensi*

Previously annotated *Agam-Obp7* gene sequence was used to construct *Obp7* gene probe to screen a bacterial artificial chromosome (BAC) library derived from *An. stephensi* genomic DNA (see Materials and methods). Six positive clones were identified from a total of 9,216 clones screened, which represents approximately 5-fold coverage of the genome, assuming that the genome size of *An. stephensi* is approximately 240 Mbp (Rai and Black, 1999). One positive BAC clone was sequenced, which produced 421 contigs, and a single *An. stephensi Obp7* gene (*Aste-Obp7*) was identified in a 12 kb contig. As shown in the alignment of the genomic regions encompassing the *Obp7* genes in *An. gambiae* and *An. stephensi* (Fig. 2.1), the coding sequences of the *Obp7* genes as well as the order of neighboring genes are conserved between the two species. Furthermore, we mapped *Aste-Obp7 gene* on the region 9C of the chromosomal arm 2R of the ovarian chromosomes of *An. stephensi* by fluorescent *in situ* hybridization analysis (Fig. 2.2). This region is homologous to *An. gambiae* chromosomal arm 2R 8B, the region in which *Agam-Obp7* reside (http://www.ensembl.org/Anopheles_gambiae/index.html; Sharakhova et al., 2006). Conservation in gene order and chromosomal location as well as phylogenetic analysis described later suggests that *Aste-Obp7* and *Agam-Obp7* are orthologs.

Aste-Obp7 gene structure is defined experimentally

The alignment shown in Figure 2.1 suggests a good conservation in the coding sequences of *Aste-Obp7* and *Agam-Obp7* genes. The actual gene structure of *Aste-Obp7*, however, needs to be determined by experimental methods. The 5' end of the *Aste-Obp7* transcript was determined by 5' rapid amplification of cDNA ends (5' RACE) using a total RNA sample isolated from whole female *An. stephensi* mosquitoes. Sequence comparisons between the 5' RACE product and the BAC clone revealed the existence and boundaries of a 1,302 bp intron. The comparison also indicated a transcription start site GATACAA (indicated as +1 in Fig. 2.3A) that is 154 nucleotides upstream of the initiation codon ATG. However, a TCAGG sequence (Fig. 2.3A, boldface and underlined), which is similar to the arthropod initiator consensus TCAGT (Cherbas and Cherbas, 1993), is observed 11 nucleotides upstream of the transcription start site predicted from 5' RACE. It is possible that the 5' RACE did not extend to the very beginning of the transcript. However, we are numbering the sequences according to the transcription start site as indicated by 5' RACE. A TATA box is located 32 bp upstream of the predicted transcription start site, which perfectly matches the consensus G/(A)TATAAAA from *D. melanogaster* (Breathnach and Chambon, 1981). The 3' end of the *Aste-Obp7* transcript was determined by 3' RACE, which produced a cDNA product with an expected poly(dA) tail. A 73 bp intron was removed from the cDNA. Imperfect polyadenylation signal sequences AATAA, ATTAAT and ATTAAA are found 45 bp, 48 bp and 80 bp upstream of the poly(dA) tail, respectively (Fig. 2.3A, boldface and italicized). Reverse transcription polymerase chain reaction (RT-PCR) was also performed using primers spanning the first and second predicted exons (Fig. 2.3A). Comparing sequences of the RT-PCR product and the BAC clone confirmed the existence of the first and second introns as described during 5' and 3' RACE. Thus the entire transcript of *Aste-Obp7* has been determined experimentally.

The positions of transcription start site, the initiation and stop codons, the entire ORF which is interrupted by two introns, and the putative polyadenylation signals are all shown in Figure 2.3A. The transcript is 793 bp long with an approximately 150 bp 5' untranslated region (UTR) and a 200 bp 3' UTR. The coding region is 438 bp long

encoding a 146 amino acid peptide. The overall structure of *Aste-Obp7* is highly similar to *Agam-Obp7* (Fig. 2.3B), which is annotated in Ensembl database (http://www.ensembl.org/Anopheles_gambiae/index.html).

Expression profile of *Aste-Obp7*

The initial assessment of the expression profile of *Aste-Obp7* was examined by non-quantitative RT-PCR. Our results indicate a variable expression of *Aste-Obp7* in developmental stages tested, relatively weak in early pupae stage (Fig. 2.4A). We also performed RT-PCR using different olfactory/gustatory tissues from 1-day-old and 5 to 6-day-old adults of males and females as well as females 24 h after a blood meal. *Aste-Obp7* expression is observed in wings and legs in addition to antenna, maxillary palp and proboscis from all five adult samples (Fig. 2.4B). These non-quantitative RT-PCR reactions were performed using relatively high cycle numbers (35 cycles) and were not intended to reveal quantitative differences. We also tested body samples devoid of head and appendages and either weak or no expression was observed (not shown).

To quantify the relative levels of *Aste-Obp7* mRNA in olfactory and gustatory tissues of adult mosquitoes, we performed quantitative real-time PCR (see Materials and methods for details). We analyzed the level of *Aste-Obp7* mRNA in female antenna, maxillary palp and proboscis, and legs. We observed a significantly higher (on average approximately 600-fold higher) expression in the female antenna compared to the female maxillary palp and proboscis (Table 2.1; Fig. 2.5A). Very low amount of *Aste-Obp7* is observed in the female legs, approximately 50-fold lower than in maxillary palp and proboscis (Table 2.1; Fig. 2.5A). These results indicate that *Aste-Obp7* is much more abundantly expressed in the primary olfactory organ, the antenna, of the female *An. stephensi* mosquitoes compared to the other chemosensory tissues.

In antenna, maxillary palp and proboscis, and legs, the level of *Aste-Obp7* transcript is significantly higher in the females than in the males, regardless of blood-feeding status (Fig. 2.5B-D). In the female antenna and leg samples, *Aste-Obp7* is slightly increased 24 h after a blood meal. However, *Aste-Obp7* level dropped more than

10-fold in the female maxillary palp and proboscis after a blood meal, although it was still significantly higher than in the males.

Identification and analysis of the gene structure of *Obp7* in *An. quadriannulatus*

An *An. quandriannulatus* BAC library was also screened using the *Obp7* gene probe mentioned above. Two positive clones were identified among 4,608 total clones screened, which represents approximately 2.1-fold coverage of the genome, assuming the genome size is approximately 270 Mbp, similar to that of *An. gambiae* (Besansky and Powell, 1992). One positive BAC clone was sequenced, which produced 11 contigs, and a single *An. quadriannulatus Obp7* gene (*Aqua-Obp7*) was identified in a 34,687 bp contig. As shown in the VISTA alignment of the genomic regions encompassing the *Obp7* genes in *An. gambiae* and *An. quadriannulatus* (Fig. 2.1), the coding sequences of the *Obp7* genes as well as the order of neighboring genes are conserved between the two species. As shown in Figure 2.3B, *Agam-Obp7*, *Aste-Obp7*, and *Aqua-Obp7* genes show similar exon/intron structure. The three exons are relatively conserved both in terms of their sequence and length. Although the sequences of their 5' and 3' UTR and introns are not as highly conserved, their relative lengths are similar. The comparison of the coding sequences of *Obp7* gene orthologs is discussed in detail in a later section.

Conserved non-coding sequences (CNSs) and putative transcription factor binding sites (TFBSs) identified from comparisons of Anopheles *Obp7* genes

We compared genomic regions including *Obp7* and its flanking sequences between *An. gambiae*, *An. stephensi* and *An. quadriannulatus*. As mentioned before, Figure 2.1 shows the VISTA display of a multiple sequence alignment between the three species. The alignment between *An. gambiae* and *An. quadriannulatus* shows a high level of similarity across the entire length that is possibly due to lack of sufficient divergence time between these two species. Comparison between *An. gambiae* and *An. stephensi* is more informative as it revealed general conservation at the coding regions as well as the lack of conservation in the introns, UTRs and intergenic regions. One exception is an approximate 400 bp conserved non-coding region located 1 kb upstream of the *Obp7* transcription start site (Fig. 2.1, boxed region), which showed 72.3% identity between *An.*

stephensi and *An. gambiae* and 94% identity between *An. gambiae* and *An. quadriannulatus*.

For further analysis, we used ConSite (Sandelin et al., 2004) prediction tool to determine the potential TFBSs in the conserved region. Significant hits common for the three anopheline species are highlighted as shown in Figure 2.6. We found potential binding sites for different types of factors such as C2H2-type zinc finger (*Snail, Broad-complex*), bZIP (*c-Fos*), HMG (*Sox*), Runt/AML-1 (*AML-1*), Forkhead (*HNF3β*/*Foxa2*) in the upstream sequences up to 1kb region from the start codon. There is also a putative *E74A* binding site in the 5' UTR region of the *Obp7* gene. Interestingly, *AML-1* (Daga et al., 1996) is found to be the vertebrate homolog of *lozenge* (*lz*) in *Drosophila,* which is involved in the development of the antennal olfactory sense organs (Kumar and Moses, 1997). In mosquitoes, ecdysone initiates a cascade of gene regulatory events through transcription factors such as *Broad-complex and E74A* (Raikhel et al., 2002; Zhu et al., 2007). It is possible that these factors might be involved in mosquito *Obp7* gene regulation in relation to a blood meal.

Conservation of OBP7 gene and protein structures among divergent mosquitoes

We have identified the OBP7 protein and its corresponding gene from the genome database of a non-anopheline mosquito, *Culex pipiens quinquefasciatus*. The *Ae. aegypti* homolog of OBP7, previously named AaegOBP2 (Ishida et al., 2004), was obtained from NCBI database (AY189224). In this study, we named it as *Aaeg*-OBP7 (or *Aaeg-Obp7* for the gene) for consistency. The deduced amino acid sequences of OBP7 proteins from *An. gambiae*, *An. quadriannulatus*, *An. stephensi*, *Ae. aegypti*, and *Cx. quinquefasciatus* were aligned along with a possible *Drosophila* ortholog, *Dmel*-OBP69a (Fig. 2.7). Mosquito OBP7 proteins show significant amino acid identity as well as positional conservation of six cysteines. The predicted secondary structure of *Aste*-OBP7 includes six α-helices (Fig. 2.7; solid bars above the peptide sequence) consistent with the predicted structures from other insect OBPs (Leal et al., 1999; Sandler et al., 2000; Lartigue et al., 2003, 2004; Kruse et al., 2003; Mohanty et al., 2004; Wogulis et al.,

2006). The N-terminal signal peptide sequence of mosquito OBP7 are less conserved than the rest of the protein.

OBP7 phylogeny reflects mosquito phylogeny

Phylogenetic relationship between OBP7 proteins was reconstructed in the context of additional OBPs to provide comparison and to root the OBP7 clade. Our phylogenetic analysis included OBP7 from different mosquito species as well as selected OBPs from fly and mosquitoes that show similarity to OBP7. A neighbor-joining (NJ) tree is shown in Figure 2.8, which is consistent with minimum evolution and parsimony analyses (not shown). The bootstrap values of all three analyses were labeled in Figure 2.8. Mosquito OBP7 proteins form a monophyletic clade with high bootstrap support. The phylogeny of mosquito OBP7 is congruent with their species phylogeny (Isoe, 2000). The *Drosophila Dmel*-OBP69a and the mosquito OBP7 are sister taxa although the bootstrap values for this grouping are not consistently high (Fig. 2.8).

Purifying selection has been acting on mosquito *Obp7* genes

Pairwise comparisons of mosquito *Obp7* sequences were used to determine the rates of synonymous (d_S) and nonsynonymous (d_N) codon substitutions and the ratio of d_N/d_S was calculated to provide an estimate of the selection pressure on *Obp7* genes (Table 2.2). The coding regions of *Obp7* were included in the analysis except the 5' exon regions, which encode the signal peptides that are highly divergent among OBPs. The ratio of d_N/d_S was much less than 1 for each comparison (0.134-0.202), suggesting that OBP7 is evolving under strong purifying selection for a conserved functional role.

2.5 Discussion

We experimentally defined the gene structure of *Obp7* in *An. stephensi* and determined its expression profile in pre-adult and adult stages. Using quantitative real-time PCR, we showed that the *Aste-Obp7* gene was expressed at significantly higher levels in females than males in all three chemosensory tissues tested. In adult females, *Aste-Obp7* level was the highest in antenna, the primary olfactory organ. *Aste-Obp7*

level in maxillary palp and proboscis, although much less abundant than that of the antenna, was approximately 50-fold higher than what was observed in legs. Thus it is likely that *Aste-Obp7* is involved in female olfactory response. Moreover, the level of *Aste-Obp7* transcript was reduced by more than 10-fold in female maxillary palp and proboscis after blood-feeding, further indicating a possible function in female-biased behavior relevant to blood-feeding. The observation that *Aste-Obp7* level is much less in maxillary palp and proboscis than antenna does not necessarily suggest that *Aste-Obp7* is not biologically important in maxillary palp and proboscis. It could simply be that there are much smaller number of sensilla that express *Aste-Obp7* in the maxillary palp and proboscis. The influence of blood-feeding on *Aste-Obp7* expression is also consistent with the discovery of putative response elements for transcription factors that are regulated by ecdysone, which are discussed below.

In addition to antenna and maxillary palp and proboscis, *Aste-Obp7* is also expressed in legs and wings. The expression profile of *Aste-Obp7* is consistent with the observation of its ortholog in *An. gambiae*. *Agam-Obp7* shows a high level of expression in female olfactory tissues and it is also expressed in body and legs (Li et al., 2005; Biessmann et al., 2005). However, quantitative analysis was not performed on isolated maxillary palp and proboscis in *An. gambiae*. Thus, our observation of a sharp decrease of *Aste-Obp7* mRNA in maxillary palp and proboscis after blood-feeding is new and indicates that further investigation in *An. gambiae* is warranted. *Dmel-Obp69a* is a possible homolog of mosquito *Obp7* (Fig. 2.8). In *Drosophila*, *Dmel-Obp69a* gene promoter constructs failed to drive the expression of a reporter gene in tissues other than the antenna (Galindo and Smith, 2001). *Aste-Obp7* expression is also observed in larvae and pupae stages, consistent with *An. gambiae Obp7* gene expression in these pre-adult stages (Biessmann et al., 2005). *Dmel-Obp69a* also shows a dramatic increase in its expression in dark pupae stage, in which the pigmentation of developing wings occurs soon after the complete development of the olfactory sensilla (Park et al., 2000). Thus, the expression of *Aste-Obp7* in the pre-adult stages may suggest a chemosensory role of this gene, such as locating food sources.

We are also interested in studying the evolution and regulation of genes involved in mosquito olfaction using comparative genomics approaches. Mosquito *Obp7* is a good candidate for such investigations because its higher expression in female antenna indicates a possible olfactory role of this gene. We have focused on three anopheline species, including *An. gambiae*, *An. stephensi*, and *An. quandriannulatus*. *An. gambiae* is the primary vector of malaria in Africa and it serve as the reference genome in our study. *An. stephensi* is the primary malaria vector in Asia and it is becoming a model *Anopheles* species as it is much more amenable to genetic and physiological studies than *An. gambiae*. We included *An. quadriannulatus* to our comparative analysis because it is believed that this species has a different host preference compared to *An. gambiae* and *An. stephensi*. While the last two species show a high degree of anthropophily, the former exhibits a zoophilic behavior (Curtis, 1996; Gibson, 1996).

The comparison between *An. gambiae* and *An. stephensi* appear to be most informative when determining the conservation in the non-coding regions, which may indicate regulatory sequences of the genes. The comparison between *An. gambiae* and *An. quadriannulatus* is less informative due to high degree of conservation observed in the non-coding regions of the genomes. We have detected conserved motifs in all three anopheline species that may provide important information on the regulation of *Obp7* gene. For example, we identified a conserved motif for an *AML-1* homolog, *lozenge* (*lz*), that has been shown to be involved in the development of the antennal olfactory sense organs and regulation of odorant receptor (*Or*) genes in *Drosophila* (Kumar and Moses, 2006; Ray et al., 2007). The conservation of the *AML-1* binding motif in *Obp7* of the three mosquito species suggests that this transcription factor may also be involved in the regulation of *Obp7* genes in mosquitoes. These findings are supported by the fact that *Obp7* is highly expressed in the antenna of both *An. gambiae* and *An. stephensi*. Putative binding sites for *Broad-complex* and *E74A* are also found to be conserved among the *Anopheles* mosquitoes. In mosquitoes, blood-feeding triggers a rapid increase of ecdysone, which initiates a cascade of gene regulatory events through transcription factors such as *Broad-complex and E74A* (Raikhel et al., 2002; Zhu et al., 2007). It is possible that these factors are involved in mosquito *Obp7* gene regulation after a blood

meal. A recent study in *D. melanogaster* has reported the identification of regulatory sequences of *Or85e* and *Or46a* by making constructs with deletion series of upstream sequences of these genes (Ray et al., 2007). Such experiments are needed to test whether the predicted TFBSs are indeed involved in the regulation of *Obp7* gene in mosquitoes.

We also expanded our comparative analysis to include OBP7 protein and gene sequences from *Ae. aegypti* and *Cx. quinquefasciatus*. All mosquito OBP7 orthologs analyzed so far share the hallmark features of insect OBPs. The features include the presence of N-terminal signal peptide, the conservation of six cysteines, and the protein secondary structure, such as six α-helices. Their coding sequences are conserved, showing a 60% to 90% identity. This level of conservation is remarkable considering that *Anopheles* and *Aedes*/*Culex* mosquitoes were separated approximately 145-200 million years ago (MYA) (Krzywinski et al., 2001) and that OBP sequences are generally highly divergent in insects (Vogt, 2005). Pairwise comparisons also indicated a strong purifying selection for OBP7 orthologs, which also supports its functional importance.

In the long term, systematic comparative genomics analyses coupled with functional tests of genes involved in mosquito olfaction will reveal conservation due to functional constraint and divergence underlying behavioral and physiological adaptations. Such information will provide the baseline for future analysis to test the function of predicted regulatory sequences using reporter gene constructs in transgenic mosquitoes. The comparative genomics approach will also likely identify genetic differences between mosquito species. For example, in a recent study employing the same comparative approach, our laboratory has identified a new odorant receptor gene in *An. stephensi* (Miller and Tu, unpublished data). Identification and characterization of the molecular players involved in mosquito olfaction and a better understanding of their regulation is important for the development of novel and more effective disease-control products based on the interruption of odor-mediated host-seeking behaviors.

2.6 Acknowledgements

We thank Dr. Maria V. Sharakhova for help with *in situ* hybridizations; Thomas R. Saunders for rearing *An. stephensi* mosquitoes; and Dr. James Biedler for helpful discussions. We thank Drs. Sharon Hill and Keying Ye for help with statistical analysis. We thank Dr. Brendan Loftus for coordinating BAC sequencing; Dr. Maureen Coetzee for providing *An. quadriannulatus* mosquitoes. This work was supported by the National Institutes of Health Grant AI063252.

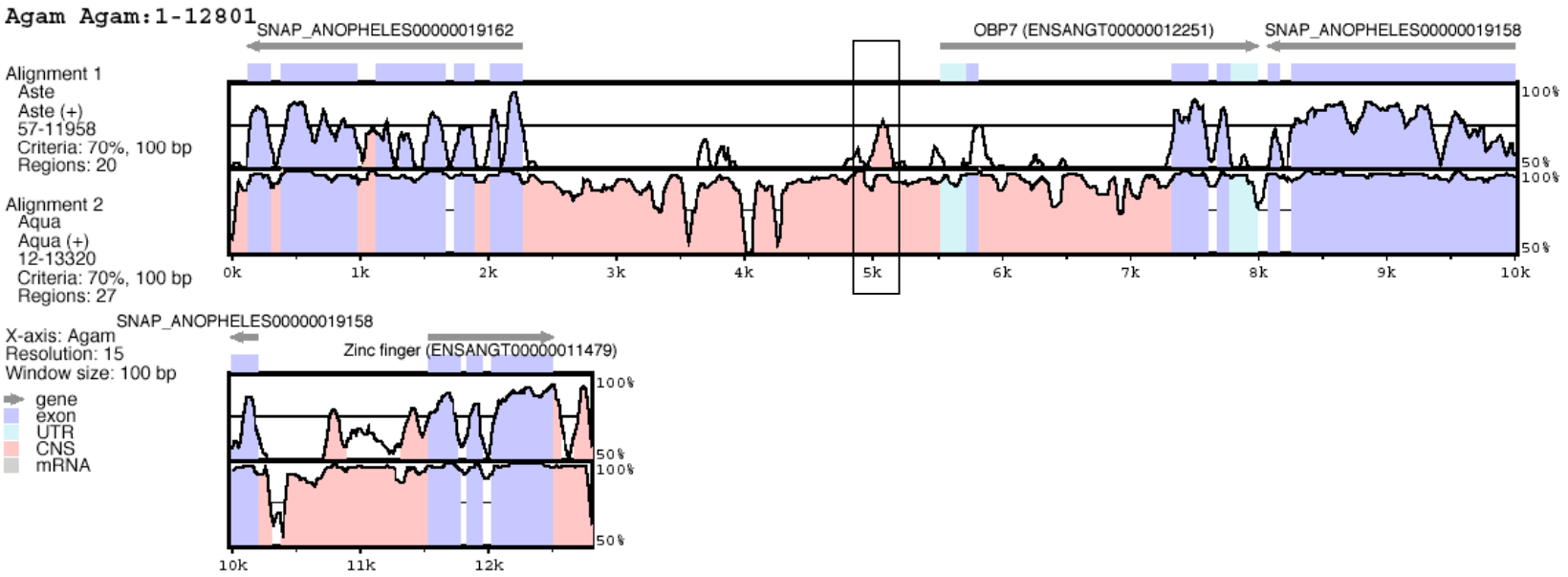

Figure 2.1 VISTA plot that shows the alignment between *An. gambiae* and *An. stephensi* (top bracket) and *An. gambiae* and *An. quadriannulatus* (bottom bracket) genomic segments including the *Obp7* gene and nearby sequences. X-axis shows the relative position of the *An. gambiae* genomic DNA used as the reference genome in the alignment. Y-axis shows the % identity between the compared species. Arrows above the plots correspond to genes or coding sequences annotated in the *An. gambiae* genome according to the Ensembl database. Coding regions are shown in blue, untranslated regions are in light blue, and conserved non-coding sequences are shown in pink. CNSs, conserved non-coding sequences. UTR, untranslated region.

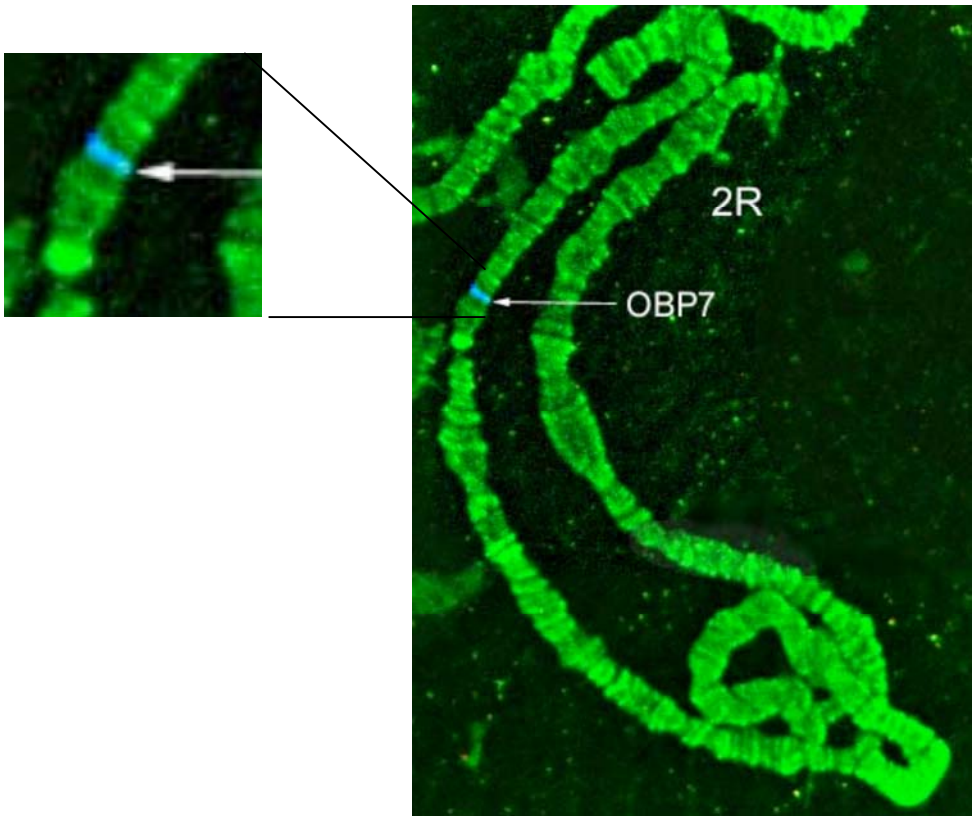

Figure 2.2 Fluorescent *in situ* hybridization performed on the polytene chromosomes of *An. stephensi*. *Aste-Obp7* probe is labeled with Cy5 (blue). The chromosomal segment including the *Aste-Obp7* gene is enlarged as shown in a separate window.

(A)

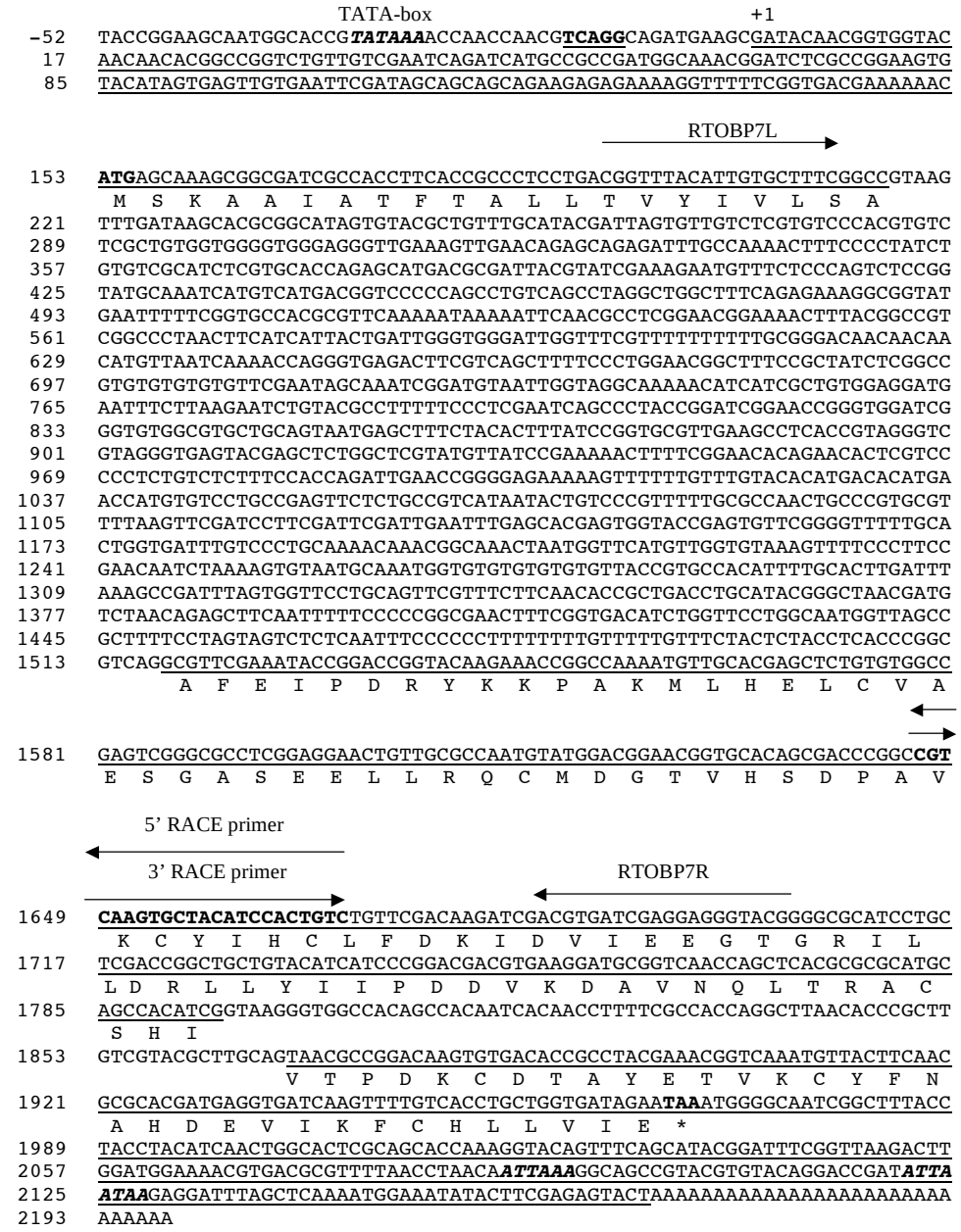

Figure 2.3 Genomic sequence and gene structure of anopheline *Obp7* genes. **(A)** *Aste-Obp7* genomic and cDNA sequences. The *Aste-Obp7* gene contains two introns between the three underlined exons. The deduced amino acid sequence of *Aste-Obp7* is shown below the coding regions. Start (ATG) and stop (TAA) codons are shown in bold. We refer the transcription start site as the first nucleotide (G) of the 5' RACE product and

(B)

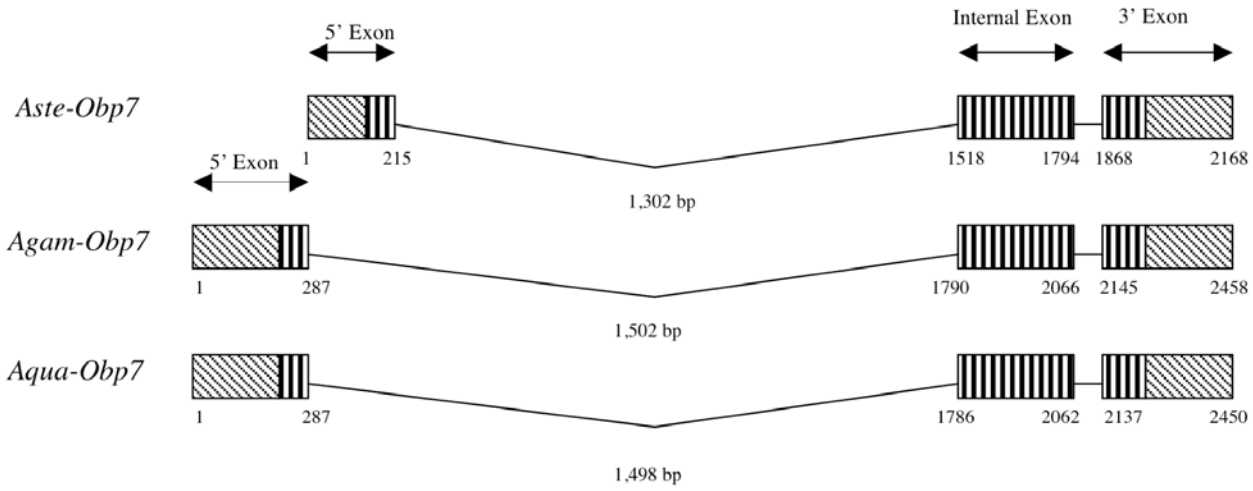

labeled it as +1. A putative initiator sequence, TCAGG, similar to the arthropod initiator consensus is in bold and underlined. See Results section for details. The consensus for TATA-box, TATAAA, and the imperfect polyadenylation signals, AATAA, ATTAAT and ATTAAA are shown in bold italics. The primers used in RT-PCR and RACE reactions are shown by arrows above the corresponding sequences. **(B)** *Aste-Obp7* gene structure is compared with that of *Agam-Obp7* and *Aqua-Obp7* genes. 5' exons, internal exons, and 3' exons are indicated. Boxes with vertical lines indicate ORFs and they are connected with lines that indicate the introns. The 5' and 3' untranslated regions (UTRs) are shown in boxes with upward diagonal lines. Numbers indicate the relative positions of UTRs, ORFs and intronic regions.

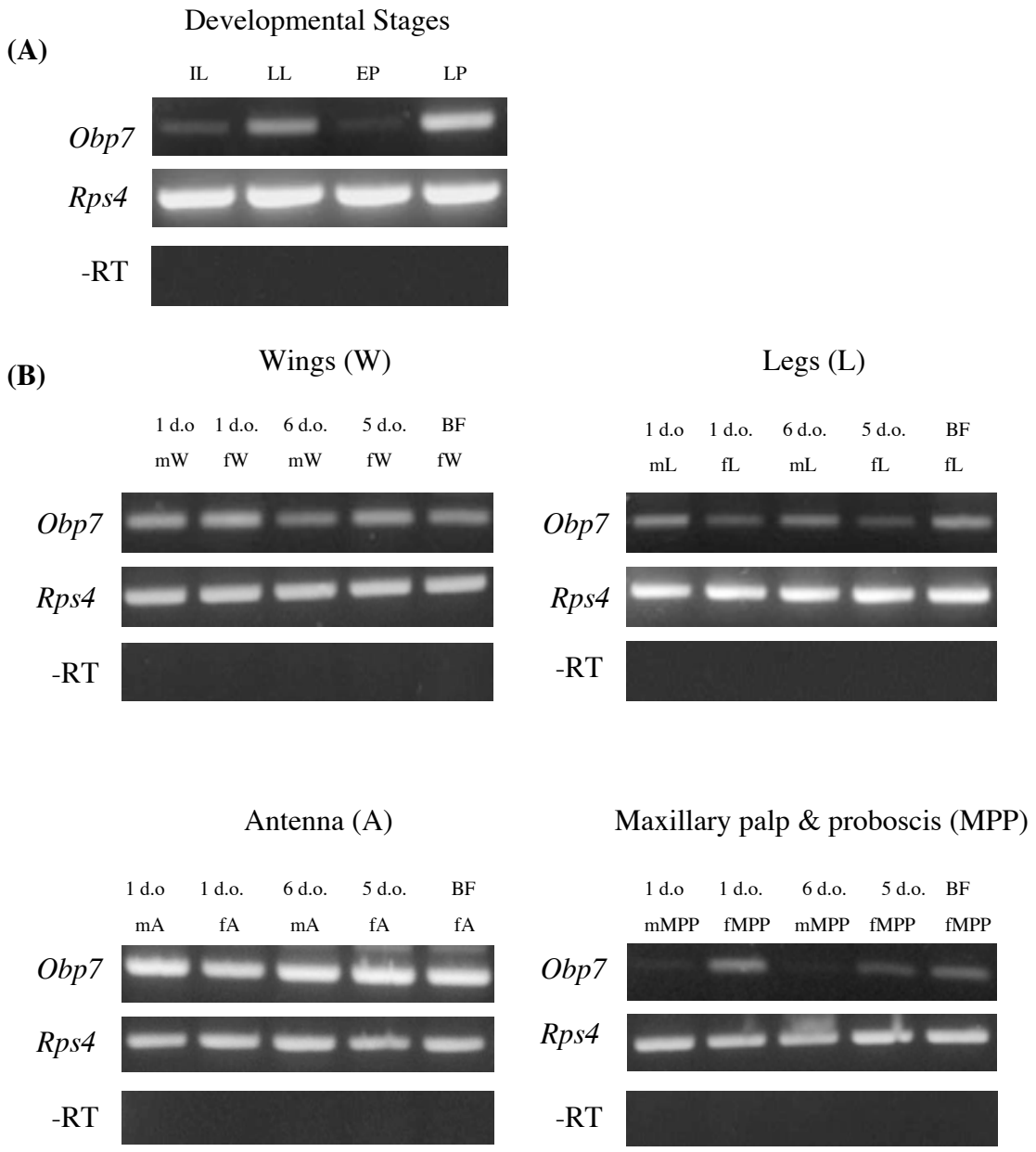

Figure 2.4 Non-quantitative RT-PCR showing the expression profile of *Aste-Obp7* in pre-adult and adult *An. stephensi*. **(A)** Expression in pre-adult stages: first instar larvae (IL), late larvae (LL), early pupae (EP), late pupae (LP). **(B)** Expression in chemosensory tissues of adult *An. stephensi*: adult male antenna (mA), adult female antenna (fA), blood-fed female antenna (BFfA), adult male maxillary palp and proboscis (mMPP), adult female maxillary palp and proboscis (fMPP), blood-fed female maxillary palp and proboscis (BFfMPP), adult male legs (mL), adult female legs (fL), blood-fed female legs

(BFfL), adult male wings (mW), adult female wings (fW), blood-fed female wings (BFfW). *Rps4* internal control gene is used as a positive control. –RT products (negative control without the use of reverse transcriptase) are also shown for each cDNA samples. Days old: d.o. All RT-PCR reactions were done with 35 cycles of amplification. Note that although it appears that the relative level of *Obp7*/*Rps4* in BFfMPP is similar to or slightly higher than fMPP, several RT-PCR reactions at 25 cycles indicated that the relative level of *Obp7*/*Rps4* was lower in BFfMPP than fMPP (not shown).

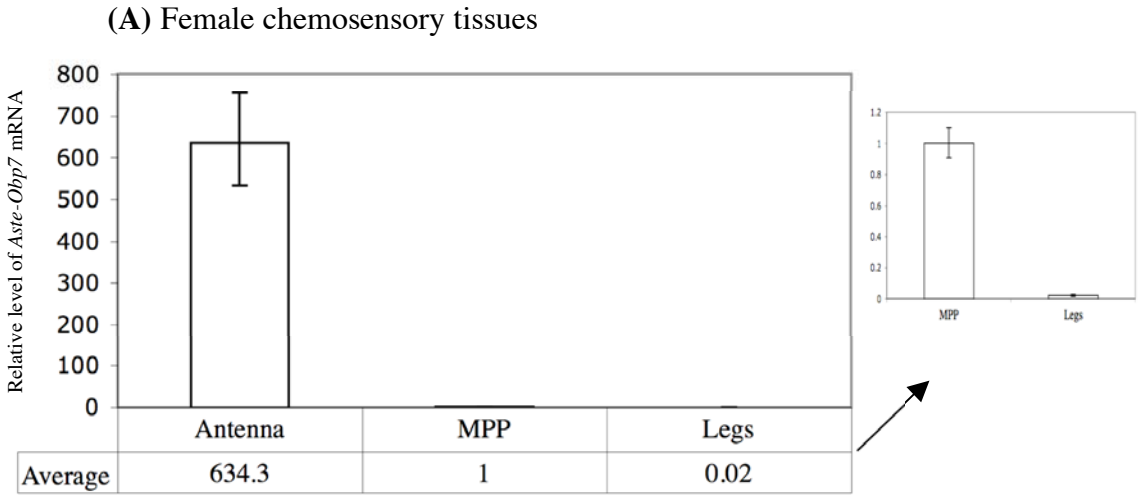

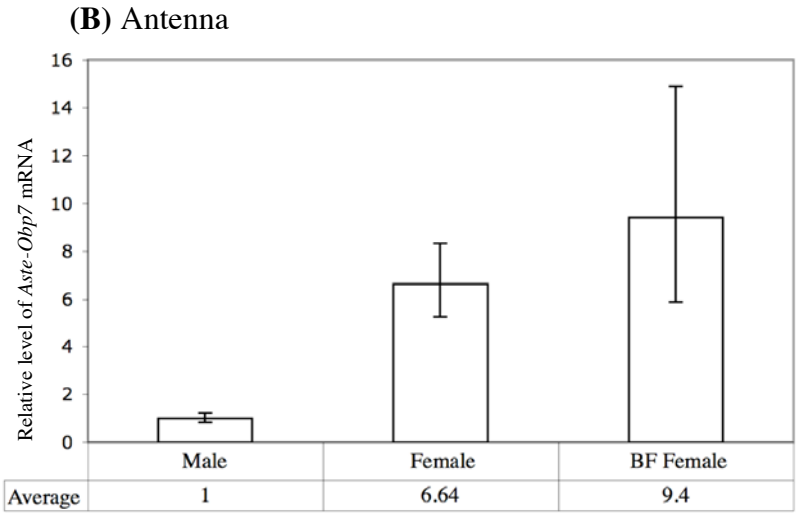

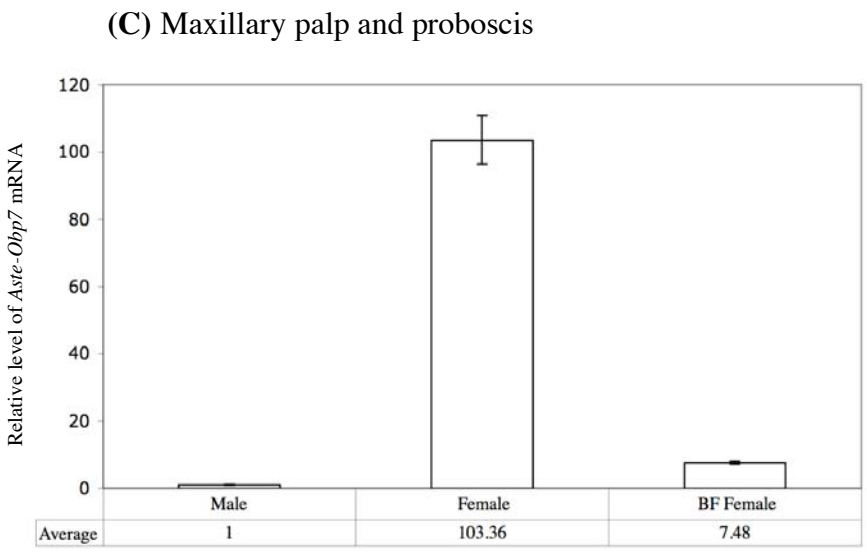

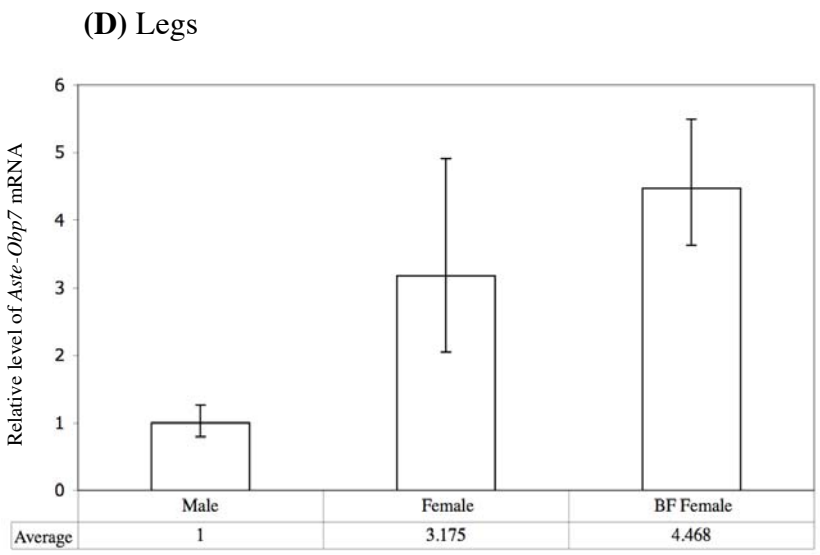

Figure 2.5 Relative amount of the *Obp7* mRNA in adult chemosensory tissues of *An. stephensi*. Y-axis is the relative level of *Aste-Obp7* mRNA as determined by the $2^{-\Delta\Delta CT}$ method. Detailed data analyses are shown in Table 1 and Table S1-S3. All data are presented

as average and a range specified by $2^{-(\Delta\Delta CT+SD)}$ and $2^{-(\Delta\Delta CT-SD)}$, where SD is the standard deviation. **(A)** Comparisons of *Aste-Obp7* expression levels in different female chemosensory tissues. **(B)** Comparisons of *Aste-Obp7* expression levels in the antenna of male, female and blood-fed females. **(C)** Comparisons of *Aste-Obp7* expression levels in the maxillary palp and proboscis of male, female and blood-fed females. **(D)** Comparisons of *Aste-Obp7* expression levels in the legs of male, female and blood-fed females. The relative amount of *Aste-Obp7* is significantly different between different chemosensory tissues in the female (Panel A) as well as in tissues between male, female and blood-fed female (Panels B-D) ($P < 0.05$). The only exception is that the relative amount of *Aste-Obp7* in legs after a blood meal is not significantly different from that of non-blood fed female ($P > 0.05$). In all cases, the calibrator sample for normalization show an average value of 1. See Materials and methods for statistical analysis.

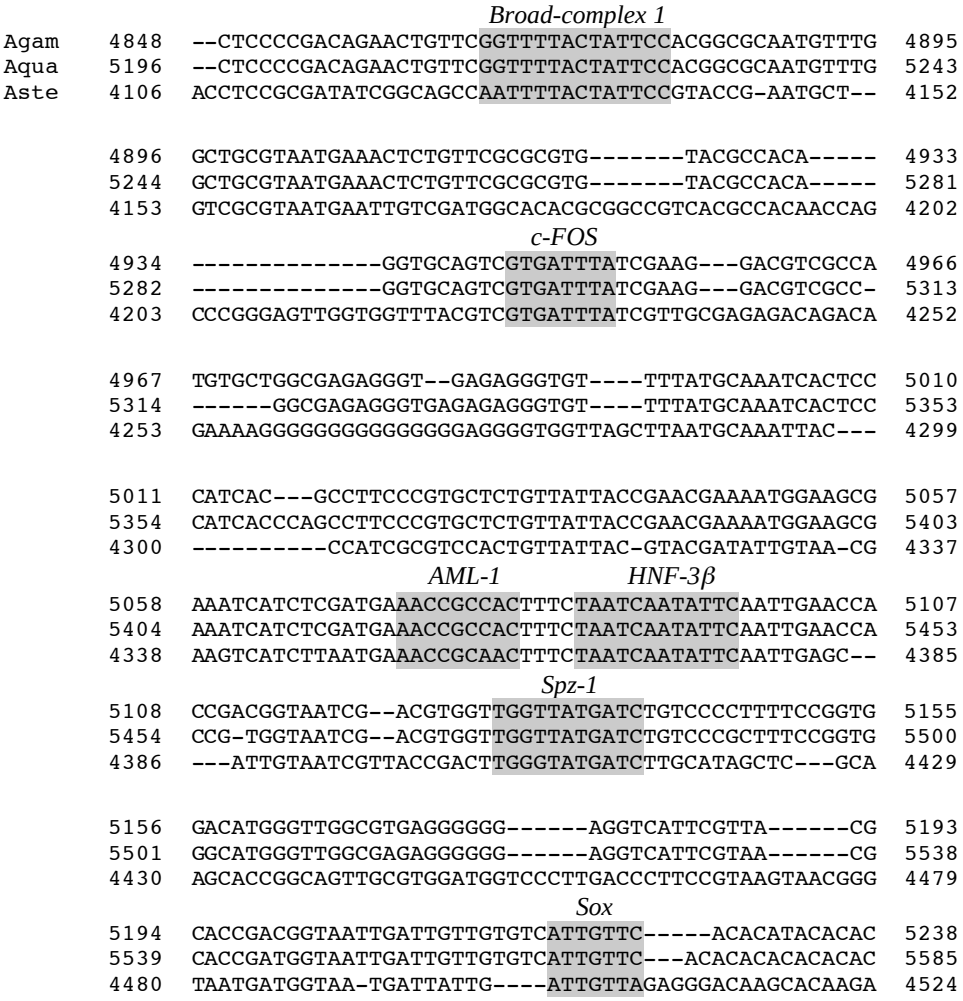

Figure 2.6 VISTA alignment between *An. gambiae*, *An. quadriannulatus* and *An. stephensi* corresponding to 1 kb upstream of *Obp7* transcription start site. Potential TFBSs that are conserved for all species are highlighted in the alignment.

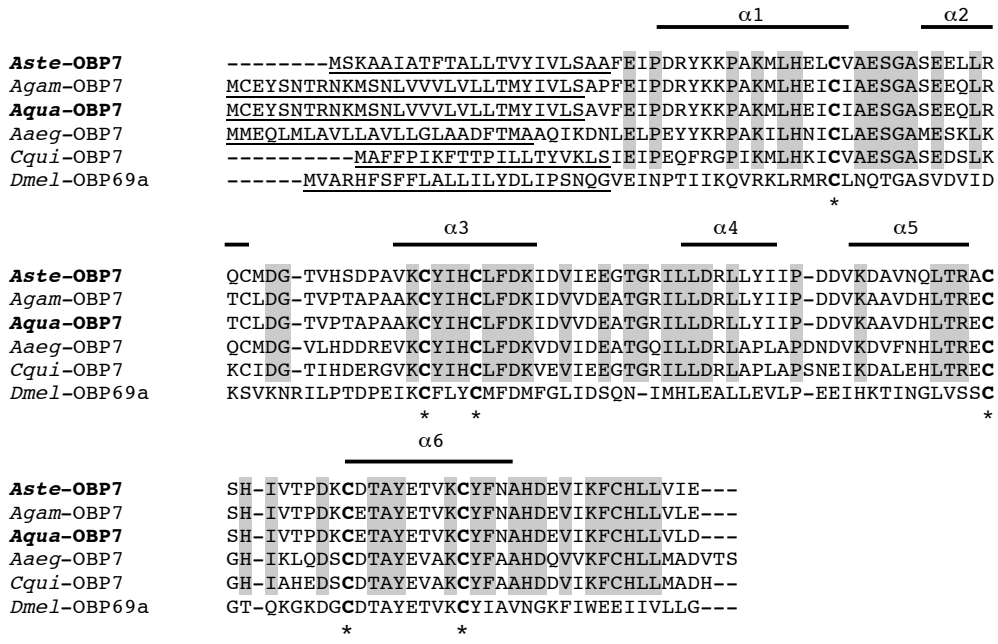

Figure 2.7 Peptide alignment of *Aste*-OBP7 with its mosquito and fly homologues. Mosquito homologues show significant amino acid identity among themselves. Conserved peptides among all mosquitoes are shaded in gray. Conserved six cysteines are shown in bold and indicated with stars. Predicted signal peptides are underlined in the sequences. The α-helices of *Aste*-OBP7 are indicated by solid bars above the amino acid sequence. Species abbreviations are Aste (*Anopheles stephensi*), Agam (*Anopheles gambiae*), Aqua (*Anopheles quadriannulatus),* Aaeg (*Aedes aegypti*), Cqui (*Culex pipiens quinquefasciatus*), and Dmel (*Drosophila melanogaster*).

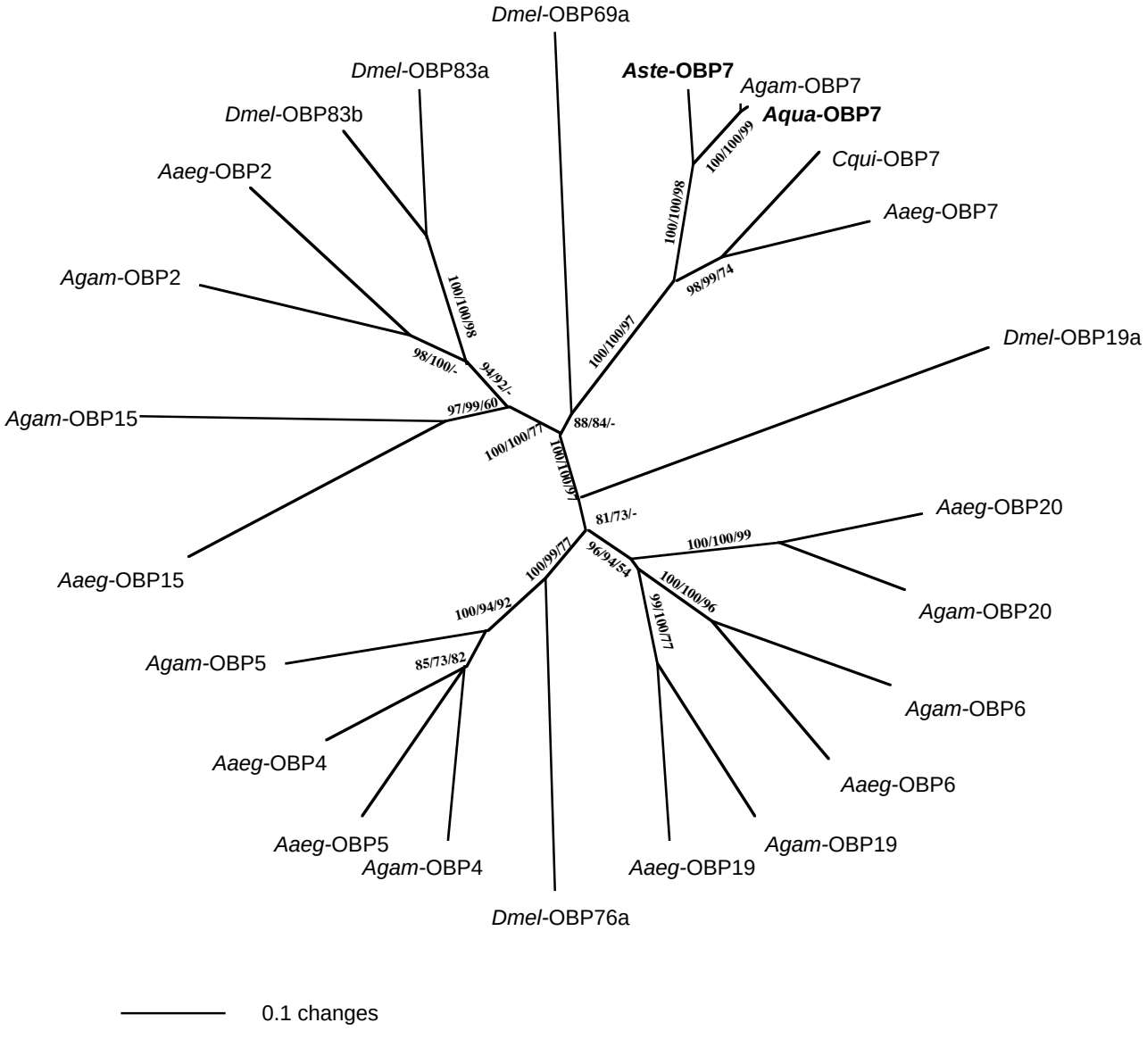

Figure 2.8 Phylogenetic relationship between OBP7 orthologs and representatives of other OBPs. An unrooted tree was constructed using the neighbor-joining algorithm based on the alignment of OBPs with removed signal peptide sequences. Two additional methods, minimum evolution and maximum parsimony, were also used. Bootstrap values are based on 1000 replicates and represented as the first, second and the third numbers above the branches derived from neighbor-joining, minimum evolution and maximum parsimony analyses, respectively. All phylogenetic analyses were performed using PAUP* 4.0b10 package (Swofford, 2002).

Table 2.1 Relative mRNA levels of *Aste-Obp7* in female antenna, maxillary palp and proboscis, and legs

Tissue		*Obp7*C_T	*Rps4*C_T	ΔC_T (*Obp7*C_T-*Rps4*C_T)	$\Delta\Delta C_T$ (ΔC_T-$\Delta C_{Tcalibrator}$	Normalized *Obp7* amount relative to the calibrator, $2^{-\Delta\Delta CT}$
Antenna	replicate1	15.772	18.968	-3.197		
	replicate2	15.546	19.225	-3.68		
	replicate3	16.039	19.681	-3.642		
	Average	15.786 +/- 0.143	19.292 +/- 0.208	-3.506 +/- 0.253	-9.309 +/- 0.253	634.3 (532.26-755.87)
Max. Palp & Proboscis (calibrator)	replicate1	24.108	18.08	6.028		
	replicate2	24.123	18.565	5.557		
	replicate3	24.095	18.272	5.824		
	Average	24.108 +/- 0.008	18.306 +/- 0.14	5.803 +/- 0.14	0 +/- 0.14	1 (0.907-1.1)
Legs	replicate1	30.516	18.913	11.603		
	replicate2	29.923	18.042	11.881		
	replicate3	29.154	18.35	10.805		
	Average	29.864 +/- 0.394	18.435 +/- 0.255	11.43 +/- 0.47	5.627 +/- 0.47	0.02 (0.0146-0.028)

Data presentation is according to Livak and Schmittgen (2001), with average and standard deviation (SD). Data in the final column are presented as average and a range specified by $2^{-(\Delta\Delta CT+SD)}$ and $2^{-(\Delta\Delta CT-SD)}$. All replicates are biological replicates.

Table 2.2 Selection pressure analysis of mosquito *Obp7* coding sequences

Sequences [1]	**ps**	**pn**	**d_S**	**d_N**	**d_N/d_S**	**% aa identity** [2]
Aste-Obp7 vs. *Agam-Obp7*	0.43	0.08	0.65	0.09	0.134	86
Aste-Obp7 vs. *Aqua-Obp7*	0.41	0.09	0.6	0.09	0.152	85
Aste-Obp7 vs. *Aaeg-Obp7*	0.65	0.25	1.53	0.31	0.202	64

1. Manually codon aligned sequences, excluding the signal peptide, of *Obp7* is used to estimate selection pressure by SNAP (http://www.hiv.lanl.gov/content/sequence/SNAP/SNAP.html) (Korber, 2000).

2. The N-terminal signal peptide sequences are not included in the amino acid identity.

ps: The proportion of observed synonymous substitutions

pn: The proportion of observed non-synonymous substitutions

d_S: The Jukes-Cantor correction for multiple hits of ps

d_N: The Jukes-Cantor correction for multiple hits of pn

d_N/d_S: The ratio of non-synonymous to synonymous substitutions

Table S2.1 Relative mRNA level of *Aste-Obp7* in antenna

Tissue		*Obp7*C_T	*Rps4*C_T	ΔC_T (*Obp7*C_T-*Rps4*C_T)	$\Delta\Delta C_T$ (ΔC_T-$\Delta C_{Tcalibrator}$	Normalized *Obp7* amount relative to the calibrator, $2^{-\Delta\Delta CT}$
Male *	replicate1	19.595	19.026	0.57		
	replicate2	18.756	18.5	0.256		
	replicate3	18.721	18.537	0.184		
	replicate4	19.363	19.216	0.147		
	Average	19.109 +/- 0.219	18.82 +/- 0.178	0.289 +/- 0.28	0 +/- 0.28	1 (0.82-1.21)
Female	replicate1	15.8	18.418	-2.618		
	replicate2	16.6	18.865	-2.265		
	replicate3	16.545	19.119	-2.574		
	replicate4	17.071	19.38	-2.309		
	Average	16.504 +/- 0.263	18.945 +/- 0.205	-2.442 +/- 0.33	-2.73 +/- 0.33	6.64 (5.28-8.34)
Blood-fed females	replicate1	18.261	21.375	-3.114		
	replicate2	17.088	19.652	-2.565		
	replicate3	16.101	19.257	-3.156		
	replicate4	17.765	20.704	-2.938		
	Average	17.304 +/- 0.467	20.247 +/- 0.484	-2.943 +/- 0.67	-3.23 +/- 0.67	9.4 (5.89-14.9)

Data presentation is according to Livak and Schmittgen (2001), with average and standard deviation (SD). Data in the final column are presented as average and a range specified by $2^{-(\Delta\Delta CT+SD)}$ and $2^{-(\Delta\Delta CT-SD)}$. All replicates are biological replicates.

* represents the calibrator.

Table S2.2 Relative mRNA level of *Aste-Obp7* in maxillary palp and proboscis

Tissue		*Obp7*C_T	*Rps4*C_T	ΔC_T (*Obp7*C_T-*Rps4*C_T)	$\Delta\Delta C_T$ (ΔC_T-$\Delta C_{Tcalibrator}$	Normalized *Obp7* amount relative to the calibrator, $2^{-\Delta\Delta CT}$
Male *	replicate1	30.887	19.193	11.695		
	replicate2	30.888	19.521	11.367		
	replicate3	29.975	19.561	10.414		
	Average	30.888 +/- 0.0004	19.425 +/- 0.117	11.463 +/- 0.117	0 +/- 0.117	1 (0.92-1.08)
Female	replicate1	23.459	18.417	5.041		
	replicate2	23.272	18.64	4.632		
	replicate3	23.2	18.561	4.64		
	Average	23.31 +/- 0.077	18.539 +/- 0.065	4.77 +/- 0.1	-6.692 +/- 0.1	103.36 (96.47-110.8)
Blood-fed females	replicate1	26.955	18.627	8.329		
	replicate2	27.119	18.415	8.704		
	replicate3	27.185	18.539	8.646		
	Average	27.086 +/- 0.068	18.527 +/- 0.061	8.56 +/- 0.092	-2.903 +/- 0.092	7.48 (7.02-7.97)

Data presentation is according to Livak and Schmittgen (2001), with average and standard deviation (SD). Data in the final column are presented as average and a range specified by $2^{-(\Delta\Delta CT+SD)}$ and $2^{-(\Delta\Delta CT-SD)}$. All replicates are biological replicates.

* represents the calibrator.

Table S2.3 Relative mRNA level of *Aste-Obp7* in legs

Tissue		*Obp7*C_T	*Rps4*C_T	ΔC_T (*Obp7*C_T-*Rps4*C_T)	$\Delta\Delta C_T$ (ΔC_T-$\Delta C_{Tcalibrator}$	Normalized *Obp7* amount relative to the calibrator, $2^{-\Delta\Delta CT}$
Male *	replicate1	31.163	19.976	11.187		
	replicate2	31.598	18.984	12.614		
	replicate3	31.318	19.805	11.514		
	Average	31.36 +/- 0.127	19.588 +/- 0.306	11.771 +/- 0.33	0 +/- 0.33	1 (0.795-1.257)
Female	replicate1	29.66	19.58	10.08		
	replicate2	28.717	18.321	10.396		
	replicate3	28.079	18.241	9.838		
	Average	28.819 +/- 0.459	18.714 +/- 0.433	10.105 +/- 0.63	-1.667 +/- 0.63	3.175 (2.05-4.91)
Blood-fed females	replicate1	28.522	18.371	10.151		
	replicate2	28.384	18.472	9.912		
	replicate3	27.818	19.046	8.772		
	Average	28.241 +/- 0.215	18.63 +/- 0.21	9.612 +/- 0.3	-2.16 +/- 0.3	4.468 (3.63-5.5)

Data presentation is according to Livak and Schmittgen (2001), with average and standard deviation (SD). Data in the final column are presented as average and a range specified by $2^{-(\Delta\Delta CT+SD)}$ and $2^{-(\Delta\Delta CT-SD)}$. All replicates are biological replicates.

* represents the calibrator.

Chapter 3

Identification and characterization of the odorant-binding protein 1 gene from the Asian malaria mosquito, *Anopheles stephensi*

3.1 Abstract

Female mosquitoes transmit major vector-borne infectious diseases, including malaria and yellow fewer. Their ability to transmit diseases is influenced by their host-seeking behavior mediated largely by olfactory cues. Odorant-binding proteins (OBPs) are involved in the transport of odorant molecules through the aqueous lymph to reach the receptors on chemosensory neurons to elicit an olfactory-mediated behavior in insects. Here we report the identification and characterization of *Aste-Obp1*, an *Obp1* gene in *Anopheles stephensi*, the major malaria vector in Asia. Through chromosomal mapping and a comparative genomics approach, we have shown that *Aste-Obp1* gene and *Anopheles gambiae Obp1* gene (*Agam-Obp1*) are orthologous and they share highly similar coding sequences, a few fragments of conserved non-coding sequences (CNSs) that may be involved in gene regulation, and a conserved neighboring gene including odorant receptor 66 gene, *Or66*. We showed that *Aste-Obp1* was expressed in larvae and pupae stages, at a relatively high level in the late pupae. We also determined the expression profile of *Aste-Obp1* in adult mosquito chemosensory organs. The level of *Aste-Obp1* transcript was much higher in the female antenna, the primary olfactory tissue, than that of the other female chemosensory tissues. *Aste-Obp1* level was significantly reduced in maxillary palp and proboscis 24 h after a blood meal. We also found that *Aste-Obp1* was expressed in the gustatory tissues such as legs and wings. Our results indicate that *Aste-Obp1* may have a primary function in olfaction and possibly a secondary role in gustation and it may also be involved in mosquito blood-feeding behavior.

3.2 Introduction

Mosquito behaviors are mediated by both internal and external factors and olfactory cues are undoubtedly the most important external stimuli that affect mosquito behaviors (Takken and Knols, 1999). They include host-seeking (e.g. human or animal) for a blood meal, looking for suitable oviposition sites to lay their eggs, and sugar feeding as the energy source (Takken and Knols, 1999). Behavioral studies on mosquitoes have been mainly focused on two major disease vectors *Anopheles gambiae* and *Aedes aegypti*, which are anthropophilic (i.e. tendency to feed on humans) species. These studies are corroborated with the electrophysiological recordings of the stimulated neurons of olfactory organs (e.g. antennae and maxillary palp) of mosquitoes to determine the chemical nature of host odors as potential attractants or repellents. *Anopheles stephensi* is an important malaria vector in Asia and it is becoming a model Anopheles mosquito for physiological and genetic studies because it is easy to work with and much more amenable to genetic transformation.

Our understanding of insect olfaction has been dramatically improved in recent years as the molecular basis of odor perception is being uncovered. The peripheral events in insect olfaction include major molecular players, which are odorant-binding proteins (OBPs; Vogt and Riddiford, 1981), odorant receptors (ORs; Clyne et al., 1999; Vosshall et al., 1999), and odorant-degrading enzymes (ODEs; Vogt and Riddiford, 1981). OBPs are involved in the transport of odorant molecules through the aqueous lymph to the receptors on chemosensory neurons. With the availability of many insect genomes, OBPs have been identified from various insect orders, including Lepidoptera (moths and butterflies; Vogt and Riddiford, 1981; Vogt et al., 1989); Hymenoptera (bees, wasps, and ants; Danty et al., 1999), Diptera (flies and mosquitoes; Pikielny et al., 1994; Galindo and Smith, 2001; Graham and Davies, 2002; Biessmann et al., 2002; Xu et al., 2003), Coleoptera (beetles; Wojtasek et al., 1998, 1999), and Hemiptera (true bugs; Vogt et al., 1999), suggestive of their important role in insect olfaction. Identification of these proteins in different insect species also revealed general properties of OBPs such that they are small (15-17kDa), water-soluble, extracellular proteins present in the sensillum

lymph of the sensilla. Most insect OBPs share a pattern of six cysteines, whose relative positions are conserved. This has been accepted as the hallmark feature of OBPs in insects.

In Diptera, the genomes of the *D. melanogaster* and *An. gambiae* encode 51 and 57 *Obp* genes, respectively (Hekmat-Scafe et al., 2002; Vogt, 2002; Xu et al., 2003). In *Drosophila*, two physically linked olfactory specific genes, *OS-E* and *OS-F* (*Dmel*-OS-E and *Dmel*-OS-F), show substantial sequence similarity (69% amino acid identity) and share similar expression patterns (McKenna et al., 1994; Hekmat-Scafe et al., 1997). These two genes are expressed in the antenna of adult flies, while their expression has not been determined in other chemosensory tissues (Galindo and Smith, 2000). *An. gambiae Obp1* (henceforth referred as *Agam-Obp1*) are homologous to *Drosophila OS-E*/*OS-F* genes (Biessmann et al., 2002). *Agam-Obp1* was found at high levels in female antenna; although, the expression was observed in maxillary palp and proboscis and headless bodies as well (Biessmann et al., 2002). A later study indicated that *Agam-Obp1* is expressed exclusively in female heads (Li et al., 2005). Interestingly, they found that the expression in female heads was higher in *An. gambiae* compared to that of *An. arabiensis*. Reduction in expression of an olfactory gene after blood meal is regarded as indication of a possible role in host-seeking behavior of female mosquitoes. It was observed that *Obp1* expression was reduced after blood-feeding in a non-quantitative RT-PCR (Justice et al., 2003). More recently, less than 2-fold reduction of mRNA levels of *Obp1* was observed in heads of blood-fed female mosquitoes (Biessmann et al., 2005).

In this study, we cloned, mapped, and characterized the *Obp1* gene in *An. stephensi* (henceforth referred as *Aste-Obp1*). The relative mRNA level of *Aste-Obp1* is significantly higher in the antenna that suggests its primary function in female olfaction. Its expression is also observed in gustatory tissues, such as legs and wings. This may indicate a possibly secondary and broad role of *Aste-Obp1* in mosquito chemoperception. There is also indication that *Aste-Obp1* may be involved in behaviors associated with blood-feeding. Comparative analysis of the genomic segments including *Agam-Obp1* and *Aste-Obp1* genes revealed conserved non-coding sequences (CNSs) that may potentially

be the regulatory sequences of these genes. We have also shown that *Obp1* has been subject to strong purifying selection, consistent with the notion of its functional importance.

3.3 Materials and methods

Mosquitoes

We used the Indian strain of *Anopheles stephensi* in this study. The rearing conditions and the mosquitoes used for tissue collections were previously described (see Chapter 2, pp. 34).

Generation of DIG-labeled, single-stranded DNA (ssDNA) probes and BAC library screening

An amino acid alignment of *Agam*-OBP3 (AF437886; Biessmann et al., 2002), *Agam*-OBP1 (AF4377884; Biessmann et al., 2002), *Dmel*-OS-F (U02542; McKenna et al., 1994), and *Dmel*-OS-E (U02543; McKenna et al., 1994) has been performed using Clustal X (1.8) (Thompson et al., 1997). This alignment was used to design the following degenerate primers; OBP1F1: 5'-TGYTAYATGAAYTGYYTNTTYCA-3' corresponding to the motif CYMVCLFH and OBP1R1: 5'-CARCAYTTRTGNARCCARAANGC -3' corresponding to the motif AFWLHKCW. The genomic DNAs were isolated from individual mosquitoes of *An. stephensi* using DNAzol Genomic DNA Isolation Reagent (MRC, Inc.). Degenerate primers (mentioned above) were used to amplify a 186 bp sequence in the second exon region of the *Aste-Obp1* gene. The PCR product was cloned using pGEM-T-Easy vector systems (Promega, Madison, WI) and confirmed by sequencing (Virginia Bioinformatics Institute, Blacksburg, VA). The plasmid that contains *Obp1* gene sequence was used as a template in an asymmetric PCR using the primer, OBP1probe: 5'-GTTTGTTTCACGAGGCCAAG-3' and DIG-dUTP labeling mixture (Roche Diagnostics, IN) to generate single stranded DNA (ssDNA) probes.

The construction of bacterial chromosome library for *An. stephensi* was previously described (see Chapter 2, pp. 34). This BAC library was screened with the

DIG-labeled ssDNA OBP1 probe under moderate conditions. Hybridization was carried out at 55°C overnight. Two set of washes were performed at 55°C with 2X and 0.5X SSC. The positive clones were colorimetrically detected by following the protocol of Boehringer Mannheim, Biochemicals (Indianapolis, IN).

Sequence analysis of BACs and identification of mosquito OBP1 orthologs

The positive clones from the BAC library screening were determined as discussed before (see Chapter 2; pp. 35). The sequenced BAC contigs from *An. stephensi* that had significant matches to the *Agam-Obp1* gene sequence and the nearby coding sequences were determined by using BLAST (Altschul et al., 1990). The orthologs of OBP1 from *Ae. aegypti*, *Aaeg*-OBP1 (AY189223; Ishida et al., 2004), and from *Cx. quinques-fasciatus*, *Cqui*-OBP1 (AF468212; Ishida et al., 2002) was obtained from GenBank data base.

Fluorescent in situ hybridization analysis of *Aste-Obp1*

MapOBP1L: 5'-GCTCGTGTTTGCTTCAGTTG-3' and MapOBP1R: 5'-ACCC ACACCGATTAAAGTGC-3' primer pair was used to amplify a 1,054 bp genomic sequence of *Aste-Obp1* gene. Gel purified PCR product was used to make probe by labeling 1 μg of DNA with Cy5-AP3-dUTP (GE Healthcare, Little Chalfont, Buckinghamshire, UK) using Random Primers DNA Labeling System (Invitrogen, Carlsbad, CA). Cy5 fluorescently labeled *Obp1* gene probe was used for *in situ* hybridization on the polytene chromosomes of *An. stephensi* prepared from ovarian nurse cells. Chromosome preparation and hybridization were performed as previously described (Sharakhova et al., 2006).

Expression analysis of *Aste-Obp1* by Reverse Transcription-Polymerase Chain Reaction (RT-PCR) and quantitative Real-time PCR

Total RNA was isolated from various *An. stephensi* developmental stages and manually dissected adult tissues using TRIzol reagent (Invitrogen, Carlsbad, CA). Following DNase treatment (Ambion, Inc., Austin, TX), samples were reverse transcribed using Superscript II reverse transcriptase (Invitrogen, Carlsbad, CA) at 42°C

for 1.5 hr followed by heat inactivation at 70°C for 15 minutes. All cDNA synthesis reactions were carried out in the absence of reverse transcriptase (-RT) in parallel for each sample. RT-PCR amplification of cDNAs were carried out using gene specific primers, RTOBP1L: 5'-GTTTGTGTCGGGTTGATGTG-3' and RTOBP1R: 5'-TTGTCGCAAAGATTTTCACC-3' that span the first intron sequence of *Aste-Obp1* gene to control for any genomic DNA contamination (Fig. 3.3A). Accordingly, PCR products with an expected size of 356 bp from cDNA amplification can be differentiated from genomic DNA amplification of a 477 bp product. We used *Aste-Rps4* gene as an internal control in the RT-PCR reactions to determine the integrity of cDNA templates. RT-PCR primer pair; Rps4L: 5'-CACGAGGATGGATGTTGGAC-3' and Rps4R: 5'-ATCAGGCGGAAGTATTCACC-3' amplified a cDNA product of about 260 bp long. The optimal annealing temperature for the RT-PCR was 60°C for both *Aste-Obp1* and *Aste-Rps4* genes. Both reactions were run for a total of 35 cycles. PCR products were analyzed by 2% agarose-gel electrophoresis.

For the quantitative real-time PCR, total RNA from selected tissues were isolated from adult male and female mosquitoes as well as blood-fed females and used for cDNA synthesis as mentioned above. Our analyses included three or more biological replicates for all samples. The real-time PCR was performed using the TaqMan probe-based chemistry with an ABI Prism 7300 Sequence Detection System (SDS) (Applied Biosystems, Foster City, CA). Briefly, for each 25 μl PCR reaction, 2 μl of cDNA was used with 9.25 μl nuclease-free water, 12.5 μl 2 X TaqMan Universal PCR Master Mix (Applied Biosystems, Foster City, CA), and 1.25 μl 20 X assay mix designed by ABI. The assay mixture for *Obp1* and the control gene consists of 5'FAM labeled, non-fluorescent quencher (NFQ) probes and the primer pairs designed for the corresponding sequences below:

*Aste-Obp1*primerF: 5'- AACCGCTGCACGATATTTGC-3'
*Aste-Obp1*primerR: 5'- GGATCTCTTCGTCGCTGAACTTTT-3'
*Aste-Obp1*probe: 5'FAM- ATCGCTTCCTCAGTAACAC -NFQ
*Aste-Rps4*primerF: 5'- TTCGCACCGATCCGAACTAC-3'

*Aste-Rps4*primerR: 5'- GAAGTATTCACCGGTCTTGTGGAT-3'
*Aste-Rps4*probe: 5'FAM- TTGATCACATCCATGAAACC -NFQ

The thermocycler program consisted of 50°C for 2 min, 95°C for 10 min, 40 cycles of 95°C for 15 sec and 60°C for 1 min. Since the relative mRNA amount of *Aste-Obp1* is being determined, parallel TaqMan assays were done for the control gene, *Aste-Rps4,* as well.

Validation of the amplification efficiencies for the qRT-PCR reactions was determined as previously described (Chapter 2, pp. 38). All TaqMan PCR data were analyzed using SDS Software based on the comparative method ($\Delta\Delta C_T$) (Livak and Schmittgen, 2001). Briefly, for every sample, an amplification plot was generated showing the reporter dye fluorescence (ΔRn) at each PCR cycle. For each amplification, a threshold cycle (C_T) was calculated, representing the cycle number at which the fluorescence passes the threshold, giving the relative amounts of *Aste-Obp1* and *Aste-Rps4* for each cDNA sample. The difference between these two values was calculated, giving the ΔC_T value. Then, the ΔC_T value of each sample has been normalized to that of the calibrator sample (5-day-old female maxillary palp and proboscis is selected for comparison of female tissues, Table 3.1; 6-day-old male is selected for male, female and blood-fed female tissue comparisons, Tables 3.2-3.4) resulting in the determination of $\Delta\Delta C_T$ value. And finally, $2^{-\Delta\Delta CT}$ values were calculated to estimate the fold variation in the mRNA levels of *Aste-Obp1* in different samples.

Statistical analysis of real-time PCR data was performed using One-way ANOVA with Tukey's post test using GraphPad Prism version 3.00 for Windows (GraphPad Software, San Diego, CA). Significance in treatments is assumed if $P < 0.05$ is obtained in the appropriate test.

Rapid Amplification of cDNA Ends (RACE)

5' and 3' RACE were performed using the BD Smart RACE cDNA amplification kit (BD Biosciences Clontech, Palo Alto, CA) according to the manufacturers

instructions. After the first strand cDNA synthesis, PCR was performed using the adapter primer and the gene specific primers, 5'RACE-OBP1: 5'-TTCATCGCCTCCAGCAAC TC-3' and 3'RACE-OBP1: 5'-GGCAAACGATGCCTCTATCC-3' (Fig. 3.3A). The PCR products were cloned into pGEM-T-Easy vector (Promega, Madison, WI) and confirmed by sequencing (Virginia Bioinformatics Institute, Blacksburg, VA).

Sequence analyses of OBP1

The complete gene structure of *Aste-Obp1* is confirmed by RT-PCR and RACE. The peptide alignment of OBP1 orthologs was generated by using Clustal X (1.8) (Thompson et al., 1997). The following parameters were used for the alignment: pairwise gap penalty (open=35, extension=0.75), multiple gap penalty (open=15, extension=0.3). N-terminal signal peptide sequences of OBP1 were predicted by the SignalP V 3.0 program (Bendtsen et al., 2004; http://www.cbs.dtu.dk/services/SignalP/). Putative α-helical regions were predicted using Jpred (Cuff and Barton, 1999; http://www.compbio.dundee.ac.uk/~www-jpred/).

Pair-wise comparison and prediction of transcription factor binding sites (TFBSs)

The genome comparisons to identify conservation in coding and non-coding regions of *Obp1* from *An. stephensi* and *An. gambiae* were established by using MLAGAN (Multi-LAGAN) multiple alignment program (Brudno et al., 2003; http://genome.lbl.gov/vista/lagan/submit.shtml). The cut-off for sequence conservation is 75% over 100 bp. The *An. gambiae* genome annotation (Holt et al., 2002) is used to determine the coding regions in the alignment. The alignment was visualized by VISTA (Mayor et al., 2000), which gives a VISTA plot output calculating the percent identity over the window at each base pair. The X-axis shows the relative position of the *An. gambiae* genomic DNA, and the Y-axis shows the % identity between *An. stephensi* and *An. gambiae* sequences. ConSite program (Sandelin et al., 2004; http://asp.ii.uib.no:8090/cgi-bin/CONSITE/consite/) is used to predict potential transcription factor binding sites for the 5' upstream sequences of *Obp1*, up to 1 kb region from the translation start site, of the aligned sequences between *An. gambiae* and *An. stephensi*. The cut-off for sequence conservation is 74%, and transcription factor score threshold is set to 80%.

d_N and d_S calculations

Synonymous and nonsynonymous mutations were analyzed by the method of Nei and Gojobori, 1986. SNAP program (Synonymous/Nonsynonymous Analysis Program; http://www.hiv.lanl.gov/content/sequence/SNAP/SNAP.html) (Korber, 2000) was used to calculate d_N, d_S and to determine d_N/d_S ratios for mosquito OBP1 orthologs.

3.4 Results

Identification and chromosomal mapping of *Obp1* in *An. stephensi*

Previously annotated *Obp1* gene (AY146721) and *Obp17* gene (AY146723) in *An. gambiae* are nearly identical to each other. Currently, the updated Ensembl annotation shows only a single gene with two possible transcripts: Q8I8TO_ANOGA (AY146721) and OBP17 (AY146723), the former of which codes for the *Agam*-OBP1 peptide (Biessmann et al., 2002). Accordingly, we used the gene sequence of *Agam-Obp1* (AY146721) to construct an *Obp1* gene probe to screen a bacterial artificial chromosome (BAC) library derived from *An. stephensi* genomic DNA (see Materials and methods). Three positive clones were identified from a total of 9,216 clones screened, which represents ~ 5-fold coverage of the genome, assuming that the genome size of *An. stephensi* is approximately 240 Mbp (Rai and Black, 1999). One positive BAC clone was sequenced, which produced 2 contigs. A single *Aste-Obp1* was identified in the 98.5 kb contig. We mapped the *Aste-Obp1 gene* on the region corresponding to 17A of the *An. stephensi* chromosomal arm 2R of the ovarian chromosomes of *An. stephensi* by fluorescent *in situ* hybridization analysis (Fig. 3.1). This region is homologous to *An. gambiae* region 14E of arm 2R, the region in which *Agam-Obp1* resides (http://www.ensembl.org/Anopheles_gambiae/index.html; Sharakhova et al., 2006). Thus *Agam-Obp1* and *Aste-Obp1* are orthologous. Our mapping and BAC sequencing results indicate that *Aste-Obp1* gene exits as a single copy gene in the *An. stephensi* genome.

Comparison of genomic sequences of *An. gambiae* and *An. stephensi* including *Obp1* gene

Figure 3.2A shows the VISTA display of the sequence alignment between *An. gambiae* and *An. stephensi* for genomic region including *Obp1* gene and nearby sequences. Overall, it is found that the coding sequences of the *Obp1* genes as well as the order of neighboring genes are conserved between the two species. A G-protein coupled odorant receptor (*Or*) gene, similar to *An. gambiae Or66*, is identified approximately 10 kb downstream of *Aste-Obp1*.

The VISTA alignment revealed high level of conservation in the coding regions of *Obp1* gene, ranging between 77% to 95% identity at the nucleotide level. Additionally, there are a few conserved non-coding sequences (CNSs) at the 5' and 3' flanking regions as well as in an intron (Fig. 3.2A, pink peaks). These regions exhibited >75% identity between the two species. In order to determine whether these regions contain any transcription factor binding sites (TFBSs), we used ConSite prediction tool (Sandelin et al., 2004) and found significant hits for *RXR-VDR* (a nuclear receptor factor) and HMG (*Sox*) (Fig. 3.2B, i) and *Broad-complex* (Fig. 3.2B, ii) binding sites upstream of *Obp1* genes. Highly conserved motifs have also been observed in the alignment that did not show any significant hits for a known transcription factor in the database.

Characterization of the *Aste-Obp1* gene structure

The alignment shown in Figure 3.2A suggests a good conservation in the coding sequences of *Aste-Obp1* and *Agam-Obp1* genes. The actual gene structure of *Aste-Obp1* is further determined by experimental methods. 5' and 3' RACE were performed to determine the full length *Aste-Obp1* transcript using a total RNA sample isolated from whole female *An. stephensi* mosquitoes. Unfortunately, our attempts for 5'RACE have failed and thus we could not experimentally confirm the transcription start site for *Aste-Obp1* gene. However, the observed conservation between *Agam-Obp1* and *Aste-Obp1* genes indicates potential TATA box and transcription start site. A TCAGT sequence (Fig. 3.3A, boldface and italicized), which is similar to the arthropod initiator consensus TCAGT (Cherbas and Cherbas, 1993), is observed 69 nucleotides upstream of the

translation initiation codon, ATG. A consensus for TATA-box is located 101 bp upstream of the ATG as well (Fig. 3.3A; boldface and boxed). The 3' end of the *Aste-Obp1* transcript was determined by 3' RACE, which produced a cDNA product with an expected poly(dA) tail, 422 bp untranslated region (UTR) and a removed intron. RT-PCR was also performed using primers spanning the first predicted intron (Fig. 3.3A). Comparing sequences of the RT-PCR, 3'RACE products and the BAC clone confirmed the existence the first and second introns of 121 bp and 461 bp in length, respectively. Overall, we characterized the entire open reading frame (ORF) of *Aste-Obp1* interrupted by two introns as shown in Figure 3.3A. The coding region is 432 bp long encoding a 144 amino acid peptide. The overall gene structure of *Aste-Obp1* is highly similar to that of *Agam-Obp1* (Fig. 3.3B) as annotated in Ensembl database (http://www.ensembl.org/ Anopheles_ gambiae/index.html).

Expression profile of *Aste-Obp1*

The expression profile of *Aste-Obp1* was initially examined by non-quantitative RT-PCR. We found that a higher level of *Aste-Obp1* expression in late pupae stage compared to other pre-adult stages (Fig. 3.4A). A weak or no expression is observed for late larvae and early pupae stages. We also performed RT-PCR using different olfactory and gustatory tissues from 1-day-old and 5 to 6-days-old adults of both sexes as well as females 24 h after a blood meal. Broad distribution of *Aste-Obp1* gene expression in most of the chemosensory tissues of mosquitoes is observed (Fig. 3.4B, C). It is found that *Aste-Obp1* is expressed in mosquito antenna, maxillary palp and proboscis, and mosquito body parts such as legs and wings. *Aste-Obp1* expression appears to be reduced in maxillary palp and proboscis in females after a blood meal (Fig. 3.4C). Either very weak or no expression was observed in body samples devoid of head and appendages (not shown). These reactions were performed using 35 cycles of PCR reactions and do not give any indication of the relative amount of *Aste-Obp1* in these tissues.

Quantitative real-time PCR was performed to compare the *Aste-Obp1* mRNA levels in the antenna, maxillary palp and proboscis, and legs from adult females. We observed a significantly higher (~900-fold) expression in female antenna compared to

that of the maxillary palp and proboscis (Table 3.1). Very low amount of *Aste-Obp1* is observed in female legs, approximately 15-fold lower than in maxillary palp and proboscis (Table 3.1). These results clearly show that *Aste-Obp1* is much more abundantly expressed in the primary olfactory organ, the antenna, of the *An. stephensi* mosquitoes compared to the other chemosensory tissues. Although the expression level in maxillary palp and proboscis is low, the level is significant and likely biologically relevant.

We also determined expression levels of *Aste-Obp1* in different tissues between males, females and blood-fed females. We observed a significantly higher expression of *Aste-Obp1* in the female antenna (~7-fold) and maxillary palp and proboscis (~80-fold) than those in males (Tables 3.2 and 3.3). The expression in legs is not significantly different between male and females (Table 3.4). However, the expression in legs is increased by > 2-fold in blood-fed females (Table 3.4). Given the low level of transcripts in the legs, it is unclear whether the difference before and after blood-feeding is biologically relevant. Blood meal did not affect the mRNA level of *Aste-Obp1* in the antennae of female mosquitoes (Table 3.2). However, we observed a significant reduction (~20-fold) of *Aste-Obp1* gene expression in maxillary palp and proboscis of blood-fed females compared to that of in females before a blood meal (Table 3.3).

Conservation of OBP1 protein structures among divergent mosquito species

The deduced amino acid sequences of OBP1 from *An. gambiae*, *An. stephensi*, *Ae. aegypti*, and *Cx. quinquefasciatus* were aligned along with the *D. melanogaster* OBPs OS-E and OS-F (Fig. 3.5). Mosquito OBP1 show significant amino acid identity, ranging between 76% to 86% identity, as well as positional conservation of six cysteines. The predicted secondary structure of *Aste*-OBP1 includes six α-helices (Fig. 3.5; solid bars above the peptide sequence) consistent with the predicted structures from other insect OBPs (Leal et al., 1999; Sandler et al., 2000; Lartigue et al., 2003, 2004; Kruse et al., 2003; Mohanty et al., 2004; Wogulis et al., 2006). The N-terminal signal peptide sequence (Fig. 3.5, underlined) of mosquito OBP1 are less conserved than the rest of the protein.

Selective pressure acting on *Obp1* genes

Pairwise comparisons of mosquito OBP1 sequences were used to determine the rates of synonymous (d_S) and nonsynonymous (d_N) codon substitutions and the ratio of d_N/d_S was calculated to provide an estimate of the selection pressure on *Obp1* genes in *An. gambiae and An. stephensi*. The d_N/d_S ratio is determined as 0.1, suggesting that OBP1 is evolving under strong purifying selection for a conserved functional role in mosquitoes.

3.5 Discussion

In this study, we report identification and characterization of an *Obp* gene form the Asian malaria mosquito *Anopheles stephensi* in an effort to understand common molecular aspects of olfaction in mosquitoes. We named it *Aste*-OBP1 because it shows high sequence identity (86% amino acid identity) to *Agam*-OBP1 (Biessmann et al., 2002). We determined the expression profile of *Aste-Obp1* in different chemosensory tissues using quantitative real-time PCR. Our results clearly showed that *Aste-Obp1* gene is expressed at significantly higher levels in female olfactory organs, such as antenna and maxillary palp and proboscis, when compared to those of male mosquitoes. The expression of *Obp1* in legs was quite low and did not differ significantly between females and males. These results indicate that *Obp1* gene is likely to play a role in female olfactory perception. *Aste-Obp1* expression is reduced by approximately 20-fold in female maxillary palp and proboscis 24 h after blood-feeding, indicating a possible involvement in blood-feeding related behavior. We did not observe any significant change in its antennal expression after blood-feeding. Additionally, much more abundant expression of *Aste-Obp1* in female antenna is determined when compared to that of female maxillary palp and proboscis, which further supports its olfactory role. *Agam-Obp1* also has an expression profile mostly consistent with our data. For example, a microarray data indicates a ~3-fold higher expression of *Agam-Obp1* in female antenna compared to that of males (Biessmann et al., 2005). A semi-quantitative measurement of *Agam-Obp1* expression in head tissues of females suggests a lower expression after a blood meal (Justice et al., 2003). However, we did not observe significant reduction in

antenna, which is the predominant source of *Aste-Obp1* transcripts in the head. The *Drosophila* ortholog of *Obp1* gene is also expressed exclusively in the antennal sensilla. The common antennal expression of *Obp1* as well as high sequence identity observed in divergent insect species may suggest that *Obp1* orthologs undergone little structural changes during the evolution due to functional constraint in odor perception. In fact, we determined a strong purifying selection among anopheline *Obp1* genes, supporting its conserved functional role in mosquito olfaction-mediated behavior.

A better understanding of the function of OBPs may come from the structural studies of different OBPs in various insect species. In mosquitoes, the crystal structure of OBP1 in *An. gambiae* has been determined (Wogulis et al., 2006), representing the only known OBP structure from mosquito species. This protein is crystallized as a dimer with a unique binding pocket, consisting of a single tunnel running through both subunits. It has been found that *Agam*-OBP1 undergoes a pH dependent conformational change, similar to the ligand binding and releasing mechanism proposed for PBP in *B. mori* (*Bmor*PBP) (Horst et al., 2001). It is found that at neutral pH, *Bmor*PBP binds its ligand bombykol at the hydrophobic binding pocket and the flexible N-terminus part of the *Bmor*PBP helps to close the bombykol-PBP complex (Sandler et al., 2000). When the pH drops, it undergoes a conformational change in which the C-terminal end forms an additional α-helix and fills the ligand binding pocket and thus releasing the bombykol to reach to odorant receptor in the membrane (Horst et al., 2001). In *Agam*-OBP1, the C-terminus is too short to form a helix that fits in the binding pocket. Instead, its interaction with the N-terminus will be disrupted at a lower pH leaving the binding pocket open to the solvent. This would eventually decrease the binding affinity of the protein for its ligand and thus releasing it. The similar pH dependent conformational change in the ligand binding and releasing roles for the two distantly related OBPs, *Bmor*PBP and *Agam*-OBP1, would indicate a common mechanism of odorant transport in insect OBPs. In this notion, characterization and determination of mosquito OBP1 orthologs would provide invaluable data for performing homology modeling using the known structure of *Agam*-OBP1 and determine motifs involved in ligand binding and release as well as any unique sites influencing functional differences involved in odor discrimination. The

alignment of *Aste*-OBP1 with *Agam*-OBP1 and other mosquito orthologs as well as that of *Drosophila* showed a high level of conservation in the primary sequences as well as the determined secondary structures that are important for the overall protein function (Fig. 3.5). With the known structure of *Agam*-OBP1, a comparison between the protein structure and its function can be made in these two mosquito species. Thus, we believe that the primary and secondary structure of *Aste*-OBP1 will provide further insights into the function of this gene in mosquitoes.

A comparative approach was also used to determine the regulatory elements of *Obp1* gene in *An. gambiae* and *An. stephensi* by determining the conservation in the non-coding regions. Previously, by using a similar approach, we have determined conserved motifs in the 5' upstream sequences of *Obp7* gene in three anopheline mosquitoes, including *An. gambiae*, *An. stephensi* and *An. quadriannulatus* (see Chapter 2). In the 5' upstream regions of *Obp1* genes, we observed conserved binding sites for *Broad-complex* and *RXR-VDR* transcription factors. However, much of the conservation in other regions did not give any hits for a known transcription factor. Thus, it is possible that our results identified novel binding sites that may likely play a role in *Obp* gene regulation in mosquitoes. Such comparative analysis will identify potential regulatory elements of these genes, which can be experimentally tested for their function using reporter gene constructs in transgenic mosquitoes. Comparative genomics also helped us determining conserved coding sequences in the nearby regions of *Obp1* gene in *An. stephensi*. We have identified an odorant receptor gene ortholog of the *An. gambiae Or66*. This *Or* gene is also found in the *Drosophila* as *Or83c*, that is expressed only in the antennal olfactory sensory neurons (Vosshall et al., 2000). Besides, *Or83c* is also located in close proximity to *Drosophila OS-E/OS-F* genes (Hekmat-Scafe et al., 2002). It would be interesting to know whether the close chromosomal localization of *Obp1* and *Or66* genes in these species has any impact in the regulation of these genes to carry out its function.

The identification of *Obp1* gene in *An. stephensi*, a species in the same subgenus as *An. gambiae*, the complete and tissue specific characterization of its expression profile as well as comparative genomics between *An. gambiae* provide the basis for

understanding the possible function of *Obp1* gene in mosquitoes. Further studies revealing its structure and regulation are needed for a better knowledge on whether and how these genes influence the olfactory-mediated behavior of mosquitoes.

3.6 Acknowledgements

We thank Dr. Maria V. Sharakhova for help with *in situ* hybridizations; Thomas R. Saunders for rearing *An. stephensi* mosquitoes. We also thank Brendan Loftus for coordinating the sequencing of the BAC clone. This work was supported by the National Institutes of Health Grant AI063252.

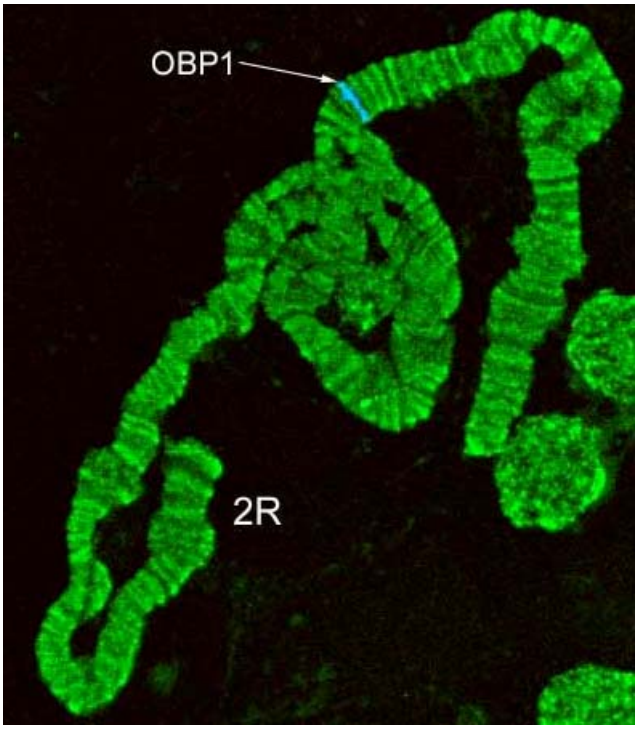

Figure 3.1 Mapping of *Aste-Obp1* on the polytene chromosomes of *An. stephensi* by fluorescent *in situ* hybridization. *Aste-Obp1* is labeled with Cy5 (blue).

(A)

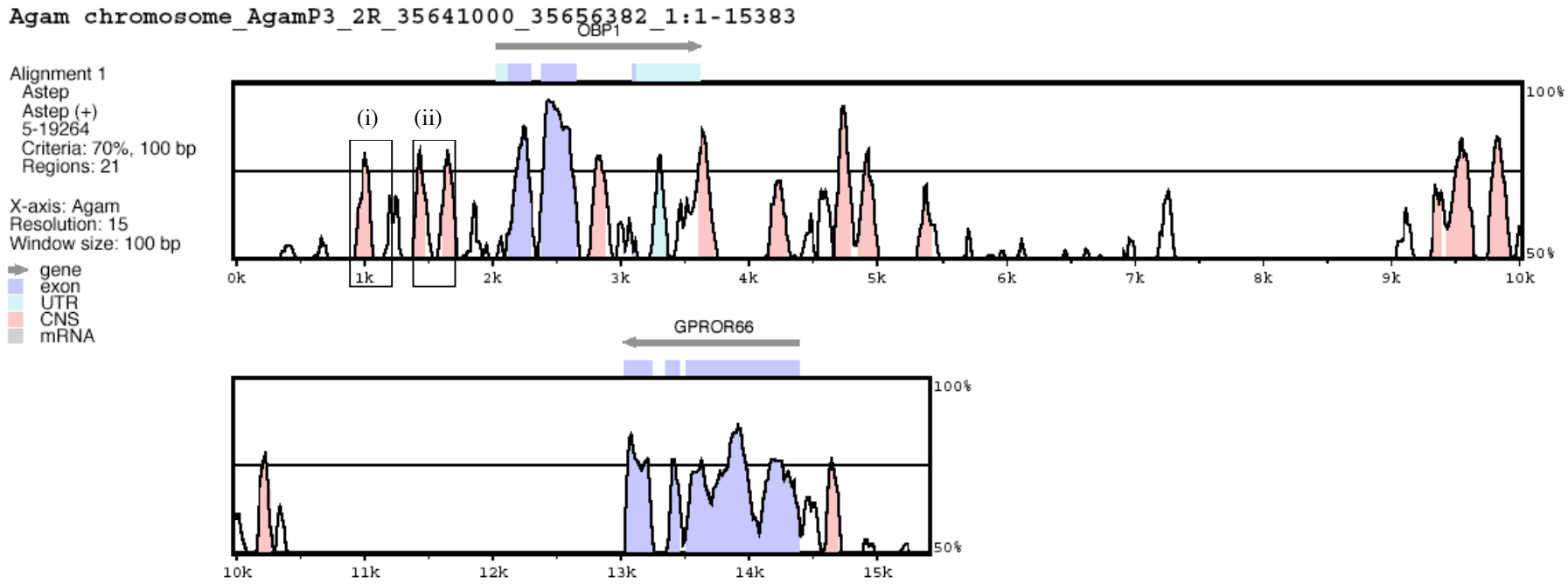

(B)

(i)

```
                                  Sox                 RXR-VDR
Agam   1015  GTGGAGCGCATAATTATTTCTACCCATGAACTTAATTACACCGCCACCCATGCGGTTGAT  1074
       >>>>  ||||||||||||||||| |||||||||||||||| ||||         ||||  ||   <<<<
Aste   1038  CGAAGGCGCATAATTATTTCTAGCCATGAACTTAATTACTCCGC-------ACGGTCGAC  1090
```

Figure 3.2 Pair-wise comparison between *An. gambiae* and *An. stephensi*. **(A)** VISTA plot that shows the alignment between *An. gambiae* and *An. stephensi* genomic segments including the *Obp1* gene and the nearby coding sequences. X-axis shows the relative position of the *An. gambiae* genomic DNA used as the reference genome in the alignment. Y-axis shows the % identity between the

(ii)

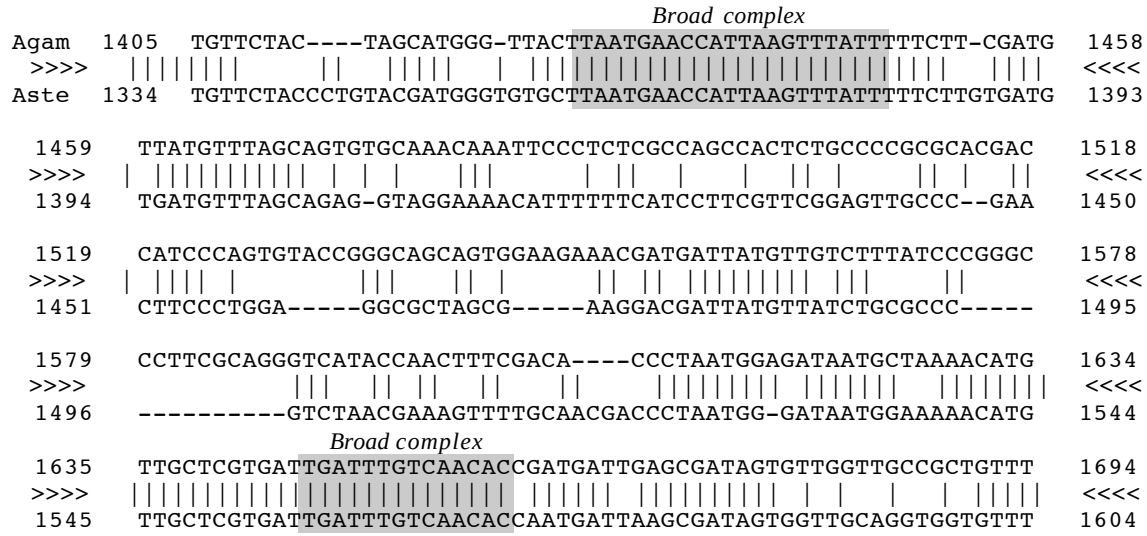

compared species. Arrows above the plots correspond to genes or coding sequences annotated in the *An. gambiae* genome according to the Ensembl database. Exons and coding regions are shown in blue, and conserved non-coding sequences are shown in pink. CNSs, conserved non-coding sequences. UTR, untranslated region. **(B)** VISTA alignment between *An. gambiae* and *An. stephensi*. **(i)** The sequence alignment corresponding to the boxed region up to 1kb region upstream of the start site, **(ii)** the alignment corresponding to the boxed region between 400-600 bp upstream of the start site. Potential TFBSs that are conserved for the two species are highlighted in the alignment.

(A)

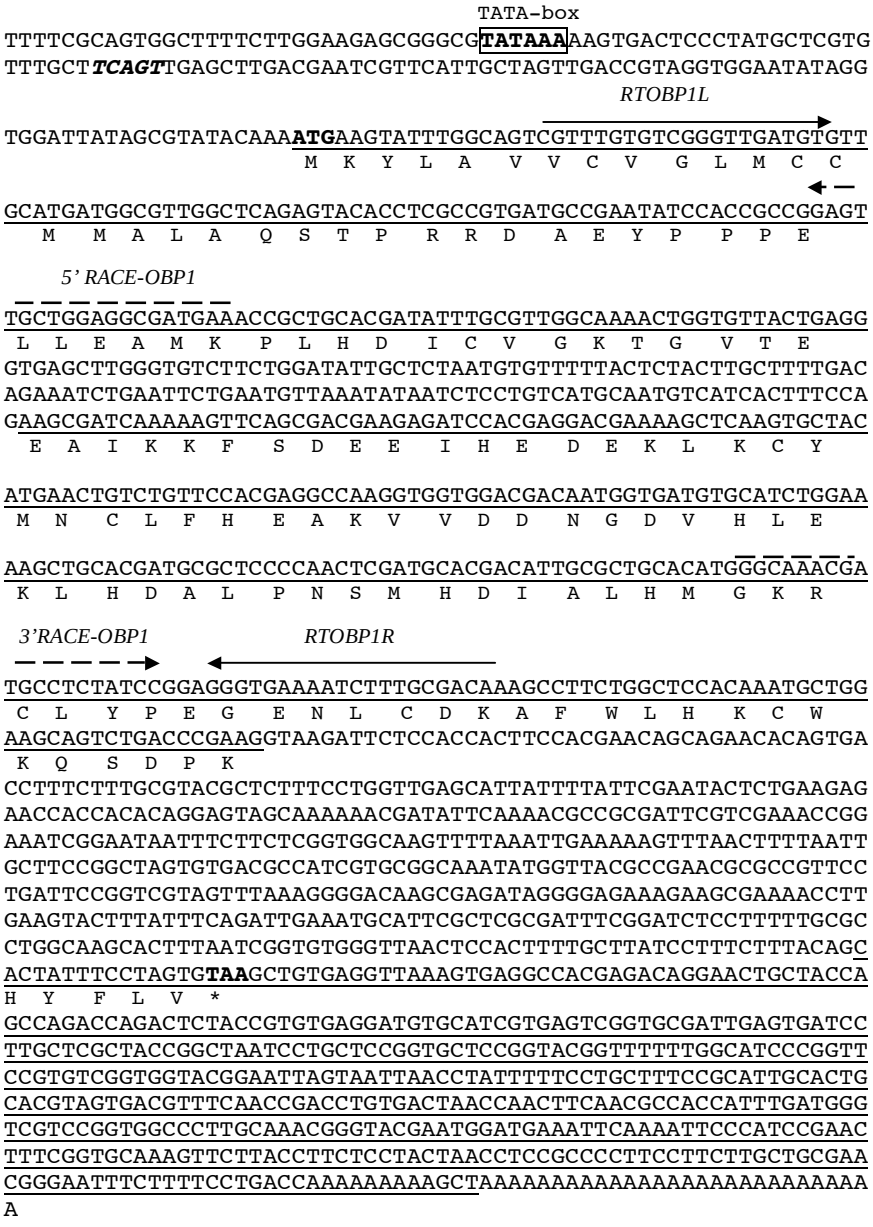

Figure 3.3 Sequence and gene structure of anopheline *Obp1* genes. **(A)** *Aste-Obp1* genomic and cDNA sequences. *Aste-Obp1* gene contains two introns between the three underlined exons. The deduced amino acid sequence of *Aste-Obp1* is shown below the coding regions. Start (ATG) and stop (TAA) codons are shown in bold. A putative initiator sequence, TCAGT, similar to the arthropod initiator consensus is in bold and

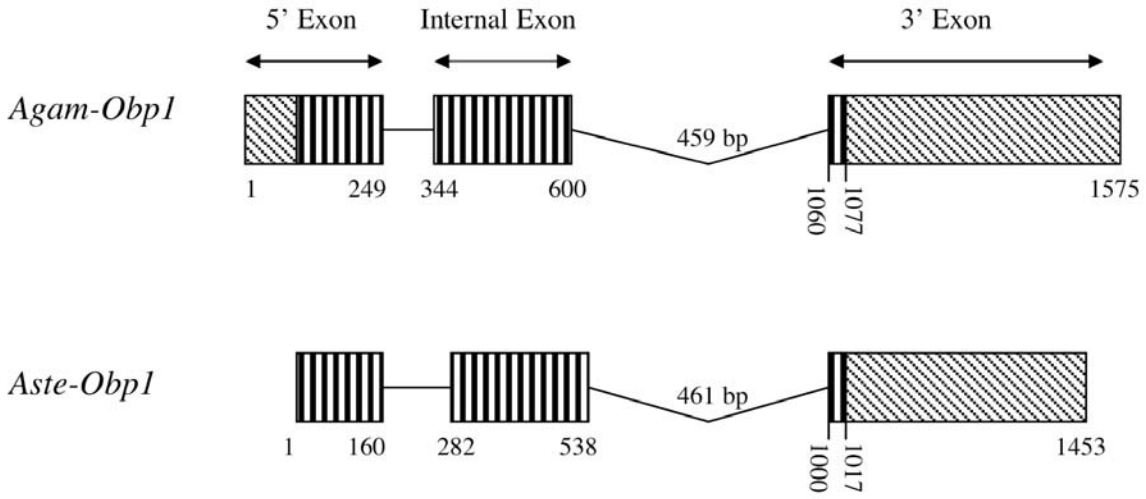

italicized. The consensus for TATA-box, TATAAA, is shown in bold and boxed. The primers used in RT-PCR and RACE reactions are shown by arrows above the corresponding sequences. **(B)** Aste-Obp1 gene structure is compared with that of Agam-Obp1. 5' exons, internal exons, and 3' exons are indicated. Boxes with vertical lines indicate ORFs and they are connected with lines that indicate the introns. The 5' and 3' untranslated regions (UTRs) are shown in boxes with upward diagonal lines. Numbers indicate the relative positions of UTRs, ORFs and intronic regions.

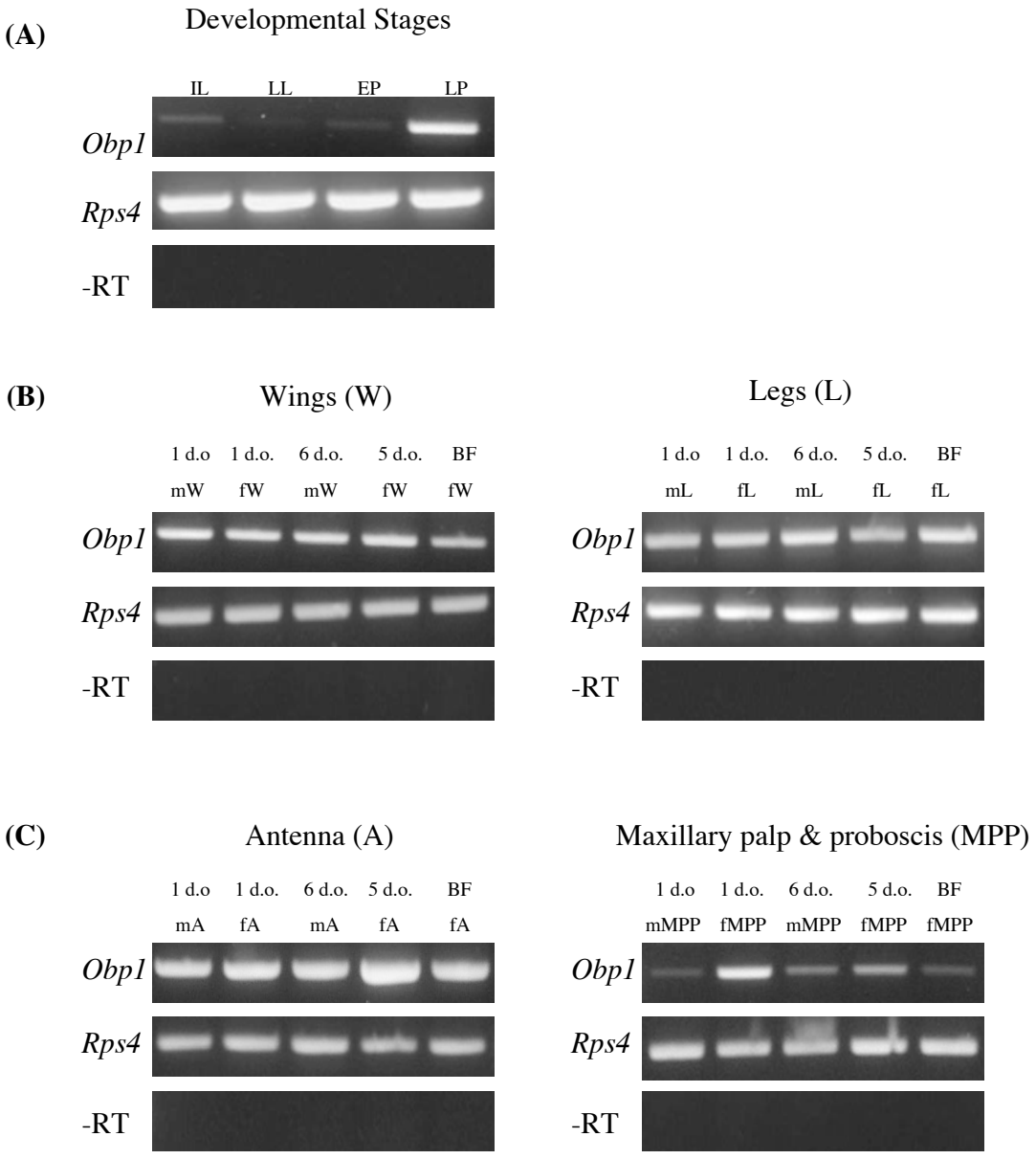

Figure 3.4 Non-quantitative RT-PCR showing expression profile of *Aste-Obp1*. **(A)** Expression of *Aste-Obp1*in pre-adult stages: first instar larvae (IL), late larvae (LL), early pupae (EP), late pupae (LP). **(B)** Expression of *Aste-Obp1* in gustatory tissues: adult male legs (mL), adult female legs (fL), blood-fed female legs (BFfL), adult male wings (mW), adult female wings (fW), blood-fed female wings (BFfW). **(C)** Expression of *Aste-Obp1* in olfactory tissues; adult male antenna (mA), adult female antenna (fA), blood-fed

female antenna (BFfA), adult male maxillary palp and proboscis (mMPP), adult female maxillary palp and proboscis (fMPP), blood-fed female maxillary palp and proboscis (BFfMPP). *Rps4* internal control gene is used as a positive control. –RT products (negative control without the use of reverse transcriptase) are also shown for each cDNA samples. Days old: d.o.

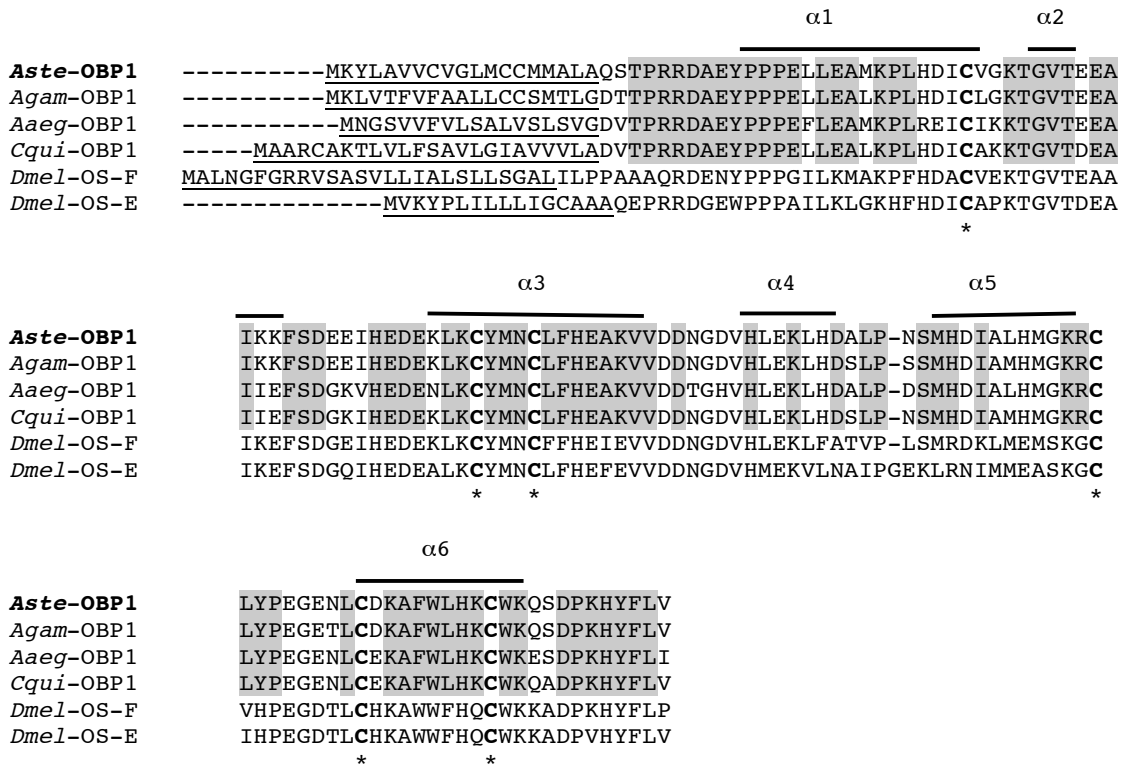

Figure 3.5 Peptide alignment of *Aste*-OBP1 with its mosquito and fly homologues. Mosquito homologues show significant amino acid identity among themselves. Conserved peptides among all mosquitoes are shaded in gray. Conserved six cysteines are shown in bold and indicated with stars. Predicted signal peptides are underlined in the sequences. The alpha-helices of *Aste*-OBP1 are indicated by solid bars above the amino acid sequence. Species abbreviations are Aste (*Anopheles stephensi*), Agam (*Anopheles gambiae*), Aaeg (*Aedes aegypti*), Cqui (*Culex pipiens quinquefasciatus*), and Dmel (*Drosophila melanogaster*).

Table 3.1 Relative mRNA levels of *Aste-Obp1* in female antenna, maxillary palp and proboscis, and legs

Tissue		*Obp1* C_T	*Rps4* C_T	ΔC_T (*Obp1* C_T - *Rps4* C_T)	$\Delta\Delta C_T$ (ΔC_T - $\Delta C_{Tcalibrator}$)	Normalized *Obp1* amount relative to the calibrator, $2^{-\Delta\Delta CT}$
Antenna	replicate1	14.322	18.968	-4.647		
	replicate2	14.226	19.225	-5		
	replicate3	14.7	19.681	-4.982		
	Average	14.416 +/- 0.145	19.292 +/- 0.208	-4.876 +/- 0.254	-9.838 +/- 0.254	915 (767.5-1090)
Max. Palp & Proboscis *	replicate1	23.73	18.08	5.651		
	replicate2	22.889	18.565	4.323		
	replicate3	23.183	18.272	4.912		
	Average	23.267 +/- 0.247	18.306 +/- 0.141	4.962 +/- 0.284	0 +/- 0.284	1 (0.82-1.217)
Legs	replicate1	28.209	18.913	9.295		
	replicate2	26.354	18.042	8.312		
	replicate3	27.125	18.35	8.776		
	Average	27.229 +/- 0.538	18.435 +/- 0.255	8.794 +/- 0.595	3.833 +/- 0.595	0.07 (0.046-0.106)

Data presentation is according to Livak and Schmittgen (2001), with average and standard deviation (SD). Data in the final column are presented as average and a range specified by $2^{-(\Delta\Delta CT+SD)}$ and $2^{-(\Delta\Delta CT-SD)}$. All replicates are biological replicates.

* represents the calibrator.

Table 3.2 Relative mRNA level of *Aste-Obp1* in antenna

Tissue		*Obp1* C_T	*Rps4* C_T	ΔC_T (*Obp1* C_T - *Rps4* C_T)	$\Delta\Delta C_T$ (ΔC_T - $\Delta C_{Tcalibrator}$	Normalized *Obp1* amount relative to the calibrator, $2^{-\Delta\Delta CT}$
Male *	replicate1	17.181	18.606	-1.424		
	replicate2	16.396	18.169	-1.773		
	replicate3	16.632	18.201	-1.569		
	replicate4	17.27	18.878	-1.608		
	Average	16.87 +/- 0.212	18.463 +/- 0.17	-1.594 +/- 0.272	0 +/- 0.272	1 (0.828-1.207)
Female	replicate1	13.457	18.098	-4.642		
	replicate2	14.319	18.472	-4.154		
	replicate3	14.331	18.751	-4.42		
	replicate4	14.659	19.077	-4.417		
	Average	14.191 +/- 0.257	18.6 +/- 0.208	-4.408 +/- 0.331	-2.815 +/- 0.331	7.035 (5.59-8.852)
Blood-fed females	replicate1	16.537	21.067	-4.529		
	replicate2	15.108	19.301	-4.193		
	replicate3	14.51	18.939	-4.429		
	replicate4	16.028	20.347	-4.319		
	Average	15.546 +/- 0.455	19.913 +/- 0.487	-4.368 +/- 0.666	-2.774 +/- 0.666	6.839 (4.31-10.85)

Data presentation is according to Livak and Schmittgen (2001), with average and standard deviation (SD). Data in the final column are presented as average and a range specified by $2^{-(\Delta\Delta CT+SD)}$ and $2^{-(\Delta\Delta CT-SD)}$. All replicates are biological replicates.

* represents the calibrator.

Table 3.3 Relative mRNA level of *Aste-Obp1* in maxillary palp and proboscis

Tissue		*Obp1* C_T	*Rps4* C_T	ΔC_T (*Obp1* C_T- *Rps4* C_T)	$\Delta\Delta C_T$ (ΔC_T- $\Delta C_{Tcalibrator}$	Normalized *Obp1* amount relative to the calibrator, $2^{-\Delta\Delta CT}$
Male *	replicate1	31.264	19.193	12.072		
	replicate2	28.682	19.521	9.161		
	replicate3	32.038	19.561	12.477		
	Average	30.662 +/- 1.01	19.425 +/- 0.117	11.237 +/- 1.021	0 +/- 1.021	1 (0.49-2.03)
Female	replicate1	23.439	18.417	5.021		
	replicate2	22.962	18.64	4.323		
	replicate3	23.719	18.561	5.158		
	Average	23.373 +/- 0.221	18.539 +/- 0.065	4.834 +/- 0.23	-6.403 +/- 0.23	84.6 (72.1-99.2)
Blood-fed	replicate1	30.15	18.627	11.524		
females	replicate2	26.365	18.415	7.95		
	replicate3	26.005	18.539	7.467		
	Average	27.507 +/- 1.326	18.527 +/- 0.061	8.98 +/- 1.327	-2.257 +/- 1.327	4.78 (1.9-12)

Data presentation is according to Livak and Schmittgen (2001), with average and standard deviation (SD). Data in the final column are presented as average and a range specified by $2^{-(\Delta\Delta CT+SD)}$ and $2^{-(\Delta\Delta CT-SD)}$. All replicates are biological replicates.

* represents the calibrator.

Table 3.4 Relative mRNA level of *Aste-Obp1* in legs

Tissue		*Obp1* C_T	*Rps4* C_T	ΔC_T (*Obp1* C_T - *Rps4* C_T)	$\Delta\Delta C_T$ (ΔC_T - $\Delta C_{Tcalibrator}$	Normalized *Obp1* amount relative to the calibrator, $2^{-\Delta\Delta CT}$
Male *	replicate1	27.424	18.772	8.652		
	replicate2	27.471	17.815	9.656		
	replicate3	27.247	18.652	8.595		
	Average	27.381 +/- 0.118	18.413 +/- 0.521	8.968 +/- 0.535	0 +/- 0.535	1 (0.69-1.45)
Female	replicate1	27.364	18.415	8.949		
	replicate2	25.632	17.187	8.445		
	replicate3	26.321	17.134	9.188		
	Average	26.439 +/- 0.872	17.579 +/- 0.725	8.861 +/- 1.13	-0.107 +/- 1.13	1.077 (0.49-2.36)
Blood-fed females	replicate1	25.091	17.236	7.856		
	replicate2	25.036	17.331	7.705		
	replicate3	25.501	17.883	7.618		
	Average	25.209 +/- 0.254	17.483 +/- 0.35	7.726 +/- 0.43	-1.242 +/- 0.43	2.36 (1.75-3.18)

Data presentation is according to Livak and Schmittgen (2001), with average and standard deviation (SD). Data in the final column are presented as average and a range specified by $2^{-(\Delta\Delta CT+SD)}$ and $2^{-(\Delta\Delta CT-SD)}$. All replicates are biological replicates.

* represents the calibrator.

Chapter 4

Expression analysis and knockdown of two antennal odorant-binding protein genes in *Aedes aegypti*

Submitted for Publication in*: Insect Biochemistry and Molecular Biology*

4.1 Abstract

The transmission of mosquito-borne infectious diseases, such as malaria and dengue fever, are heavily influenced by the olfactory behavior of mosquitoes. The abundance of odorant-binding proteins (OBPs) in the olfactory sensillum lymph suggests that they are important for mosquito chemosensory systems. However, no direct evidence has been found for specific functions of mosquito OBPs. Thus, it is important to establish a method in which a loss-of-function test can be performed to determine the possible role of these genes in olfactory tissues. In this study, we use a double subgenomic Sindbis (dsSIN) virus expression system as a tool to reduce the expression of two *Obp* genes in *Aedes aegypti*, *Aaeg-Obp1* and *Aaeg-Obp7*. Using quantitative real-time-PCR (qRT-PCR), we showed that both genes are predominantly expressed in the female antenna, the primary olfactory tissue of mosquitoes. Moreover, the mRNA levels of *Aaeg-Obp1* and *Aaeg-Obp7* were significantly reduced in olfactory tissues of recombinant dsSIN virus-inoculated female mosquitoes compared to that of controls by approximately 8 and 100-fold, respectively, at 11 days post virus-inoculation (p.i.). Our data suggest that the dsSIN virus system can be efficiently used to knockdown *Obp* gene expression in olfactory tissues of mosquitoes. We discuss the potential for a systematic analysis of the molecular players involved in mosquito olfaction using this newly developed technique. Such analysis will provide an important step to interfere with the host-seeking behavior of mosquitoes to prevent the transmission of diseases.

4.2 Introduction

Mosquitoes are the most important vectors for human diseases, such as malaria, dengue fever, and yellow fever. Most female mosquitoes require a blood meal to complete their reproductive cycle and their blood-feeding behavior enables the transmission of the vector-borne diseases to their hosts. Olfaction plays a critical role in host-seeking behaviors of mosquitoes (Takken and Knols, 1999). Current strategies to control the transmission of vector-borne diseases are ineffective. Thus, novel approaches are desperately needed to reduce the disease transmission including new ways to interfere with mosquito host-seeking behavior. In this respect, mosquito odorant-binding proteins (OBPs), which are small, water-soluble molecules that transport the hydrophobic odorants through the aqueous lymph of the sensilla to their receptors in the olfactory receptor neurons (ORNs), represent good candidate targets for interference.

Several *Obp* genes, including *Anopheles gambiae Obp1* and *Obp7* (*Agam-Obp1* and *Agam-Obp7*, respectively), show high levels of expression in the antenna and a general female-bias in their expression patterns (Biessmann et al., 2005; Li et al., 2005). Thus, mosquito *Obp1* and *Obp7* are likely involved in female olfactory response and are good candidates for further investigation. Unfortunately, no direct evidence has been found for specific functions of any mosquito OBPs. Functional assignment of mosquito olfactory genes will undoubtedly benefit from effective and efficient *in vivo* gene knockdown methods, which are currently lacking.

Transformation technology provides the ability to study heterologous gene expression and analysis of gene regulatory elements, and permits gene knockdown experiments designed to study gene function and perhaps to reduce the ability for mosquitoes to transmit diseases. For example, transformation of mosquitoes based on transposable elements, such as *mariner* and *Hermes*, has been shown to integrate heterologous genes into the *Aedes aegypti* mosquitoes (Sarkar et al., 1997; Coates et al., 1998). However, the lack of high transformation frequency and effective screening

methods causes researchers search for alternative tools for efficient molecular analysis. In this aspect, virus-derived infectious-clone technology provides a powerful alternative.

Among the virus expression systems, double subgenomic Sindbis (dsSIN) virus expression systems have been most frequently used in mosquitoes. They have been used to introduce the gene of interest into mosquitoes *in vivo* (Higgs et al., 1993; Olson et al., 1994; Kamrud et al., 1995; Rayms-Keller et al., 1995) and facilitate the expression of heterologous genes in mosquitoes (Hahn et al., 1992; Olson et al., 1994, 2000). These expression systems have also been used to silence gene expression in mosquitoes (Olson et al., 1996, 2002; Johnson et al., 1999; Adelman et al., 2001; Shiao et al., 2001; Tamang et al., 2004). However, it is not known whether olfactory genes can be efficiently silenced using this method.

Sindbis (SIN) viruses are arboviruses (genus *Alphavirus*, family *Togaviridae*) that naturally cycles between mosquitoes of the *Culex* genus and the avian hosts (Taylor et al., 1955). They are enveloped viruses that replicate exclusively in the cytoplasm of the infected cells (Strauss et al., 1984; Strauss and Strauss, 1994). SIN virus genome is a positive-sense, single stranded RNA and is about 11.7 kb in length. The 5'end is capped and the 3' end contains a poly (A) tail. The 5' two- thirds of the genomic RNA is translated to produce the non-structural polyproteins for viral replication machinery. The 3' one-third of the genome is translated to generate structural proteins, capsid (C) protein and envelope glycoproteins (E1 and E2). A noncoding region (NCR) exists at both 5' and 3' ends. It has been found that 3' NCR contains repeated sequence elements (Strauss and Strauss, 1994) that may play a role in host specificity by interacting with host proteins (Kuhn et al., 1991). SIN and other alphaviruses gain entry into vertebrate and invertebrate cells by receptor-mediated endocytosis (Strauss and Strauss, 1994). The TE/3'2J double subgenomic SIN virus was developed from infectious cDNA clones of the manipulated viral RNA genome of a mouse neurovirulent strain of AR339 SIN virus (Lustig et al., 1988; Hahn et al., 1992). The TE/3'2J viruses contain a second subgenomic promoter between the structural protein coding region and the 3'NCR. The exogenous gene is

inserted at the 3' end of this promoter that enables the expression (or silencing via RNA interference, RNAi) of the gene of interest.

In this study, we describe the construction of recombinant dsSIN viruses that produce an antisense transcript of each of the two *Obp* genes, henceforth referred to as *Aaeg-Obp1* and *Aaeg-Obp7* genes, in *Aedes aegypti*. The recombinant dsSIN virus-inoculated mosquitoes showed dramatic decrease in the mRNA levels for both *Obp* genes at 11 days post virus-inoculation (p.i.). We showed that these genes are abundantly expressed in the female antenna compared to the other female mosquito chemosensory tissues, which may indicate a significant role for both *Obp* genes in mosquito olfactory behavior. Our results provide the use of dsSIN virus expression system to effectively knockdown olfactory genes in the antenna of mosquitoes. The establishment of this efficient method to knockdown olfactory genes opens the door to future systematic analysis of the molecular players involved in mosquito olfaction and will, in turn, facilitate the development of novel targets or compounds that interfere with mosquito behaviors that are relevant to disease transmission.

4.3 Materials and methods

Cells and medium

Baby hamster kidney cells (BHK-21, ATCC no. CCL-10) and *Aedes albopictus* C6/36 cells (ATCC no. CRL-1660) were grown in Dulbecco's minimal essential medium (DMEM) containing 10% fetal bovine serum (FBS), L-glutamine, 100 U/ml penicillin, and 100 μg/ml streptomycin and were maintained at 37°C and 28°C, respectively.

Mosquitoes

Aedes aegypti (Liverpool strain) were reared at 28°C, 80% relative humidity and photoperiod of 12 h Light:12 h Dark.

Expression analyses of *Obp* genes by quantitative Real-time PCR (qRT-PCR)

Total RNA was isolated from antenna, maxillary palp and proboscis, legs, and body devoid of appendages from 5-day-old female mosquitoes. First-strand cDNA was synthesized from 0.8 μg total RNA. qRT-PCR was performed using the TaqMan probe-based chemistry with an ABI Prism 7300 Sequence Detection System (SDS) (Applied Biosystems, Foster City, CA). Briefly, 2 μl of cDNA was used with 9.25 μl nuclease-free water, 12.5 μl 2 X TaqMan Universal PCR Master Mix (Applied Biosystems, Foster City, CA), and 1.25 μl 20 X Assay mix designed by ABI in a 25 μl PCR reaction volume. Each assay mix included 5'FAM and 3'non-fluorescent quencher (NFQ) labeled probe corresponding to a cDNA fragment that is separated by an intron, ensuring that only cDNA products were quantified. qRT-PCR for *Aaeg-Obp1* and *Aaeg-Obp7* genes and the internal control, *ribosomal protein S7* gene (*Aaeg-Rps7*), were carried out using the following primer pairs and probes:

*Aaeg-Obp1*primerF: 5'-GCACAAATGCTGGAAGGAGTCT-3'
*Aaeg-Obp1*primerR: 5'-CCATGTTTCGGTTCTGCATTTCTT-3'
*Aaeg-Obp1*probe: 5'FAM-ACCCCAAGCATTACTTC-3'NFQ
*Aaeg-Obp7*primerF: 5'-CGGGCTCGTAGCAGATGTTAC-3'
*Aaeg-Obp7*primerR: 5'-CGGGTAGCTCCAAATTGTCCTT-3'
*Aaeg-Obp7*probe: 5'FAM-ATGGCCGCTCAAATC-3'NFQ
*Aaeg-Rps7*primerF: 5'-CGCGCTCGTGAGATCGA-3'
*Aaeg-Rps7*primerR: 5'-GCACCGGGACGTAGATCA-3'
*Aaeg-Rps7*probe: 5'FAM-ACAGCAAGAAGGCTATCG-3'NFQ

The thermocycler program consisted of 50°C for 2 min, 95°C for 10 min, 40 cycles of 95°C for 15 sec and 60°C for 1 min. The goal is to determine the relative amounts of *Obp7* and *Obp1* mRNA. Thus, TaqMan assays were done in parallel for the control gene, *Rps7,* as well. All test samples and the controls were done in triplicate.

We used the ABI Assays-on-Demand setup for our TaqMan Gene Expression Assays. ABI does not recommend testing of amplification efficiency because their

extensively tested assay design ensures near 100% (+/- 10%) efficiency and because commonly used testing methods tend to produce unreliable results (ABI Publication 127AP05-01). However, to be sure, we performed assay validation by checking the amplification curves (Bohbot and Vogt, 2005). All TaqMan PCR data were analyzed using SDS Software based on the comparative method ($\Delta\Delta C_T$) (Livak and Schmittgen, 2001). Briefly, for every sample, an amplification plot was generated showing the reporter dye fluorescence (ΔRn) at each PCR cycle. For each amplification, a threshold cycle (C_T) was determined, representing the cycle number at which the fluorescence passes the threshold. This is how the C_T values of *Aaeg-Obp7*, *Aaeg-Obp1* and the control gene (*Aaeg-Rps7*) were determined. The C_T value of the control gene was then subtracted from the C_T value of the *Obp* gene giving the ΔC_T value. Then, the ΔC_T value of each sample was normalized to that of the calibrator sample (i.e. maxillary palp and proboscis was used as the calibrator for comparison of *Obp* gene expression in selected tissues of females, Tables 4.1 and 4.2) resulting in the determination of $\Delta\Delta C_T$ value. Finally, $2^{-\Delta\Delta CT}$ values were calculated to estimate the fold variations in the mRNA levels of *Obp7* and *Obp1* in different tissues in females relative to the calibrator, maxillary palp and proboscis.

Construction of *Aaeg-Obp1* and *Aaeg-Obp7* cDNA clones

Total RNA was isolated from whole *Ae. aegypti* mosquitoes using TRIzol reagent (Invitrogen, Carlsbad, CA). DNase treated RNA was used to synthesize first-strand cDNA using oligo (dT) primers and the SuperScript II reverse transcriptase (Invitrogen, Carlsbad, CA). The primer pairs used in PCR reactions included *Xba*I and *Pac*I restriction enzyme sites at the 5' ends (Figs. 4.1A, B). Accordingly, the primer pair SINV-Obp7L: 5'-TTAATTAAGGACAATTTGGAGCTACCC-3' and SINV-Obp7R: 5'-TCTAGATAACATCAGCCATCAACAGG-3' were used to amplify 386 bp of *Aaeg-Obp7* cDNA in the antisense orientation in a PCR with annealing temperature of 61°C for a total of 35 cycles. The primer pair SINV-Obp1R: 5'-TCTAGACAGACTCCTTCC AGCATTTG-3' and SINV-Obp1L: 5'-TTAATTAACGGATCGGTAGTTTTTGTGC-3' were used to amplify a 401 bp of *Aaeg-Obp1* cDNA in the antisense orientation in a PCR with annealing temperature of 64°C for a total of 35 cycles. The PCR products were

cloned into pGEM-T-Easy vector (Promega, Madison, WI) and confirmed by sequencing (Virginia Bioinformatics Institute, Blacksburg, VA).

Construction of Sindbis vectors

The pTE/3'2J viral construct was obtained from Dr. K. Myles (Virginia Polytechnic Institute and State University, Blacksburg, VA) and has been previously described (Hahn et al., 1992). This plasmid was modified by adding a *Pac*I site downstream of the *Xba*I site (Fig. 4.2) and the two sites were used for our cloning purposes. Either *Aaeg-Obp7* cDNA or *Aaeg-Obp1* cDNAs were cloned into the *Xba*I/*Pac*I digested pTE/3'2J plasmid in the antisense orientation. We named these recombinant plasmids pTE/3'2J/AaegOBP1^{as} and pTE/3'2J/AaegOBP7^{as}. Antisense orientation of each cDNA insert in these recombinant plasmids was confirmed by PCR using primers complementary to the pTE/3'2J viral plasmid sequence flanking the inserted cDNA sequences.

dsSIN virus production

dsSIN plasmids were linearized at the *Xho*I site and their genomic RNA was transcribed *in vitro* using SP6 RNA polymerase (Promega, Madison, WI) and capped with 7-methylguanosine (Ambion Inc., Austin, TX). The RNA products were electroporated into BHK-21 cells with two consecutive pulses at 460 V, 725 ohms, and 75 μF. Following incubation at 37°C for 48 h, the viruses were harvested and stored in aliquots at -80°C. The dsSIN viruses were propagated once in C6/36 cells and harvested from the medium 48 h and 72 h later. An aliquot of virus was titrated in BHK-21 cells using tissue culture infectious dose 50% end-points ($TCID_{50}$) assay.

Mosquito infections

Five-day-old female *Ae. aegypti* mosquitoes were intrathoracically inoculated with dsSIN viruses pTE/3'2J (8.5 $\log_{10}TCID_{50}$), pTE/3'2J/AaegOBP1^{as} (7.3$\log_{10}TCID_{50}$) or pTE/3'2J/AaegOBP7^{as} (8.5 $\log_{10}TCID_{50}$), respectively. For all experiments, uninfected mosquitoes and pTE/3'2J virus-inoculated mosquitoes were used as controls. Mosquitoes were collected at 3 days, 7 days and 11 days post virus-inoculation (p.i.), homogenized

and stored at –80°C until processing. Head tissues were also dissected at 11 days p.i. from uninfected and recombinant dsSIN virus-inoculated mosquitoes.

Obp gene expression in dsSIN virus-inoculated mosquitoes

Aaeg-Obp1 and *Aaeg-Obp7* mRNA levels in recombinant dsSIN virus-inoculated mosquitoes were determined by using non-quantitative reverse transcription-polymerase chain reaction (RT-PCR) and qRT-PCR. Our experiments included three sets of independent replicates for each uninfected, pTE/3'2J, pTE/3'2J/AaegOBP1^{as} and pTE/3'2J/AaegOBP7^{as} virus-inoculated mosquitoes. Whole mosquitoes were collected at 3 days, 7 days and 11 days p.i. Moreover, head tissues (antenna, maxillary palp and proboscis) of viral infected and control mosquitoes were collected in triplicates during three independent experiments at 11 days p.i. Total RNA isolation and cDNA synthesis were performed as mentioned above. cDNA synthesis reactions were also carried out in the absence of reverse transcriptase (-RT) in parallel for each sample as a control for the reactions. In addition, *Aaeg-Rps7* gene was used as an internal control. RT-PCR was performed using the following gene specific primer pairs:

RT-Obp1L: 5'-TGGGTTCCAGCTTTCACAAT-3'
RT-Obp1R: 5'-GGAAGTAATGCTTGGGGTCA-3'
RT-Obp7L: 5'-TTATGCTGGCAGTTTTGCTG-3'
RT-Obp7R: 5'-AGCTGGTAACATCAGCCATC-3'
RT-Rps7L: 5'-GCTTTCGAGGGACAAATCG-3'
RT-Rps7R: 5'-CAATGGTGGTCTGCTGGTTC-3'

Optimal annealing temperatures were 60°C for *Aaeg-Obp1,* 58°C for *Aaeg-Obp7*, and 61°C for *Aaeg-Rps7* genes and the amplification was performed for twenty-five cycles. PCR products were analyzed by 2% agarose-gel electrophoresis.

Furthermore, cDNAs from head tissues (antenna, maxillary palp and proboscis) of infected and control mosquitoes were used to compare the level of *Obp* gene expression by TaqMan based qRT-PCR (see above for details). The primers used for real-time PCR

ensure that the *Obp* RNA derived from recombinant dsSIN virus will not be amplified. The TaqMan assay primers and probes were described above.

Statistical analysis

We used ΔC_T values for analysis of real-time PCR data. One-way ANOVA with Tukey's post test was performed using GraphPad Prism version 3.00 for Windows (GraphPad Software, San Diego, CA). Significance in comparisons is assumed if $P < 0.05$ is obtained in the appropriate test.

4.4 Results

Identification of *Obp1* and *Obp7* genes in *Aedes aegypti*

We decided to establish a dsSIN virus based *Obp* gene knockdown method for *Ae. aegypti* because the SIN virus is known to be infectious to *Ae. aegypti* nervous systems. We chose *Obp1* and *Obp7* genes, which were previously annotated in *An. gambiae,* as our targets for the *Obp* gene knockdown in *Ae. aegypti*. In order to achieve this, we first needed to identify and characterize these two genes in *Ae. aegypti*.

Obp genes have been identified during recent genome annotation of *Ae. aegypti* (Nene et al., 2007) based on similarities to OBPs in *An. gambiae* (Vogt, 2002; Xu et al., 2003) and *D. melanogaster* (Hekmat-Scafe et al., 2002). Among these, *Ae. aegypti* OBP56e showed highest amino acid sequence identity (50%) to *Agam*-OBP7 while a putative OBP (GenBank accession no: EAT38681) showed the highest identity (70%) to *Agam*-OBP1. Phylogenetic analysis suggest that these two *Ae. aegypti* OBPs, *Aaeg*-OBP7 and *Aaeg*-OBP1 are the homologs of *Agam*-OBP7 and *Agam*-OBP1, respectively (data not shown).

Expression of *Aaeg-Obp1* and *Aaeg-Obp7* genes in female *Ae. aegypti* mosquitoes

The expression of *Obp1 and Obp7* genes have only been investigated in anopheline mosquitoes (Biessmann et al., 2005; Li et al., 2005; see Chapters 2 and 3) Our RT-PCR and subsequent cloning and sequencing results confirmed the splicing of introns

that are encompassed by the RT-PCR primers (Figs. 4.1A, B) in the two *Ae. aegypti Obp* genes. To determine the mRNA levels of *Aaeg-Obp1* and *Aaeg-Obp7* genes, we performed real-time PCR using 5- day-old female *Ae. aegypti* mosquitoes, which are ready to take a blood meal. mRNA levels of *Aaeg-Obp1* and *Aaeg-Obp7* have been examined in antenna, maxillary palp and proboscis, legs, and body devoid of appendages. The results indicated that *Obp7* mRNA level in the antenna is approximately 260-fold higher than that of the maxillary palp and proboscis (Table 4.1). The level of *Obp7* in maxillary palp and proboscis, on the other hand, is significantly higher than female legs as well as bodies devoid of appendages, approximately 200-fold and 600-fold higher, respectively. We also observed an approximately 500-fold more abundant *Obp1* mRNA level in the female antenna compared to that of the maxillary palp and proboscis (Table 4.2). The level of *Obp1* in maxillary palp and proboscis is again significantly higher than female legs as well as bodies devoid of appendages, approximately 2.5-fold and 70-fold higher, respectively. These results clearly indicate that *Aaeg-Obp1* and *Aaeg-Obp7* are predominantly expressed in the antennae, the primary olfactory tissues of mosquitoes, indicating a possible olfactory function. The expression levels of these two genes in the maxillary palp and proboscis, although much lower when compared to that of the antenna, are significant and likely biologically important as well.

Generation of recombinant dsSIN viruses for *Obp* gene knockdown

A 386 bp *Aaeg-Obp7* cDNA and a 401 bp *Aaeg-Obp1* cDNA have been cloned in antisense orientation using primers with *Pac*I and *Xba*I restriction enzyme sites (Figs. 4.1A, B; see Materials and methods). These cDNA sequences were inserted at the 3' end of the second subgenomic promoter (S2) using the *Pac*I/*Xba*I sites in the pTE/3'2J plasmid (Fig. 4.2A). The RNA was transcribed *in vitro* from the SP6 bacteriophage promoter of the pTE/3'2J recombinant plasmids and then electroporated into BHK-21 cells. Upon infection, three virus-specific double stranded RNAs (dsRNAs) would be produced (Fig. 4.2B). DsSIN virus harvested after 48 h was further propagated by passage through *Ae. albopictus* C6/36 cells to obtain higher viral titers. dsSIN viruses were harvested after 48 h and 72 h and their titers were determined using tissue culture infectious dose 50% end-points ($TCID_{50}$) assay. pTE/3'2J and pTE/3'2J/AaegOBP7^{as}

viruses had similar growth patterns and attained a titer of 8.5 $\log_{10}$TCID$_{50}$/ml at 72 h post-infection (Fig. 4.3). The concentration of pTE/3'2J/AaegOBP1^{as} virus stayed the same at 48 h and 72 h post-infection, reaching a maximum titer of 7.3$\log_{10}$TCID$_{50}$/ml (Fig. 4.3). As a result, we were able to generate three recombinant dsSIN virus constructs, one without an insert that was used as a negative control (pTE/3'2J) and those that were used as experimental samples producing dsRNAs targeting either *Aaeg-Obp7* (pTE/3'2J/AaegOBP7^{as}) or *Aaeg-Obp1* (pTE/3'2J/AaegOBP1^{as}) mRNA.

dsRNA-mediated interference of *Obp* gene expression

Female mosquitoes were intrathoracically inoculated with either the pTE/3'2J, pTE/3'2J/AaegOBP7^{as} or pTE/3'2J/AaegOBP1^{as} dsSIN virus. On the 3rd, 7th and 11th days p.i., four groups of mosquitoes (uninfected, pTE/3'2J infected, pTE/3'2J/ AaegOBP7^{as} infected, and pTE/3'2J/AaegOBP1^{as} infected) with the survival rate ranged between 88-94% were collected and analyzed for *Obp7* and *Obp1* mRNA levels using whole body preparations. Non-quantitative RT-PCR results showed progressive and apparent reduction of the *Aaeg-Obp1* and *Aaeg-Obp7* gene expressions in recombinant dsSIN virus-inoculated mosquitoes to that of the pTE/3'2J and uninfected controls at 3, 7, and 11 days p.i. (Fig. 4.4A). In order to determine the mRNA levels of these *Obp* genes in olfactory tissues of *Ae. aegypti*, head tissues (including antenna, maxillary palp and proboscis) were collected from recombinant dsSIN virus-inoculated mosquitoes at 11 days p.i. RT-PCR results showed a dramatic decrease for both gene transcripts in pTE/3'2J/AaegOBP1^{as} or pTE/3'2J/AaegOBP7^{as} virus-inoculated mosquitoes (Fig. 4.4B). The internal control gene, *Aaeg-Rps7*, was robustly expressed for the tissue samples examined for all the RT-PCR reactions.

In accordance with the RT-PCR data, qRT-PCR analysis also confirmed that the transcript levels of *Aaeg-Obp1* and *Aaeg-Obp7* were decreased significantly in head tissues of dsSIN virus-inoculated mosquitoes (Fig. 4.5). We observed an 8-fold decrease in *Aaeg-Obp1* mRNA levels in head tissues of pTE/3'2J/AaegOBP1^{as} virus-inoculated mosquitoes (Fig. 4.5A; Table 4.3); whereas, > 100-fold reduction is observed for *Aaeg-Obp7* expression in head tissues of pTE/3'2J/AaegOBP7^{as} virus-inoculated mosquitoes

(Fig. 4.5B; Table 4.4). As expected, there is no significant differences between uninfected and the control pTE/3'2J virus-infected samples. The observed decrease in *Obp1* and *Obp7* transcript levels are indicative of knockdown for both genes in the olfactory tissues of *Ae. aegypti* females.

4.5 Discussion

We have shown that *Aaeg-Obp1* and *Aaeg-Obp7* genes are expressed at higher levels in the antennae compared to the other chemosensory tissues of female mosquitoes. This is consistent with what has been previously reported in *An. gambiae* species (Biessmann et al., 2005; Li et al., 2005). Thus, these two *Obp* genes are likely involved in female olfaction in both Aedes and Anopheles mosquitoes. We also found that these genes are expressed at lower levels in the maxillary palp and proboscis of females. The low expression may be due in part to the fact that maxillary palp contains fewer sensilla than the antenna (Mclver, 1982). Although these two genes might be primarily involved in the olfactory behavior of female mosquitoes, they may also recognize different chemical molecules for a gustation-mediated behavior, such as sugar feeding. Overlapping expression of *Obp* genes in maxillary palps and antennae have also been shown in *An. gambiae* (Biessmann et al., 2005) and *D. melanogaster* (Galindo and Smith, 2001). It has been found that 1-octen-3-ol, an attractant for *Ae. aegypti* mosquitoes, stimulates neurons on both palps (Lu et al., 2007) and antennae (Grant and O'Connell, 1996). In *Drosophila*, the neurons of the palps and the antennae were stimulated by common chemical cues as well (de Bruyne et al., 1999). Thus, it is possible that maxillary palps and antennae have overlapping functions where an *Obp* gene may be involved in the perception of a common odorant in both tissues or it is involved in both olfactory and gustatory chemoreception.

Using *Aaeg-Obp1* and *Aaeg-Obp7* as targets, we established an effective method to knockdown *Obp* gene expression in *Ae. aegypti*. This method is based on dsRNA-mediated gene silencing using the dsSIN virus expression system. We demonstrated that both *Aaeg-Obp1* and *Aaeg-Obp7* gene expressions were reduced significantly in female

head tissues (antenna and maxillary palp and proboscis) after infection with the recombinant dsSIN viruses when compared to those of the uninfected and control virus-inoculated samples. We achieved 8-fold and >100-fold reduction in transcript levels of these two genes in head tissues of recombinant virus-inoculated female mosquitoes, which are the main sources of mRNAs for both genes (Tables 4.1 and 4.2). Given that the two *Obp* transcripts showed 259- and 480-fold higher levels in the antenna than in the maxillary palp and proboscis of females, the significant level of reduction in head tissues should mainly result from gene knockdown in the antenna. On the other hand, knockdown in maxillary palp and proboscis are likely masked by transcript levels in the antennae. In any case, we demonstrated successful knockdown of two antennal *Obp* genes in the primary olfactory tissue, the antennae, of mosquitoes.

As discussed above, the effectiveness of the gene knockdown in virus-inoculated mosquitoes is likely facilitated by RNAi-mediated inhibition of endogenous *Obp* gene expression. During the virus life cycle, dsRNAs, which are complementary to the endogenous *Obp* mRNA, are produced by the recombinant virus. These dsRNAs will trigger RNA interference against the expression of endogenous mosquito *Obp* genes, and, thus, reduce mRNA transcripts of these genes. As mentioned in the introduction, dsSIN virus based expression system has been successfully used to silence several immunity-related genes in Aedes mosquitoes. Our study shows for the first time that the same effective strategy can be used to knockdown genes in olfactory tissues. Thus, the power and the relative ease of using an infectious clone technology by simple manipulation can be harvested to allow the systematic investigation of the function of many olfactory genes by relatively efficient gene knockdown in mosquitoes.

Although insect OBPs are known to be involved in odorant perception by transferring odorants to the olfactory receptor neurons, their specific functions have not been determined in mosquitoes. Our findings provide a potentially powerful new tool for assigning the functions of *Obp* genes, or other genes involved in olfaction in mosquitoes. Achieving this goal will likely be challenging and require extensive collaborations between mosquito geneticists and behavioral biologists. The reward, however, will be

great improvement in our understanding of the molecular basis of mosquito olfaction that will lead to possible new targets and compounds to interfere with mosquito behaviors that are relevant to disease transmission.

4.6 Acknowledgements

We thank Drs. Kevin M. Myles and Zachary N. Adelman (Department of Entomology, Virginia Polytechnic Institute and State University) for providing the pTE/3'2J plasmid and leading us through the work with Sindbis viruses. We also thank Dr. Yumin Qi for assistance in cell culture and Thomas R. Saunders for rearing *Ae. aegypti* mosquitoes. We thank Dr. Keying Ye for help with statistical analysis. This work was supported by National Institutes of Health Grant AI063252.

(A)

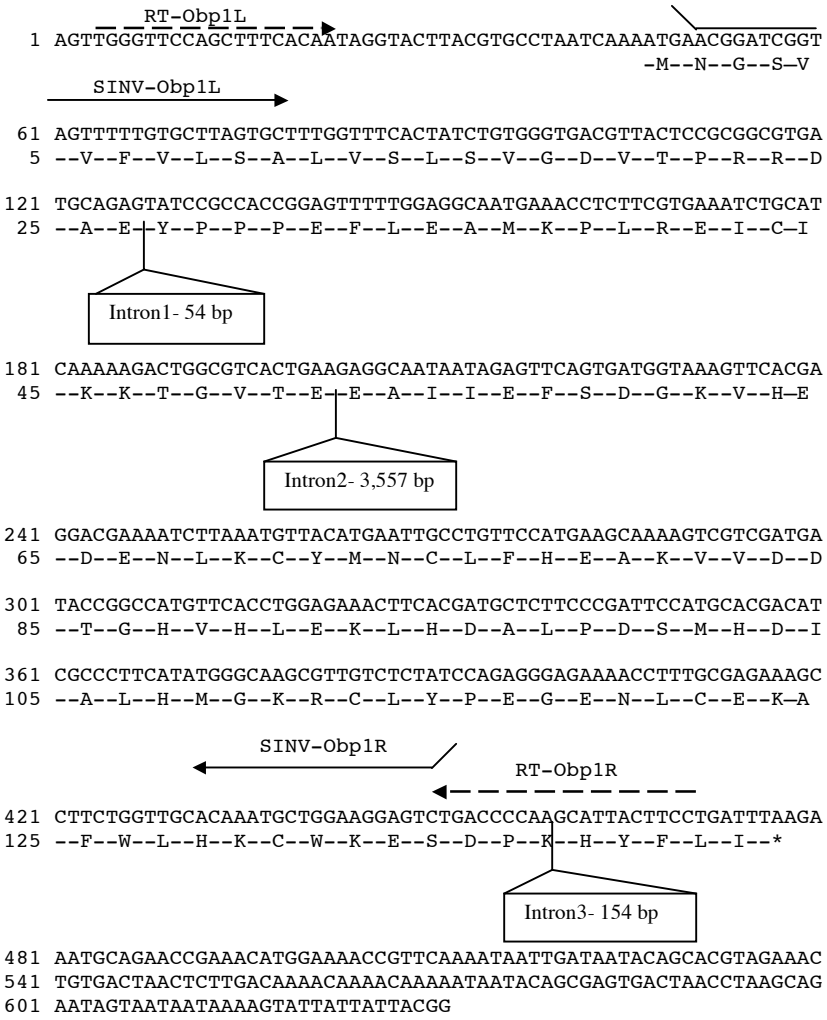

Figure 4.1 cDNA sequences of *Obp1* and *Obp7* genes in *Ae. aegypti*. **(A)** *Aaeg-Obp1* cDNA **(B)** *Aaeg-Obp7*cDNA. Deduced peptide sequences are also shown. Solid arrows depict the primers used for recombinant dsSIN virus plasmid construction, and dashed arrows indicate primers used for non-quantitative RT-PCR. The locations of introns are indicated as box inserts and the lengths of intron sequences are shown in the boxes.

(B)

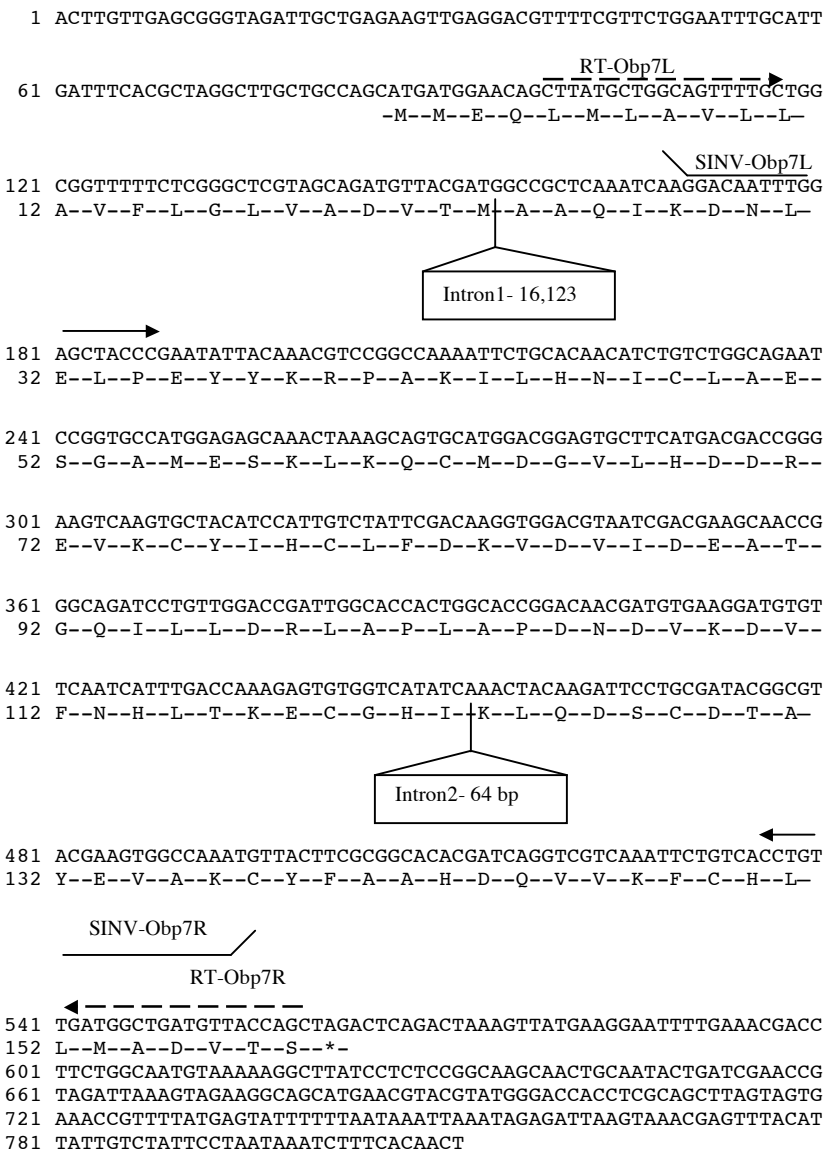


```
  1 ACTTGTTGAGCGGGTAGATTGCTGAGAAGTTGAGGACGTTTTCGTTCTGGAATTTGCATT

 61 GATTTCACGCTAGGCTTGCTGCCAGCATGATGGAACAGCTTATGCTGGCAGTTTTGCTGG
                            -M--M--E--Q--L--M--L--A--V--L--L-

121 CGGTTTTTCTCGGGCTCGTAGCAGATGTTACGATGGCCGCTCAAATCAAGGACAATTTGG
 12 A--V--F--L--G--L--V--A--D--V--T--M--A--A--Q--I--K--D--N--L-

181 AGCTACCCGAATATTACAAACGTCCGGCCAAAATTCTGCACAACATCTGTCTGGCAGAAT
 32 E--L--P--E--Y--Y--K--R--P--A--K--I--L--H--N--I--C--L--A--E--

241 CCGGTGCCATGGAGAGCAAACTAAAGCAGTGCATGGACGGAGTGCTTCATGACGACCGGG
 52 S--G--A--M--E--S--K--L--K--Q--C--M--D--G--V--L--H--D--D--R--

301 AAGTCAAGTGCTACATCCATTGTCTATTCGACAAGGTGGACGTAATCGACGAAGCAACCG
 72 E--V--K--C--Y--I--H--C--L--F--D--K--V--D--V--I--D--E--A--T--

361 GGCAGATCCTGTTGGACCGATTGGCACCACTGGCACCGGACAACGATGTGAAGGATGTGT
 92 G--Q--I--L--L--D--R--L--A--P--L--A--P--D--N--D--V--K--D--V--

421 TCAATCATTTGACCAAAGAGTGTGGTCATATCAAACTACAAGATTCCTGCGATACGGCGT
112 F--N--H--L--T--K--E--C--G--H--I--K--L--Q--D--S--C--D--T--A-

481 ACGAAGTGGCCAAATGTTACTTCGCGGCACACGATCAGGTCGTCAAATTCTGTCACCTGT
132 Y--E--V--A--K--C--Y--F--A--A--H--D--Q--V--V--K--F--C--H--L-

541 TGATGGCTGATGTTACCAGCTAGACTCAGACTAAAGTTATGAAGGAATTTTGAAACGACC
152 L--M--A--D--V--T--S--*-
601 TTCTGGCAATGTAAAAAGGCTTATCCTCTCCGGCAAGCAACTGCAATACTGATCGAACCG
661 TAGATTAAAGTAGAAGGCAGCATGAACGTACGTATGGGACCACCTCGCAGCTTAGTAGTG
721 AAACCGTTTTATGAGTATTTTTTAATAAATTAAATAGAGATTAAGTAAACGAGTTTACAT
781 TATTGTCTATTCCTAATAAATCTTTCACAACT
```

(A)

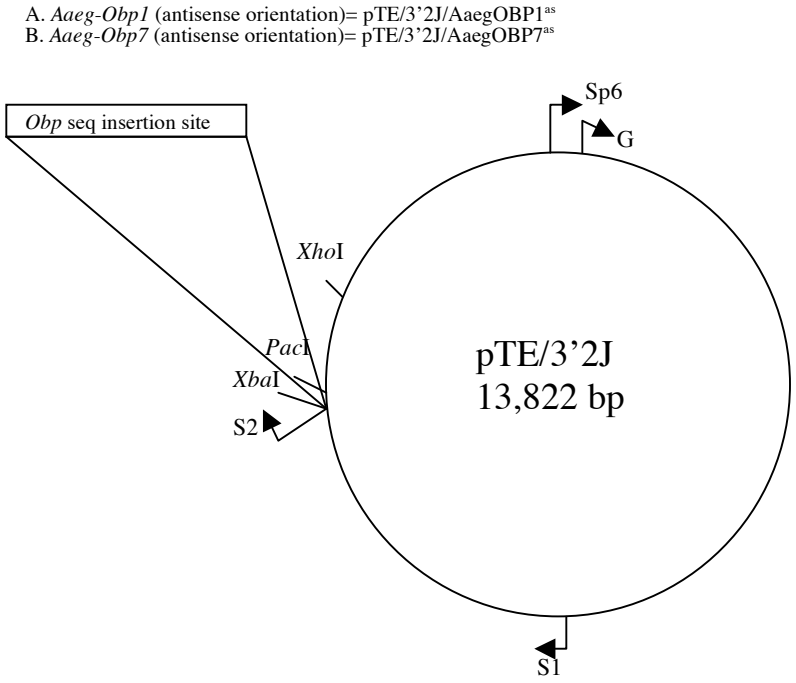

(B)

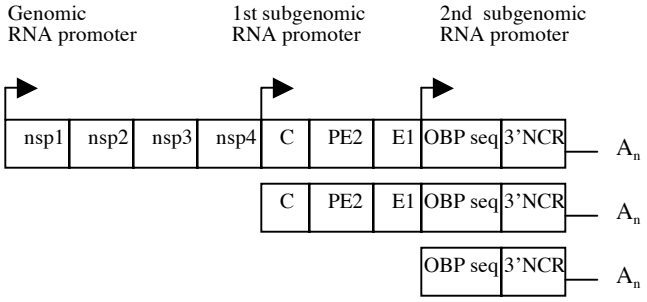

Figure 4.2 Recombinant pTE/3'2J viral plasmids and RNA transcripts produced upon viral infection. **(A)** Plasmid map of pTE/3'2J and construction of recombinant viral plasmids for *Obp* genes. The PCR amplified antisense transcript of *Aaeg-Obp1* and *Aaeg-Obp7* genes were cloned into the *Xba*I and *Pac*I sites at the 3' end of the second subgenomic promoter (S2), producing pTE/3'2J/AaegOBP1^{as} or pTE/3'2J/AaegOBP7^{as} recombinant viral plasmids. The location of the SP6 promoter used for *in vitro* transcription, genomic RNA promoter (G), 1st subgenomic RNA promoter (S1), and 2nd subgenomic RNA promoter (S2) are also indicated. **(B)** Representation of the genomic

and subgenomic transcripts produced by the recombinant dsSIN viruses upon infection. Double stranded RNAs are produced during the virus life cycle. Parts of the construct are not to scale. Nsp 1-4: nonstructural protein 1-4, C: capsid, PE2: precursor envelope glycoprotein 2, E1: envelope glycoprotein 1, NCR: noncoding region.

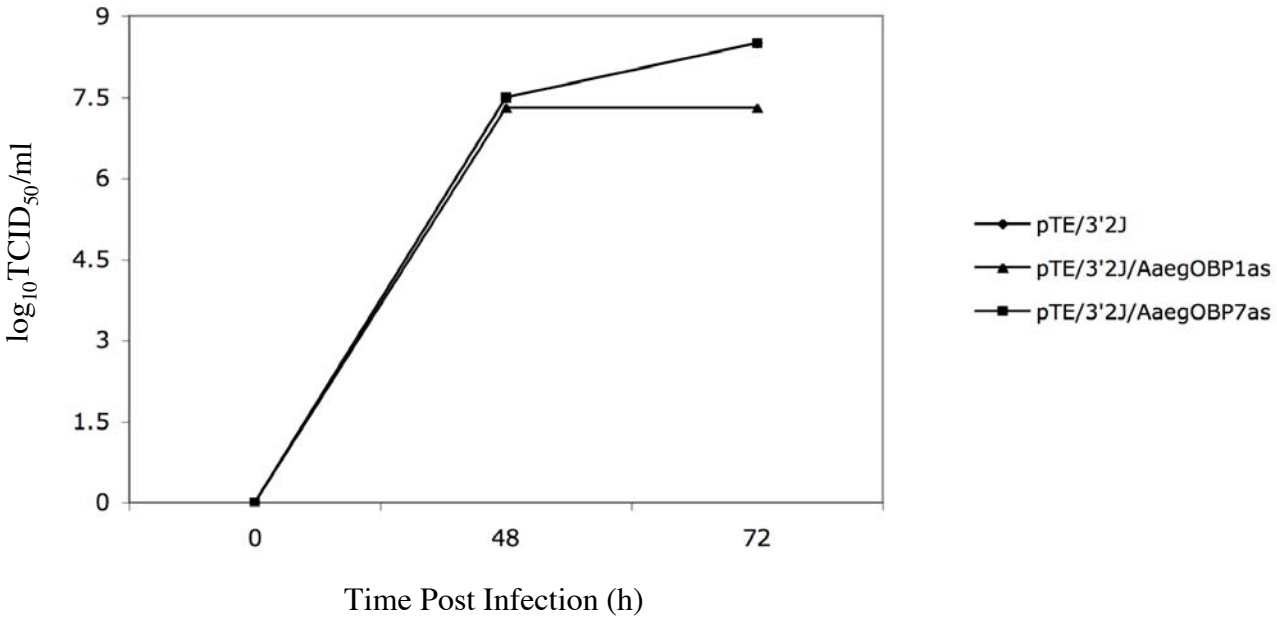

Figure 4.3 pTE/3’2J, pTE/3’2J/AaegOBP1^{as} and pTE/3’2J/AaegOBP7^{as} virus growth in C6/36 cells. C6/36 cells were infected with each recombinant virus and the virus titer was determined at 48 and 72 h p.i. in BHK-21 cells by using the end-point dilution method ($TCID_{50}$) (see Materials and methods). pTE/3’2J and pTE/3’2J/AaegOBP7^{as} virus titers show overlapping data points at 48 and 72 h p.i.

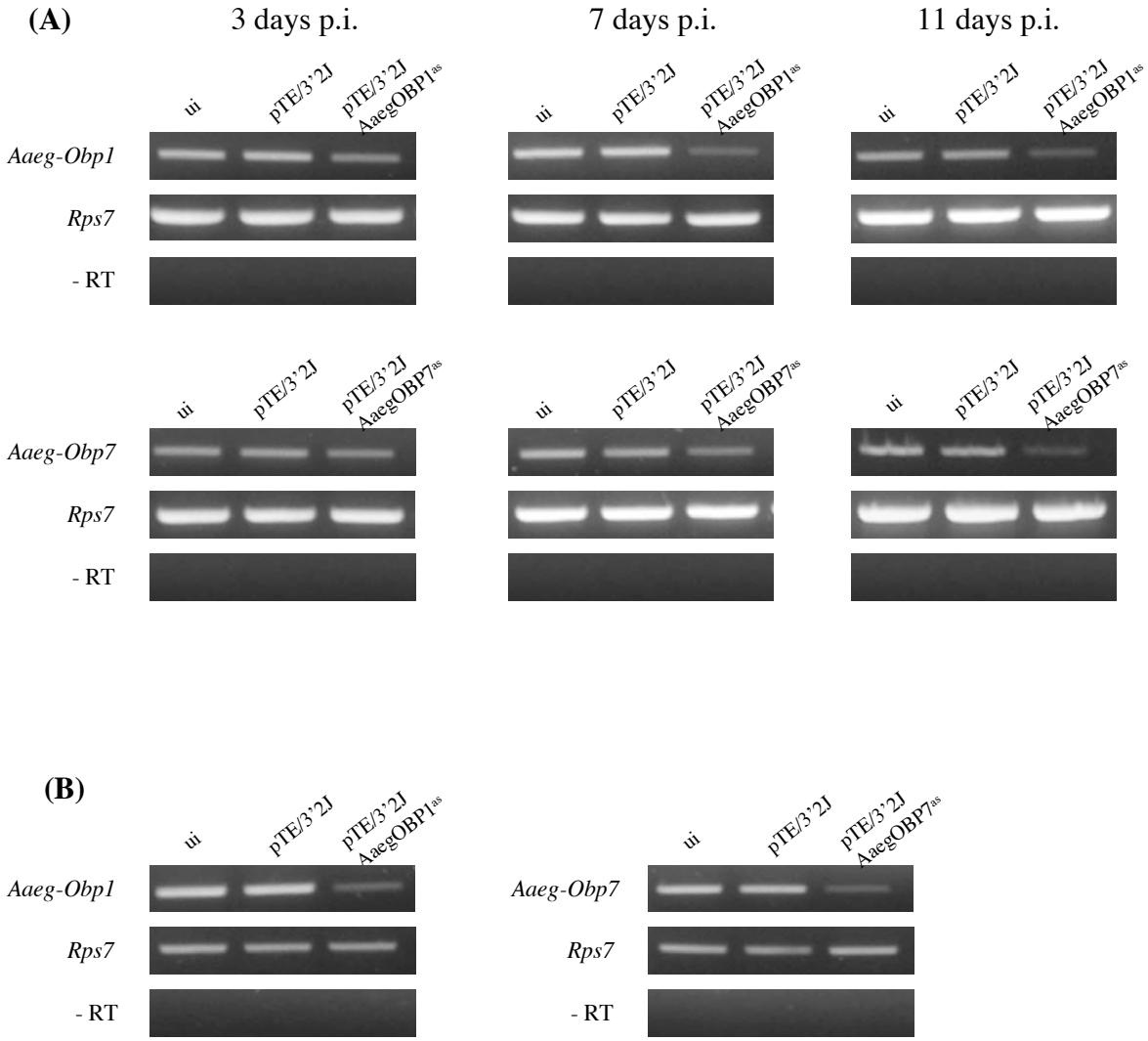

Figure 4.4 Non-quantitative RT-PCR analyses of *Aaeg-Obp1* and *Aaeg-Obp7* mRNA levels in uninfected, pTE/3'2J, pTE/3'2J/AaegOBP1^{as} or pTE/3'2J/AaegOBP7^{as} virus-inoculated *Ae. aegypti* female mosquitoes. **(A)** mRNA levels at 3, 7, and 11 days p.i. in whole mosquitoes. **(B)** mRNA levels in the head tissues (antenna, maxillary palp and proboscis) of female mosquitoes at 11 days p.i.

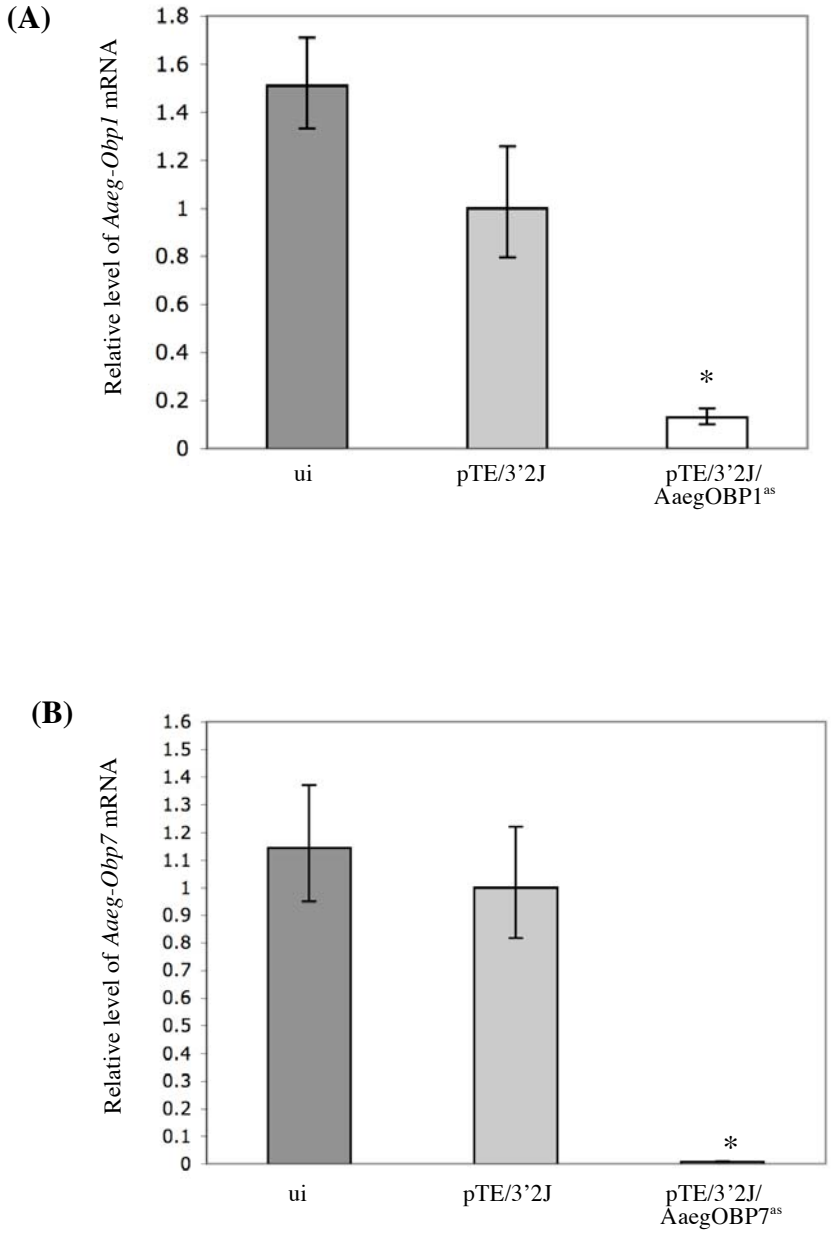

Figure 4.5 Real-time PCR detection of *Aaeg-Obp1* and *Aaeg-Obp7* mRNA levels in uninfected, pTE/3'2J, pTE/3'2J/AaegOBP1^{as} or pTE/3'2J/AaegOBP7^{as} virus-inoculated female *Ae. aegypti* mosquitoes at 11 days p.i. Total RNA from head tissues were used to synthesize cDNA for the detection of *Aaeg-Obp1* mRNA levels in pTE/3'2J/AaegOBP1^{as}

virus-inoculated female mosquitoes **(A)**, and *Aaeg-Obp7* mRNA levels in pTE/3'2J/AaegOBP7^{as} virus-inoculated female mosquitoes **(B)**, and compared to that of uninfected and pTE/3'2J control virus-inoculated females. Vertical bars represent the standard deviation representing the range of variation in three independent experiments. Asterisks indicate significant differences ($P < 0.05$). See Tables 4.1 and 4.2 for C_T, ΔC_T, $\Delta\Delta C_T$ and $2^{-\Delta\Delta CT}$ values.

Table 4.1 Relative level of *Aaeg-Obp7* mRNA in female antenna, maxillary palp and proboscis, legs and body devoid of appendages

Tissue	*Obp7*C_T	*Rps7*C_T	ΔC_T (Avg. *Obp7*C_T - Avg. *Rps7*C_T)	$\Delta\Delta C_T$ (Avg. ΔC_T - Avg. $\Delta C_{T,MPP}$)	Normalized *Obp7* amount relative to MPP $2^{-\Delta\Delta CT}$
Antenna	19.048	22.509	-3.461		
	18.91	22.487	-3.577		
	18.97	22.489	-3.519		
Average	18.976 +/- 0.069	22.495 +/- 0.012	- 3.519 +/- 0.07	-8.017 +/- 0.07	259 (246.76-270)
Max. Palp &	25.164	20.734	4.43		
Proboscis	25.241	20.747	4.494		
(MPP)*	25.302	20.731	4.571		
Average	25.236 +/- 0.069	20.738 +/- 0.008	4.498 +/- 0.07	0.00 +/- 0.07	1 (0.952-1.0497)
Legs	31.504	19.787	11.717		
	31.665	19.766	11.899		
	31.522	19.801	11.721		
Average	31.564 +/- 0.088	19.785 +/- 0.017	11.779 +/- 0.09	7.281 +/- 0.09	0.006 (0.006-0.0068)
Body -	32.485	18.706	13.779		
appendages	32.294	18.716	13.578		
	32.434	18.794	13.64		
Average	32.404 +/- 0.099	18.739 +/- 0.048	13.666 +/- 0.11	9.168 +/- 0.11	0.0017 (0.00161-0.00187)

Data presentation is according to Livak and Schmittgen (2001), with average and standard deviation (SD). Data in the final column are presented as average and a range specified by $2^{-(\Delta\Delta CT+SD)}$ and $2^{-(\Delta\Delta CT-SD)}$.

* represents the calibrator.

Table 4.2 Relative level of *Aaeg-Obp1* mRNA in female antenna, maxillary palp and proboscis, legs and body devoid of appendages

Tissue	*Obp1*C_T	*Rps7*C_T	ΔC_T (Avg. *Obp1*C_T - Avg. *Rps7*C_T)	$\Delta\Delta C_T$ (Avg. ΔC_T - Avg. $\Delta C_{T.MPP}$)	Normalized *Obp1* amount relative to MPP $2^{-\Delta\Delta CT}$
Antenna	18.427	22.509	-4.082		
	18.306	22.487	-4.181		
	18.28	22.489	-4.209		
Average	18.338 +/- 0.079	22.495 +/- 0.012	- 4.157 +/- 0.08	-8.909 +/- 0.08	480 (454.77-508.11)
Max. Palp & Proboscis (MPP)*	25.504	20.734	4.77		
	25.591	20.747	4.844		
	25.374	20.731	4.643		
Average	25.49 +/- 0.109	20.738 +/- 0.008	4.752 +/- 0.11	0.00 +/- 0.11	1 (0.926-1.079)
Legs	25.808	19.787	6.021		
	25.823	19.766	6.057		
	25.862	19.801	6.061		
Average	25.831 +/- 0.028	19.785 +/- 0.017	6.046 +/- 0.033	1.294 +/- 0.033	0.408 (0.398-0.417)
Body - appendages	29.56	18.706	10.854		
	29.581	18.716	10.865		
	29.644	18.794	10.85		
Average	29.595 +/- 0.043	18.739 +/- 0.048	10.856 +/- 0.065	6.104 +/- 0.065	0.015 (0.0138-0.0152)

Data presentation is according to Livak and Schmittgen (2001), with average and standard deviation (SD). Data in the final column are presented as average and a range specified by $2^{-(\Delta\Delta CT+SD)}$ and $2^{-(\Delta\Delta CT-SD)}$.

* represents the calibrator.

Table 4.3 Relative level of *Aaeg-Obp1* mRNA in olfactory tissues of uninfected, pTE/3'2J and pTE/3'2J/AaegOBP1^{as} virus-inoculated mosquitoes

Sample		*Obp1*C_T	*Rps7*C_T	ΔC_T (*Obp1*C_T-*Rps7*C_T)	$\Delta\Delta C_T$ (ΔC_T-$\Delta C_{Tcalibrator}$)	Normalized *Obp1* amount relative to the calibrator, $2^{-\Delta\Delta CT}$
uninfected	replicate1	15.445	17.056	-1.611		
	replicate2	15.378	17.345	-1.966		
	replicate3	15.378	17.673	-2.295		
	Average	15.4 +/- 0.02	17.358 +/- 0.178	-1.958 +/- 0.18	-0.595 +/- 0.18	1.51 (1.33-1.71)
pTE/3'2J control (calibrator)	replicate1	16.323	17.607	-1.283		
	replicate2	16.392	17.542	-1.15		
	replicate3	15.469	17.124	-1.655		
	Average	16.06 +/- 0.297	17.424 +/- 0.151	-1.363 +/- 0.33	0 +/- 0.33	1 (0.796-1.257)
pTE/3'2J/ AaegOBP1^{as}	replicate1	19.452	17.86	1.591		
	replicate2	18.503	17.109	1.393		
	replicate3	19.29	17.523	1.767		
	Average	19.081 +/- 0.293	17.497 +/- 0.217	1.584 +/- 0.365	2.947 +/- 0.365	0.13 (0.1-0.167)

Data presentation is according to Livak and Schmittgen (2001), with average and standard deviation (SD). Data in the final column are presented as average and a range specified by $2^{-(\Delta\Delta CT+SD)}$ and $2^{-(\Delta\Delta CT-SD)}$. All replicates are biological replicates.

Table 4.4 Relative level of *Aaeg-Obp7* mRNA in olfactory tissues of uninfected, pTE/3'2J and pTE/3'2J/AaegOBP7^{as} virus-inoculated mosquitoes

Sample		*Obp7*C_T	*Rps7*C_T	ΔC_T (*Obp7*C_T-*Rps7*C_T)	$\Delta\Delta C_T$ (ΔC_T-$\Delta C_{Tcalibrator}$)	Normalized *Obp7* amount relative to the calibrator, $2^{-\Delta\Delta CT}$
uninfected	replicate1	17.574	17.056	0.518		
	replicate2	16.893	17.345	-0.451		
	replicate3	17.182	17.673	-0.492		
	Average	17.216 +/- 0.197	17.358 +/- 0.178	-0.142 +/- 0.266	-0.193 +/- 0.266	1.143 (0.95-1.37)
pTE/3'2J control (calibrator)	replicate1	17.968	17.607	0.361		
	replicate2	17.246	17.542	-0.296		
	replicate3	17.214	17.124	0.09		
	Average	17.476 +/- 0.246	17.424 +/- 0.151	0.052 +/- 0.289	0 +/- 0.289	1 (0.818-1.22)
pTE/3'2J/ AaegOBP7^{as}	replicate1	24.273	17.145	7.128		
	replicate2	23.893	17.19	6.703		
	replicate3	24.433	17.403	7.03		
	Average	24.199 +/- 0.16	17.246 +/- 0.08	6.953 +/- 0.179	6.902 +/- 0.179	0.008 (0.007-0.0094)

Data presentation is according to Livak and Schmittgen (2001), with average and standard deviation (SD). Data in the final column are presented as average and a range specified by $2^{-(\Delta\Delta CT+SD)}$ and $2^{-(\Delta\Delta CT-SD)}$. All replicates are biological replicates.

Chapter 5

Summary and Future Directions

This study demonstrates the identification and characterization of two *Obp* genes in the mosquito species *Anopheles stephensi*, which is the major malaria vector in Asia. The expression profiles of the *Obp1* and *Obp7* genes indicate that they are highly expressed in the antennae of female mosquitoes. Similar expression profile is also observed in another mosquito species, *Aedes aegypti*. These results are consistent with what was previously determined in *Anopheles gambiae* and indicate that both genes are possibly involved in olfaction-mediated behavior in diverse mosquito species. This study provides the molecular foundation for further analysis of the function of these *Obp* genes in *An. stephensi* and *Ae. aegypti*, which are important disease vectors and much more amenable to genetic and physiological studies than *An. gambiae*.

The discovery of the significant reduction of *Obp1* and *Obp7* mRNA levels in maxillary palp and proboscis after blood-feeding is novel and suggests that these two genes may be involved in behaviors relevant to blood-feeding. This is significant in light of recent studies indicating that maxillary palp is likely an important and underestimated olfactory organ in mosquitoes. Future experiments that investigates the spatial expression profile of these genes within olfactory as well as other chemosensory organs may show where they are specifically expressed in the sensilla. Moreover, ligand-binding experiments and structural studies will further identify the potential chemical compounds that these OBPs bind and reveal possible mechanisms that mediate odorant-OBP interaction. This will be an important step towards developing attractants and/or repellents that can be used to interfere with mosquito host-seeking behavior.

The comparative approach used in this study also revealed potential regulatory sequences of *Obp1* and *Obp7* genes. Although the TFBSs determined in the regulatory regions of these genes are highly significant and some are found to be involved in the

development of olfactory organs or odorant receptor gene regulation in *Drosophila*, our results need to be supported experimentally. Deletion constructs containing different lengths of the 5'upstream sequences of the *Obp1* and *Obp7* genes can be prepared for functional analysis of the promoter regions of these genes. This will provide new insights into the regulation of *Obp* genes in mosquito olfaction that may provide the basis for their biological adaptations and behavioral differences.

This study also established an effective method to knockdown *Obp1* and *Obp7* genes in the adult olfactory organs of *Ae. aegypti*. This is an important step towards assigning biological functions of *Obp* genes involved in mosquito host-seeking behavior. Mosquitoes with disrupted *Obp* gene function can be generated and examined for their behavioral response to known attractants or repellents. The established method can also be used for other genes of the mosquito olfactory systems, such as odorant receptors, or on pre-adult mosquito stages.

Overall, the results of this research provide useful information as well as novel and effective approaches to study the molecular aspects of olfaction in mosquitoes. With the improved knowledge on mosquito olfactory systems, effective tools can be developed to control the transmission of mosquito-borne diseases.

References

Acree F. Jr., Turner, R.B, Couck, H.K., Beroza, M., and Smith, N. (1968) L-Lactic acid: a mosquito attractant isolated from humans. *Science* **161**: 1346-1347.

Adams, M.D., Celniker, S.E., Holt, R.A., Evans, C.A., Gocayne, J.D., Amanatides, P.G., Scherer, S.E., Li, P.W., Hoskins, R.A., Galle, R.F., George, R.A., Lewis, S.E., Richards, S., Ashburner, M., Henderson, S.N., Sutton, G.G., Wortman, J.R., Yandell, M.D., Zhang, Q., Chen, L.X., Brandon, R.C., Rogers, Y.H., Blazej, R.G., Champe, M., Pfeiffer, B.D., Wan, K.H., Doyle, C., Baxter, E.G., Helt, G., Nelson, C.R., Gabor, G.L., Abril, J.F., Agbayani, A., An, H.J., Andrews-Pfannkoch, C., Baldwin, D., Ballew, R.M., Basu, A., Baxendale, J., Bayraktaroglu, L., Beasley, E.M., Beeson, K.Y., Benos, P.V., Berman, B.P., Bhandari, D., Bolshakov, S., Borkova, D., Botchan, M.R., Bouck, J., Brokstein, P., Brottier, P., Burtis, K.C., Busam, D.A., Butler, H., Cadieu, E., Center, A., Chandra, I., Cherry, J.M., Cawley, S., Dahlke, C., Davenport, L.B., Davies, P., de Pablos, B., Delcher, A., Deng, Z., Mays, A.D., Dew, I., Dietz, S.M., Dodson, K., Doup, L.E., Downes, M., Dugan-Rocha, S., Dunkov, B.C., Dunn, P., Durbin, K.J., Evangelista, C.C., Ferraz, C., Ferriera, S., Fleischmann, W., Fosler, C., Gabrielian, A.E., Garg, N.S., Gelbart, W.M., Glasser, K., Glodek, A., Gong, F., Gorrell, J.H., Gu, Z., Guan, P., Harris, M., Harris, N.L., Harvey, D., Heiman, T.J., Hernandez, J.R., Houck, J., Hostin, D., Houston, K.A., Howland, T.J., Wei, M.H., Ibegwam, C., et al. (2000) The genome sequence of *Drosophila melanogaster*. *Science* **287**: 2185-2195.

Adelman, Z.N., Blair, C.D., Carlson, J.O., Beaty, B.J. and Olson, K.E. (2001) Sindbis virus-induced silencing of dengue viruses in mosquitoes. *Insect Mol Biol* **10**: 265-273.

Altschul, S.F., Gish, W., Miller, W., Myers, E.W. and Lipman, D.J. (1990) Basic local alignment search tool. *J Mol Biol* **215**: 403-410.

Anton, S. and Hansson, B.S. (1996) Antennal lobe interneurons in the desert locust *Schistocerca gregaria* (Forskal): processing of aggregation pheromones in adult males and females. *J Comp Neuro* **370**: 85-96.

Beehler, J., Lohr, S. and DeFoliart, G. (1992) Factors influencing oviposition in *Aedes triseriatus* (Diptera: Culicidae). *Great Lakes Entomol* **25**: 259-264.

Bendtsen, J.D., Nielsen, H., von Heijne, G. and Brunak, S. (2004) Improved prediction of signal peptides: SignalP 3.0. *J Mol Biol* **340**: 783-795.

Bently, M.D. and Day, J.D. (1989) Chemical ecology and behavioral aspects of mosquito oviposition. *Annu Rev Entomol* **34**: 401-421.

Benton, R. (2006) On the ORigin of smell: odorant receptors in insects. *Cell Mol Life Sci* **63**: 1579-1585.

Benton, R., Sache, S., Michnick, S.W. and Vosshall, L.B. (2006) Atypical membrane topology and heteromeric function of *Drosophila* odorant receptors in vivo. *Plos Biol* **4**: 240-257.

Besansky, N. J. and Powell, J. R. (1992) Reassociation kinetics of *Anopheles gambiae* (Diptera: Culicidae) DNA. *J Med Entomol* **29**: 125-128.

Biessmann H., Walter M. F., Dimitratos S. and Woods D. (2002). Isolation of cDNA clones encoding putative odourant binding proteins from the antennae of the malaria-transmitting mosquito, *Anopheles gambiae*. *Insect Mol Biol* **11**: 123-132.

Biessmann, H., Nguyen, Q.K., Le, D. and Walter, M.F. (2005) Microarray-based survey of a subset of putative olfactory genes in the mosquito *Anopheles gambiae*. *Insect Mol Biol* **14**: 575-589.

Boekhoff, I., Strotmann, J., Raming, K., Tareilus, E. and Breer, H. (1990a) Odorant-sensitive phospholipase C in insect antennae. *Cell Signal* **2**: 49-56.

Boekhoff, I., Raming, K. and Breer, H. (1990b) Pheromone-induced stimulation of inositoltriphosphate formation in insect antennae is mediated by G-proteins. *J Comp Physiol B* **160**: 99-103.

Boekhoff, I., Seifert, E., Goggerle, S., Lindermann, M. Kruger, B-W. and Breer, H. (1993) Pheromone-induced second messenger signaling in insect antennae. *Insect Biochem Mol Biol* **23**: 757-762.

Bohbot, J. and Vogt, R.G. (2005) Antennal expressed genes of the yellow fever mosquito (*Aedes aegypti* L.); characterization of odorant-binding protein 10 and takeout. *Insect Biochem Mol Biol* **35**: 961-979.

Bohbot, J., Pitts, R.J., Kwon, H.W., Rutzler, M., Robertson, H.M. and Zwiebel, L.J. (2007) Molecular characterization of the *Aedes aegypti* odorant receptor gene family. *Insect Mol Biol* **16**: 525-537.

Bowen M.F. and Romo, J. (1995a) Host-seeking and sugar-feeding in the autogenous mosquito *Aedes bahamensis* (Diptera: Culicidae). *J Vector Ecology* **20**: 211-215.

Braks, M.A.H and Takken, W. (1999) Incubated human sweat but not fresh sweat attracts the malaria mosquito *Anopheles gambiae sensu stricto*. *J Chem Ecology* **25**: 663-672.

Braks, M.A.H., Meijerink, J. and Takken, W. (2001) The response of the malaria mosquito, *Anopheles gambiae*, to two components of human sweat, ammonia and L-lactic acid. *Physiol Entomol* **26**: 142-148.

Breathnach, R. and Chambon, P. (1981) Organization and expression of eukaryotic split genes coding for proteins. *Annu Rev Biochem* **50**: 349-383.

Breer, H., Raming, K. and Boekhoff, I. (1988) G-proteins in the antennae of insects. *Naturwiss* **75**: 627.

Breer, H., Boekhoff, I. and Tareilus, E. (1990) Rapid kinetics of second messenger formation in olfactory transduction. *Nature* **345**: 65-68.

Brudno M., Do C. B., Cooper G. M., Kim M. F., Davydov E. ; NISC Comparative Sequencing Program, Green E. D., Sidow A. and Batzoglou S. (2003) LAGAN and Multi-LAGAN: efficient tools for large-scale multiple alignment of genomic DNA. *Genome Res* **13**: 721-731.

Buck, L. and Axel, R. (1991) A novel multigene family may encode odorant receptors: A molecular basis for odor recognition. *Cell* **65**: 175-187.

Butenandt, A., Beckmann, R., Stamm, D. and Hecker, E. (1959) On the sexattractant of silkworm moth *Bombyx mori*. Isolation and structure. *Z Natuforsch* **B14**: 283-284.

Carlson, J.R. (1996) Olfaction in Drosophila: from odor to behavior. *Trends Genet* **12**: 175-180.

Cherbas, L. and Cherbas, P. (1993) The arthropod initiator: the capsite consensus plays an important role in transcription. *Insect Biochem Mol Biol* **23**: 81-90.

Clements, A.N. (2000) The biology of mosquitoes. Volume 1: Development, nutrition and reproduction. CABI Publishing, Wallingford, UK.

Clyne, P.J., Warr, C.G., Freeman, M.R., Lessing, D., Kim, J. and Carlson, J.R. (1999) A novel family of divergent seven-transmembrane proteins: candidate odorant receptors in *Drosophila*. *Neuron* **22**: 327-338.

Coates, C.J., Jasinskiene, N., Miyashiro, L. and James, A.A. (1998) Mariner transposition and transformation of the yellow fever mosquito, *Aedes aegypti*. *Proc Natl Acad Sci USA* **95**: 3748-3751.

Costantini, C., Gibson, G., Sagnon, N., Della Torre, A., Brady, J. and Coluzzi, M. (1996) Mosquito responses to carbon dioxide in a west African Sudan savanna village. *Med Vet Entomol* **10**: 220-227.

Cork, A. (1996) Olfactory basis of host location by mosquitoes and other Haematophagous *Diptera*. *Ciba Foundation Symp* **200**: 71-84.

Cork, A. and Park, K.C. (1996) Identification of electrophysiologically active compounds for the malaria mosquito, *Anopheles gambiae*, in human sweat extracts. *Med Vet Entomol* **10**: 269-276.

Cuff, J.A. and Barton, G.J. (1999) Evaluation and improvement of multiple sequence methods for protein secondary structure prediction. *Proteins* **34**: 508-519.

Curtis, C.F. (1996) Introduction1: An overview of mosquito biology, behaviour and importance. *Ciba Foundation Symp* **200**: 3-7.

Daga, A., Karlovich, C.A., Dumstrei, K. and Banerjee, U. (1996) Patterning of cells in the *Drosophila* eye by Lozenge, which shares homologous domains with AML1. *Genes Dev* **10:** 1194-1205.

Danty, E., Briand, L., Michard-Vanhee, C., Perez, V., Arnold, G., Gaudemer, O., Huet, D., Huet, J.C., Ouali, C., Masson, C. and Pernollet, J.C. (1999) Cloning and expression of a queen pheromone-binding protein in the honeybee: an olfactory-specific, developmentally regulated protein. *J Neurosci* **19**: 7468-7475.

Day, J.F. and Van Handel, E. (1986) Differences between the nutritional reserves of laboratory-maintained and field-collected adult mosquitoes. *J Am Moqs Control Assoc* **2**: 154-157.

Dhileepan, K. (1997) Physical factors and chemical cues in the oviposition behavior of arboviral vectors *Culex annulirostris* and *Culex molestus* (Diptera: Culicidae). *Environmental Entomol* **26**: 318-326.

de Bruyne, M., Clyne, P.J. and Carlson, J.R. (1999) Odor coding in a model olfactory organ: the *Drosophila* maxillary palp. *J Neurosci* **19**: 4520-4532.

de Bruyne, M., Foster, K. and Carlson, J.R. (2001) Odor coding in the *Drosophila* antenna. *Neuron* **30**: 537-552.

de Bruyne, M. and Warr, C.G. (2006) Molecular and cellular organization of insect chemosensory neurons. *Bioessays* **28**: 23-34.

Dekker, T. and Takken, W. (1998) Differential responses of mosquito sibling species *Anopheles arabiensis* and *An. quadriannulatus* to carbon dioxide, a man or a calf. *Med Vet Entomol* **12**: 136-140.

Dekker, T., Steib, B., Carde, R.T. and Geier, M. (2002) L-lactic acid: a human-signifying host cue for the anthropophilic mosquito *Anopheles gambiae*. *Med Vet Entomol* **16**: 91-98.

Dekker, T., Geier, M. and Carde, R.T. (2005) Carbon dioxide instantly sensitizes female yellow fever mosquitoes to human skin odours. *J Exp Biol* **208**: 2963-2972.

Dobritsa, A.A., van der Goes van Naters, W., Warr, C.G., Steinbrecht, R.A. and Carlson, J.R. (2003) Integrating the molecular and cellular basis of odor coding in the *Drosophila* antenna. *Neuron* **37**: 827-841.

Du, G. and Prestwich, G.D. (1995) Protein structure encodes the ligand binding specificity in pheromone binding proteins. *Biochemistry* **34**: 8726-8732.

Ernst, K.D., Boeckh, J. and Boeckh, V. (1977) A neuroanatomical study on the organization of the central antennal pathways in insects. *Cell Tissue Res* **176**: 285-306.

Feng, L. and Prestwich, G.D. (1997) Expression and characterization of a lepidopteran general odorant binding protein. *Insect Biochem Mol Biol* **27**: 405-412.

Foster, W.A. (1995) Mosquito sugar feeding and reproductive energetics. *Annu Rev Entomol* **40**: 443-474.

Fox, A.N., Pitts, R.J, Robertson, H.M., Carlson, J. R. and Zwiebel, L.J. (2001) Candidate odorant receptors from the malaria vector mosquito *Anopheles gambiae* and evidence of down-regulation in response to blood feeding. *Proc Natl Acad Sci USA* **98**: 14693-14697.

Galindo, K. and Smith, D.P. (2001) A large family of divergent *Drosophila* odorant-binding proteins expressed in gustatory and olfactory sensilla. *Genetics* **159**: 1059-1072.

Gao, Q. and Chess, A. (1999) Identification of candidate *Drosophila* olfactory receptors from genomic DNA sequence. *Genomics* **60**: 31-39.

Gao, Q., Yuan, B. and Chess, A. (2000) Convergent projections of *Drosophila* olfactory neurons to specific glomeruli in the antennal lobe. *Nat Neurosci* **3**: 780-785.

Geier, M., Sass, H. and Boeckh, J. (1996) A search for components in human body odour that attract females of *Aedes aegypti. Ciba Foundation Symp* **200**: 132-148.

Ghaninia, M., Hansson, B.S. and Ignell, R. (2007) The antennal lobe of the African malaria mosquito, *Anopheles gambiae* - innervation and three-dimensional reconstruction. *Arthropod Struct Dev* **36**: 23-39.

Gibson, G. (1996) Genetics, ecology and behaviour of anophelines. *Ciba Foundation Symp* **200**: 22-37.

Gillies, M.T. (1980) The role of carbon dioxide in host-feeding my mosquitoes (Diptera: Culicidae) *Bull Entomol Res* **70**: 525-532.

Godfrey, P.A., Malnic, B. and Buck, L.B. (2004) The mouse olfactory receptor gene family. *Proc Natl Acad Sci USA* **101**: 2156-2161.

Goldman, A.L., Van der Goes van Naters, W., Lessing, D., Warr, C.G. and Carlson, J.R. 2005. Coexpression of two functional odor receptors in one neuron. *Neuron* **45**: 661-666.

Graham L. A., and Davies P. L. (2002) The odorant-binding proteins of Drosophila melanogaster: annotation and characterization of a divergent gene family. *Gene* **292:** 43-55.

Grant, A.J. and O'Connell, R.J. (1996) Electrophysiological responses from receptor neurons in mosquito maxillary palp sensilla. *Ciba Found Symp* **200**: 233-48.

Hallem, E.A., Nicole Fox, A., Zwiebel, L.J. and Carlson, J.R. (2004a) Olfaction: mosquito receptor for human-sweat odorant. *Nature* **427**: 212-213.

Hallem, E.A., Ho, M.G. and Carlson, J.R. (2004b) The molecular basis of odor coding in the Drosophila antenna. *Cell* **117**: 965-979.

Hallem, E.A. and Carlson, J.R. (2004) The odor coding system of Drosophila. *Trends Genet* **20**: 453-459.

Hahn, C.S., Hahn, Y.S., Braciale, T.J. and Rice, C.M. (1992) Infectious Sindbis virus transient expression vectors for studying antigen processing and presentation. *Proc Natl Acad Sci USA* **89**: 2679-2683.

Harbach, R.E. and Kitching, I.J. (1998) Phylogeny and classification of the Culicidae (Diptera). *Systematic Entomol* **23**: 327-370.

Hekmat-Scafe, D.S., Steinbrecht, R.A. and Carlson, J.R. (1997) Coexpression of two odorant-binding protein homologs in *Drosophila*: implications for olfactory coding. *J Neurosci* **17**: 1616-1624.

Hekmat-Scafe, D.S., Scafe, C.R., McKinney, A.J. and Tanouye, M.A. (2002) Genome-wide analysis of the odorant-binding protein gene family in *Drosophila melanogaster*. *Genome Res* **12:** 1357-1369.

Higgs, S., Powers, A.M. and Olson, K.E. (1993) Alphavirus expression systems: applications to mosquito vector studies. *Parasitol Today* **9**: 444-452.

Hildebrand, J.G. and Shepherd, G.M. (1997) Mechanisms of olfactory discrimination: converging evidence for common principles across phyla. *Annu Rev Neurosci* **20**: 595-631.

Hill, C.A., Fox, A.N., Pitts, R.J., Kent, L.B., Tan, P.L., Chrystal, M.A., Cravchik, A., Collins, F.H., Robertson, H.M. and Zwiebel, L.J. (2002) G protein-coupled receptors in *Anopheles gambiae*. *Science* **298**: 176-178.

Hill, D.S. (1997) The economic importance of insects. 1st Edition, Chapman & Hall, 2-6 Boundary Row, London, UK.

Holt R. A., Subramanian G. M., Halpern A., Sutton G. G., Charlab R., Nusskern D. R., Wincker P., Clark A. G., Ribeiro J. M., Wides R., Salzberg S. L., Loftus B., Yandell M., Majoros W. H., Rusch D. B., Lai Z., Kraft C. L., Abril J. F., Anthouard V., Arensburger P., Atkinson P. W., Baden H., de Berardinis V., Baldwin D., Benes V., Biedler J., Blass C., Bolanos R., Boscus D., Barnstead M., Cai S., Center A., Chaturverdi K., Christophides G. K., Chrystal M. A., Clamp M., Cravchik A., Curwen V., Dana A., Delcher A., Dew I., Evans C. A., Flanigan M., Grundschober-Freimoser A., Friedli L., Gu Z., Guan P., Guigo R., Hillenmeyer M. E., Hladun S. L., Hogan J. R., Hong Y. S., Hoover J., Jaillon O., Ke Z., Kodira C., Kokoza E., Koutsos A., Letunic I., Levitsky A., Liang Y., Lin J. J., Lobo N. F., Lopez J. R., Malek J. A., McIntosh T. C., Meister S., Miller J., Mobarry C., Mongin E., Murphy S. D., O'Brochta D. A., Pfannkoch C., Qi R., Regier M. A., Remington K., Shao H., Sharakhova M. V., Sitter C. D., Shetty J., Smith T. J., Strong R., Sun J., Thomasova D., Ton L. Q., Topalis P., Tu Z., Unger M. F., Walenz B., Wang A., Wang J., Wang M., Wang X., Woodford K. J., Wortman J. R., Wu M., Yao A., Zdobnov E. M., Zhang H., Zhao Q., et al. (2002) The genome sequence of the malaria mosquito *Anopheles gambiae*. *Science* **298:** 129-149.

Horst, R., Damberger, F., Luginbuhl, P., Guntert, P., Peng, G., Nikonova, L., Leal, W.S. and Wuthrich, K. (2001) NMR structure reveals intramolecular regulation

mechanism for pheromone binding and release. *Proc Natl Acad Sci USA* **98**: 14374-14379.

Huang, X. and Madan, A. (1999) CAP3: A DNA sequence assembly program. *Genome Res* **9**: 868-877.

Ishida, Y., Cornel, A.J. and Leal, W.S. (2002) Identification and cloning of a female antenna-specific odorant-binding protein in the mosquito *Culex quinquefasciatus*. *J Chem Ecology* **28**: 867-871.

Ishida, Y., Chen, A.M., Tsuruda, J.M., Cornel, A.J., Debboun, M. and Leal, W.S. (2004) Intriguing olfactory proteins from the yellow fever mosquito, *Aedes aegypti*. *Naturwissenschaften* **91**: 426-431.

Isoe, L. (2000) Comparative Analysis of the Vitellogenin Genes of the Culicidae, Ph.D. Dissertation. Pp.201. Insect Science. University of Arizona, Tucson.

Jacquin-Joly, E., Bohbot, J., Francois, M.C., Cain, A.H. and Nagnan-Le Meillour, P. (2000) Characterization of the general odorant-binding protein 2 in the molecular coding of odorants in *Mamestra brassicae*. *Eur J Biochem* **267**: 6708-6714.

Jacquin-Joly, E. and Merlin, C. (2004) Insect olfactory receptors: Contributions of molecular biology to chemical ecology. *J Chem Ecol* **30**: 2359-2397.

Johnson, B.W., Olson, K.E., Allen-Miura, T., Rayms-Keller, A., Carlson, J.O., Coates, C.J., Jasinskiene, N., James, A.A., Beaty, B.J. and Higgs, S. (1999) Inhibition of luciferase expression in transgenic *Aedes aegypti* mosquitoes by Sindbis virus expression of antisense luciferase RNA. *Proc Natl Acad Sci USA* **96**: 13399-13403.

Justice, R.W., Dimitratos, S., Walter, M.F., Woods, D.F., and Biessmann, H. (2003) Sexual dimorphic expression of putative antennal carrier protein genes in the malaria vector *Anopheles gambiae*. *Insect Mol Biol* **12**: 581-594.

Kamrud, K.I., Powers, A.M., Higgs, S., Olson, K.E., Blair, C.D., Carlson, J.O. and Beaty, B.J. (1995) The expression of chloramphenicol acetyltransferase in mosquitoes and mosquito cells using a packaged Sindbis replicon system. *Exp Parasitol* **81**: 394-403.

Kasang, G. and Kaissling, K-E. (1972) Specificity of primary and secondary olfactory processes in *Bombyx* antennae. In Int. symp. Olfaction and Taste IV (D. Schneider, *ed*), pp. 200-206, Verlagsgesellschaft, Stuttgart.

Kasang, G., Nicholls, M., Keil, T. and Kanaujia, S. (1989) Enzymatic conversion of sex pheromones in olfacyory hairs of the male silkworm moth *Antheraea polyphemus*. *Z Naturforsch* **44c**: 920-926.

Kim, M.S., Repp, A. and Smith, D.P. (1998) LUSH odorant-binding protein mediates chemosensory responses to alcohols in *Drosophila melanogaster*. *Genetics* **150**: 711-721.

Kim, M.S. and Smith, D.P. (2001) The invertebrate odorant-binding protein LUSH is required for normal olfactory behavior in *Drosophila*. *Chem Senses* **26**: 195-199.

Kline, D.L., Takken, W., Wood J. R. and Carlson, D.A. (1990) Field studies on the potential of butane, carbon dioxide, honey extract, 1-octen-3-ol, L-lactic acid and phenols as attractants for mosquitoes. *Med Vet Entomol* **4**: 383-391.

Klusak, V., Havlas, Z., Rulisek, L., Vondrasek, J. and Svatos, A. (2003) Sexual attraction in the silkworm moth. Nature of binding of bombykol in pheromone binding protein--an ab initio study. *Chem Biol* **10**: 331-340.

Knols, B.G.J, Van Loon, J.J.A, Cork, A., Robinson, R.D., Adam, W., Meijerink, J., de Jong, R. and Takken, W. (1997) Behavioral and electrophysiological responses of the female malaria mosquito *Anopheles gambiae s.s.* (Diptera: Culicidae) to Limburger cheese volatiles. *Bull Entomol Res* **87**: 151-159.

Korber B. (2000) Computational Analysis of HIV Molecular Sequences, Chapter 4. Pp. 55-72 *in* HIV Signature and Sequence Variation Analysis (eds. Allen G. Rodrigo and Gerald H. Learn), Kluwer Academic Publishers, Dordrecht, Netherlands.

Krieger, J., von Nickisch-Rosenegk, E., Mameli, M., Pelosi, P. and Breer, H. (1996) Binding proteins from the antennae of *Bombyx mori*. *Insect Biochem Mol Biol* **26**: 297-307.

Krieger, J., Raming, K., Dewer, Y.M., Bette, S., Conzelmann, S. and Breer, H. (2002) A divergent gene family encoding candidate olfactory receptors of the moth *Heliothis virescens*. *Eur J Neurosci* **16**: 619-628.

Krieger, J. and Breer, H. (2003) Transduction mechanism of olfactory sensory neurons. In: Insect Pheromone Biochemistry and Molecular Biology, (G.J. Blomquist and R.G. Vogt, *eds*), pp. 593-607. Elsevier Academic Press, London.

Kruse, S.W., Zhao, R., Smith, D.P. and Jones, D.N.M. (2003) Structure of a specific alcohol-binding site defined by the odorant binding protein LUSH from *Drosophila melanogaster*. *Nat Struct Biol* **10**: 694-700.

Krzywinski, J., Wilkerson, R.C. and Besansky, N.J. (2001) Toward understanding Anophelinae (Diptera, Culicidae) phylogeny: insights from nuclear single-copy genes and the weight of evidence. *Syst Biol* **50**: 540-556.

Kuhn, R.J., Niesters, H.G., Hong, Z. and Strauss, J.H. (1991) Infectious RNA transcripts from Ross River virus cDNA clones and the construction and characterization of defined chimeras with Sindbis virus. *Virology* **182**: 430-441.

Kumar, J. and Moses, K. (1997) Transcription factors in eye development: a gorgeous mosaic? *Genes Dev* **11**: 2023-2028.

Kwon, H.W., Lu, T., Rutzler, M. and Zwiebel, L.J. (2006) Olfactory responses in a gustatory organ of the malaria vector mosquito *Anopheles gambiae*. *Proc Natl Acad Sci USA* **103**: 13526-13531.

Laissue, P.P., Reiter, C., Hiesinger, P.R., Halter, S., Fischbach, K.F. and Stocker RF. (1999) Three-dimensional reconstruction of the antennal lobe in *Drosophila melanogaster*. *J Comp Neurol* **405**: 543-552.

Larsson, M.C., Domingos, A.I., Jones W.D., Chiappe, M.E. Amrein, H. and Vosshall, LB. (2004) *Or83b* encodes a broadly expressed odorant receptor essential for *Drosophila* olfaction. *Neuron* **43**: 703-714.

Lartigue, A., Gruez, A., Spinelli, S., Riviere, S., Brossut, R., Tegoni, M. and Cambillau, C. (2003) The crystal structure of a Cockroach Pheromone Binding Protein suggests a new ligand binding and release mechanism. *J Biol Chem* **278**: 30213-30218.

Lartigue, A., Gruez, A., Briand, L., Blon, F., Bezirard, V., Walsh, M., Pernollet, J.C., Tegoni, M. and Cambillau, C. (2004) Sulfure single-wavelength anomalous diffraction crystal of a pheromone-binding protein from the honeybee *Apis mellifera L. J Biol Chem* **279**: 4459-4464.

Laue, M.R., Steinbrecht, R.A. and Ziegelberger, G. (1994) Immunocytochemical localization of general odorant-binding protein in olfactory sensilla of the silkmoth *Antheraea polyphemus*. *Naturwissenschaften* **81**: 178-180.

Laue, M., Maida, R. and Redkozubov, A. (1997) G-protein activation, identification and immunolocalization in pheromone-sensitive sensilla trichodea of moths. *Cell Tissue Res* **288**: 149-158.

Leal, W.S., Nikonova, L. and Peng, G. (1999) Disulfide structure of the pheromone binding protein from the silkworm moth, *Bombyx mori*. *FEBS Lett* **464:** 85-90.

Lee, T., Lee, A. and Luo, L. (1999) Development of the *Drosophila* mushroom bodies: sequential generation of three distinct types of neurons from a neuroblast. *Development* **126**: 4065-4076.

Lee, D., Damberger, F.F., Peng, G., Horst, R., Guntert, P., Nikonova, L., Leal, W.S. and Wuthrich, K. (2002) NMR structure of the unliganded *Bombyx mori* pheromone-binding protein at physiological pH. *FEBS Lett* **531**: 314-318.

Li, Z.X., Pickett, J.A., Field, L.M. and Zhou, J.J. (2005) Identification and expression of odorant-binding proteins of the malaria-carrying mosquitoes *Anopheles gambiae* and *Anopheles arabiensis*. *Arch Insect Biochem Physiol* **58**: 175-189.

Livak, K.J. and Schmittgen, T.D. (2001) Analysis of relative gene expression data using real-time quantitative PCR and the $2^{-\Delta\Delta CT}$ Method. *Methods* **25**: 402-408.

Lu, T., Qiu, Y.T., Wang, G., Kwon, J.Y., Rutzler, M., Kwon, H.W., Pitts, R.J., van Loon, J.J., Takken, W., Carlson, J.R. and Zwiebel, L.J. (2007) Odor coding in the maxillary palp of the malaria vector mosquito *Anopheles gambiae*. *Curr Biol* **17**: 1533-1544.

Lustig, S., Jackson, A.C., Hahn, C.S., Griffin, D.E., Strauss, E.G. and Strauss, J.H. (1988) Molecular basis of Sindbis virus neurovirulence in mice. *J Virol* **62**: 2329-2336.

Maida, R., Redkozubov, A. and Ziegelberger, G. (2000) Identification of PLC beta and PKC in pheromone receptor neurons of *Antheraea polyphemus*. *Neuroreport* **11**: 1773-1776.

Maida, R., Ziegelberger, G. and Kaissling, K.E. (2003) Ligand binding to six recombinant pheromone-binding proteins of *Antheraea polyphemus* and *Antheraea pernyi*. *J Comp Physiol [B]* **173**: 565-573.

Malnic, B., Godfrey, P.A. and Buck, L.B. (2004) The human olfactory receptor gene family. *Proc Natl Acad Sci USA* **101**: 2584-2589.

Marin, E.C., Jefferis, G.S., Komiyama, T., Zhu, H. and Luo, L. (2002) Representation of the glomerular olfactory map in the Drosophila brain. *Cell* **109**: 243-255.

Mayor, C., Brudno, M., Schwartz, J.R., Poliakov, A., Rubin, E.M., Frazer, K.A., Pachter, L.S. and Dubchak, I. (2000) VISTA : visualizing global DNA sequence alignments of arbitrary length *Bioinformatics* **16**: 1046-1047.

Mboera, L.E.G. and Takken, W. (1997) Carbon dioxide chemotropism in mosquitoes (Diptera: Culicidae) and its potential in vector surveillance and management. *Rev Med Vet Entomol* **85**: 355-368.

McIver, S.B. (1982) Sensilla mosquitoes (Diptera: Culicidae). *J Med Entomol* **19**: 489-535.

McKenna, M.P., Hekmat-Scafe, D.S., Gaines, P. and Carlson, J.R. (1994) Putative *Drosophila* pheromone-binding proteins expressed in a subregion of the olfactory system. *J Biol Chem* **269**: 16340-16347.

Michel, W.C. and Ache, B.W. (1992) Cyclic nucleotides mediate an odor-evoked potassium conductance in lobster olfactory receptor cells. *J Neurosci* **12**: 3979-3984.

Millar, J.C., Chaney, J.D. and Mulla, M.S. (1992) Identification of oviposition attractants for *Culex quiquefasciatus* from fermented Bermuda grass infusion. *J Am Mosq Control Assoc* **8**: 11-17.

Millar, J.G., Chaney, J.D, Beehler, J.W. and Mulla, M.S. (1994) Interaction of the *Culex quiquefasciatus* egg raft pheromone with a natural chemical associated with oviposition sites. *J Am Mosq Control Assoc* **10**: 374-379.

Mohanty, S., Zubkova, S. and Gronenborg, A.M. (2004) The solution NMR structure of *Anthera polyphemus* PBP provides a new insight into pheromone recognition by PBP. *J Mol Biol* **337**: 443-451.

Mokany, A. and Shine, R. (2003) Oviposition selection by mosquitoes is affected by cues from conspecific larvae and anuran tadpoles. *Austral Ecology* **28**: 33-37.

Mustaparta H. (1996) Coding mechanisms in insect olfaction. *Ciba Found Symp* **200:** 149-157.

Nei, M. and Gojobori, T. (1986) Simple methods for estimating the numbers of synonymous and nonsynonymous nucleotide substitutions. *Mol Biol Evol* **3**: 418-426.

Nene, V., Wortman, J.R., Lawson, D., Haas, B., Kodira, C., Tu, Z.J., Loftus, B., Xi, Z., Megy, K., Grabherr, M., Ren, Q., Zdobnov, E.M., Lobo, N.F., Campbell, K.S., Brown, S.E., Bonaldo, M.F., Zhu, J., Sinkins, S.P., Hogenkamp, D.G., Amedeo, P., Arensburger, P., Atkinson, P.W., Bidwell, S., Biedler, J., Birney, E., Bruggner, R.V., Costas, J., Coy, M.R., Crabtree, J., Crawford, M., Debruyn, B., Decaprio, D., Eiglmeier, K., Eisenstadt, E., El-Dorry, H., Gelbart, W.M., Gomes, S.L., Hammond, M., Hannick, L.I., Hogan, J.R., Holmes, M.H., Jaffe, D., Johnston, J.S., Kennedy, R.C., Koo, H., Kravitz, S., Kriventseva, E.V., Kulp, D., Labutti, K., Lee, E., Li, S., Lovin, D.D., Mao, C., Mauceli, E., Menck, C.F., Miller, J.R., Montgomery, P., Mori, A., Nascimento, A.L., Naveira, H.F., Nusbaum, C., O'Leary, S., Orvis, J., Pertea, M., Quesneville, H., Reidenbach, K.R., Rogers, Y.H., Roth, C.W., Schneider, J.R., Schatz, M., Shumway, M., Stanke, M., Stinson, E.O., Tubio, J.M., Vanzee, J.P., Verjovski-Almeida, S., Werner, D., White, O., Wyder, S., Zeng, Q., Zhao, Q., Zhao, Y., Hill, C.A., Raikhel, A.S., Soares, M.B., Knudson, D.L., Lee, N.H., Galagan, J., Salzberg, S.L., Paulsen, I.T., Dimopoulos, G., Collins, F.H., Birren, B., Fraser-Liggett, C.M. and Severson, D.W. (2007) Genome sequence of *Aedes aegypti*, a major arbovirus vector. *Science* **316**: 1718-1723.

Ngai, J., Dowling, M.M., Buck, L., Axel, R. and Chess, A. (1993) The family of genes encoding odorant receptors in the channel catfish. *Cell* **72**: 657-666.

Olson, K.E., Higgs, S., Hahn, C.S., Rice, C.M., Carlson, J.O. and Beaty, B.J. (1994) The expression of chloramphenicol acetyltransferase in *Aedes albopictus* (C6/36) cells and *Aedes triseriatus* mosquitoes using a double subgenomic recombinant Sindbis virus. *Insect Biochem Mol Biol* **24**: 39-48.

Olson, K.E., Higgs, S., Gaines, P.J., Powers, A.M., Davis, B.S., Kamrud, K.I., Carlson, J.O., Blair, C.D. and Beaty, B.J. (1996) Genetically engineered resistance to dengue-2 virus transmission in mosquitoes. *Science* **272**: 884-886.

Olson, K.E., Myles, K.M., Seabaugh, R.C., Higgs, S., Carlson, J.O. and Beaty, B.J. (2000) Development of a Sindbis virus expression system that efficiently expresses green fluorescent protein in midguts of *Aedes aegypti* following per os infection. *Insect Mol Biol* **9**: 57-65.

Olson, K.E., Adelman, Z.N., Travanty, E.A., Sanchez-Vargas, I., Beaty, B.J. and Blair, C.D. (2002) Developing arbovirus resistance in mosquitoes. *Insect Biochem Mol Biol* **32**: 1333-1343.

Park, S.K., Shanbhag, S.R., Wang, Q., Hasan, G., Steinbrecht, R.A. and Pikielny, C.W. (2000) Expression patterns of two putative odorant-binding proteins in the olfactory organs of *Drosophila melanogaster* have different implications for their functions. *Cell Tissue Res* **300**: 181-192.

Pelosi, P. (1994) Odorant binding proteins. *Crit Rev Biochem Mol Biol* **29**: 199-228.

Pelosi, P. and Maida, R. (1995) Odorant-binding proteins in insects. *Comp Biochem Physiol* **111:** 503-514.

Pelosi, P. (1998) Odorant-binding proteins: Structural aspects. *Ann N Y Acad Sci* **30**: 281-293.

Pelosi, P., Zhou, J.J., Ban, L.P. and Calvello, M. (2006) Soluble proteins in insect chemical communication. *Cell Mol Life Sci* **63**: 1658-1676.

Pitts, R.J., Fox, A.N. and Zwiebel, L.J. (2004) A highly conserved candidate chemoreceptor expressed in both olfactory and gustatory tissues in the malaria vector *Anopheles gambiae*. *Proc Natl Acad Sci USA* **101**: 5058-5063.

Pikielny, C.W., Hasan, G., Rouyer, F. and Rosbash, M. (1994) Members of a family of *Drosophila* putative odorant-binding proteins are expressed in different subsets of olfactory hairs. *Neuron* **12**: 35-49.

Pophof, B. (2002) Moth pheromone binding proteins contribute to the excitation of olfactory receptor cells. *Naturwissenschaften* **89**: 515-518.

Pophof, B. and Van der Goes van Naters, W. (2002) Activation and inhibition of the transduction process in silkmoth olfactory receptor neurons. *Chem Senses* **27**: 435-443.

Rai, K.S. and Black IV, W.C. (1999) Mosquito genomes: structure, organization, and evolution. *Adv Genet* **41**: 1-33.

Raikhel, A.S., Kokoza, V.A., Zhu, J., Martin, D., Wang, S.F., Li, C., Sun, G., Ahmed, A., Dittmer, N. and Attardo, G. (2002) Molecular biology of mosquito vitellogenesis: from basic studies to genetic engineering of antipathogen immunity. *Insect Biochem Mol Biol* **32**: 1275-1286.

Raming, K., Krieger, J. and Breer, H. (1990) Molecular cloning, sequencing and expression of cDNA encoding a G0-protein from insect. *Cell Signal* **2**: 311-321.

Ray, A., van Naters, W.G., Shiraiwa, T. and Carlson, J.R (2007) Mechanisms of odor receptor gene choice in Drosophila. *Neuron* **53**: 353-369.

Rayms-Keller, A., Powers, A.M., Higgs, S., Olson, K.E., Kamrud, K.I., Carlson, J.O. and Beaty, B.J. (1995) Replication and expression of a recombinant Sindbis virus in mosquitoes. *Insect Mol Biol* **4**: 245-251.

Reisen, W.K., Meyer, R.P. and Milby, M.M. (1986b) Patterns of fructose feeding by

Culex tarsalis (Diptera: Culicidae). *J Med Entomol* **23**: 366-373.

Ressler, K.J., Sullivan, S.L. and Buck, L.B. (1993) A zonal organization of odorant receptor gene expression in the olfactory epithelium. *Cell* **73**: 597-609.

Riesgo-Escovar, J., Raha, D. and Carlson, J.R. (1995) Requirement for a phospholipase C in odor response: overlap between olfaction and vision in Drosophila. *Proc Natl Acad Sci USA* **92**: 2864-2868.

Riviere, S., Lartigue, A., Quennedey, B., Campanacci, V., Farine, J.P., Tegoni, M., Cambillau, C. and Brossut, R. (2003) A pheromone-binding protein from the cockroach *Leucophaea maderae*: cloning, expression and pheromone binding. *Biochem J* **371**: 573-579.

Robertson, H.M., Warr, C.G. and Carlson, J.R. (2003) Molecular evolution of the insect chemoreceptor gene superfamily in *Drosophila melanogaster*. *Proc Natl Acad Sci USA* **100** (Suppl 2):14537-14542.

Robertson, H.M. and Wanner, K.W. (2006) The chemoreceptor superfamily in the honey bee, *Apis mellifera*: Expansion of the odorant, but not, gustatory, receptor family. *Genome Res* **16**: 1395-1403.

Rutzler, M. and Zwiebel, L. (2005) Molecular biology of insect olfaction: Recent progress and conceptual models. *J Comp Physiol A Neuroethol Sens Neural Behav Physiol* **9:** 1-14.

Rybczynski, R., Reagan, J. and Lerner, M.R. (1989) A pheromone-degrading aldehyde oxidase in the antennae of the moth *Manduca sexta*. *J Neuroscience* **9**: 1341-1353.

Rybczynski, R., Vogt, R.G. and Lerner, M.R. (1990) Antennal specific pheromone-degrading aldehyde oxidases from the moths *Antheraea polyphemus* and *Bombyx mori*. *J Biol Chem* **32**: 19712-19715.

Sakurai, T., Nakagawa, T., Mitsuno, H., Mori., H., Endo, Y., et al. (2004) Identification and functional characterization of a sex pheromone receptor in the silkmoth *Bombyx mori*. *Proc Natl Acad Sci USA* **101**: 16653-16658.

Sandelin, A., Wasserman, W.W. and Lenhard, B. (2004) ConSite: web-based prediction of regulatory elements using cross-species comparison. *Nucleic Acids Res* **32**: 249-252.

Sandler, B.H., Nikonova, L., Leal, W.S. and Clardy, J. (2000) Sexual attraction in the silkworm moth: structure of the pheromone-binding-protein-bombykol complex. *Chem Biol* **7:** 143-151.

Sarkar, A., Yardley, K., Atkinson, P.W., James, A.A. and O'Brochta, D.A. (1997) Transposition of the Hermes element in embryos of the vector mosquito, *Aedes aegypti*. *Insect Biochem Mol Biol* **27**: 359-363.

Scott, K., Brady, R., Jr., Cravchik, A., Morozov, P., Rzhetsky, A., Zuker, C. and Axel, R. (2001) A chemosensory gene family encoding candidate gustatory and olfactory receptors in *Drosophila*. *Cell* **104**: 661-673.

Sharakhova, M.V., Xia, A., McAlister, S.I. and Sharakhov, I.V. (2006) A standard cytogenetic photomap for the mosquito *Anopheles stephensi* (Diptera: Culicidae): application for physical mapping. *J Med Entomol* **43**: 861-866.

Shiao, S.H., Higgs, S., Adelman, Z., Christensen, B.M., Liu, S.H. and Chen, C.C. (2001) Effect of prophenoloxidase expression knockout on the melanization of microfilariae in the mosquito *Armigeres subalbatus*. *Insect Mol Biol* **10**: 315-321.

Stengl, M. (1994) Inositol-trisphosphate-dependent calcium currents precede cation currents in insect olfactory receptor neurons in vitro. *J Comp Physiol [A]* **174**: 187-194.

Steinbrecht, R.A. (1984) Chemo-, Hygro-, and Thermoreceptors. In: Biology of the Integument, Vol I Invertebrates, (J. Bereiter-Hahn, A.G. Matoltsy, K.S. Richards, *eds*), pp. 523-553. Springer-Verlag, Berlin.

Steinbrecht, R.A., Ozaki, M. and Ziegelberger, G. (1992) Immunocytochemical localization of pheromone-binding protein in moth antenna. *Cell Tissue Res* **270**: 287-302.

Steinbrecht, R.A., Laue, M.R. and Ziegelberger, G. (1995) Immunolocalization of pheromone-binding protein and general odorant-binding protein in olfactory sensilla of the silkmoths *Antheraea* and *Bombyx*. *Cell Tissue Res* **282**: 203-217.

Steinbrecht, R.A. (1996) Structure and function of insect olfactory sensilla. *Ciba Foundation Symp* **200**: 158-174.

Steinbrecht, R.A. (1997) Pore structures in insect olfactory sensilla: a review of data and concepts. *Int J Insect Morphol Embryol* **26**: 229-245.

Steinbrecht, R.A. (1998) Odorant-binding proteins: expression and function. *Ann NY Acad Sci* **855**: 323-332.

Stocker, R.F. (1994) The organization of the chemosensory system in *Drosophila melanogaster*: a review. *Cell Tissue Res* **275:** 3-26.

Strauss, E.G., Rice, C.M. and Strauss, J.H. (1984) Complete nucleotide sequence of the genomic RNA of Sindbis virus. *Virology* **133**: 92-110.

Strauss, J.H. and Strauss, E.G. (1994) The alphaviruses: gene expression, replication, and evolution. *Microbiol Rev* **58**: 491-562.

Swofford, D.L. (2002) *Paup**: Phylogenetic Analysis Using Parsimony (* and Other Methods). Sinauer Associates, Sunderland, Massachusetts.

Tao, Q., Wang, A., and Zhang, H.B. (2002) One large-insert plant-transformation-competent BIBAC library and three BAC libraries of Japonica rice for genome research in rice and other grasses. *Theor Appl Genet* **105:** 1058-1066.

Takken, W. and Kline, D.L. (1989) Carbon dioxide and 1-octen-3-ol as mosquito attractants. *J Am Mosq Control Assoc* **5**: 311-316.

Takken, W., Dekker, T. and Wijnholds, Y.G. (1997) Odour-mediated flight behaviour of *Anopheles gambiae* Giles *sensu stricto* and *An. stephensi* Liston in response to CO_2, acetone, and 1-Octen-3-ol (Diptera: Culicidae). *J Insect Behav* **10**: 395-407.

Takken, W., Klowden, M.J. and Chambers, G.M. (1998) Effect of body size on host seeking and blood meal utilization in *Anopheles gambiae sensu stricto* (Diptera: Culicidae): the disadvantage of being small. *J Med Entomol* **35**: 639-645.

Takken, W. and Knols, B.G.J. (1999) Odor-mediated behavior of afrotropical malaria mosquitoes. *Annu Rev Entomol* **44:** 131-157.

Talluri, S., Bhatt, A. and Smith, D.P. (1995) Identification of a Drosophila G protein alpha subunit (dGq alpha-3) expressed in chemosensory cells and central neurons. *Proc Natl Acad Sci USA* **92**: 11475-11479.

Thompson, J.D., Gibson, T.J., Pleawniak F., Jeanmougin F., and Higgins D.G. (1997). The ClustalX windows interface: flexible strategies for multiple sequence alignment aided by quality analysis tools. *Nucleic Acids Res* **22:** 4673-4680.

Tamang, D., Tseng, S.M., Huang, C.Y., Tsao, I.Y., Chou, S.Z., Higgs, S., Christensen, B.M. and Chen, C.C. (2004) The use of a double subgenomic Sindbis virus expression system to study mosquito gene function: effects of antisense nucleotide number and duration of viral infection on gene silencing efficiency. *Insect Mol Biol* **13**: 595-602.

Taylor, R.M., Hurlbut, H.S., Work, T.H., Kingston, J.R. and Frothingham, T.E. (1955) Sindbis virus: a newly recognized arthropod-transmitted virus. *Am J Trop Med Hyg* **4**: 844-862.

Tolbert, L.P. and Hildebrand, J.G. (1981) Organization and synaptic ultrastructure of glomeruli in the antennal lobes of the moth *Manduca sexta*: a study using thin sections and freeze-structure. *Phil Trans R Soc Lond B* **213**: 279-301.

Van den Berg, M.J. and Ziegelberger, G. (1991) On the function of the pheromone-binding protein in the olfactory hairs of *Antheraea polyphemus*. *J Insect Physiol* **37**: 79-85.

Vassar, R., Ngai, J. and Axel, R. (1993) Spatial segregation of odorant receptor expression in the mammalian olfactory epithelium. *Cell* **74**: 309-318.

Vogt, R.G. (2002) Odorant binding proteins of the malaria mosquito *Anopheles gambiae*: possible orthologues of the OS-E and OS-F OBPs of *Drosophila melanogaster*. *J Chem Ecol* **28**: 2371-2376.

Vogt, R. G. (2005) Molecular basis of pheromone detection in insects. In: Comprehensive Insect Physiology, Biochemistry, Pharmacology and Molecular Biology, Endocrinology, (L.I. Gilbert, K. Iatro and S.S. Gill, *eds*), Vol. 3, pp. 753-804. Elsevier Academic Press, London.

Vogt, R.G. and Riddiford, L.M. (1981) Pheromone binding and inactivation by moth antennae. *Nature* **293**: 161-163.

Vogt, R.G., Riddiford, L.M. and Prestwich, G.D. (1985) Kinetic properties of a sex pheromone-degrading enzyme: the sensillar esterase of *Antheraea polyphemus*. *Proc Natl Acad Sci USA* **82**: 8827-8831.

Vogt, R.G. and Riddiford, L.M. (1986) Pheromone reception: a kinetic equilibrium. In: Mechanisms in Insect Olfaction, (T.L. Payne, M. C. Birch and C. E. J. Kennedy, *eds*), pp. 201-208. Clarnedon Press, Oxford.

Vogt, R.G., Kohne, A.C., Dubnau, J.T., and Prestwich, G.D. (1989) Expression of pheromone binding proteins during antennal development in the gypsy moth *Lymantria dispar*. *J Neurosci* **9**: 3332-3346.

Vogt, R.G., Prestwich, G.D. and Lerner, M.R. (1991a) Odorant-binding-protein subfamilies associate with distinct classes of olfactory receptor neurons in insects. *J Neurobiol* **22:** 74-84.

Vogt, R.G., Rybczynski, R. and Lerner, M.R. (1991b) Molecular cloning and sequencing of general odorant-binding proteins GOBP1 and GOBP2 from tobacco hawk moth *Manduca sexta*: comparisons with other insect OBPs and their signal peptides. *J Neurosci* **11**: 2972-2984.

Vogt, R.G., Callahan, F.E., Rogers, M.E. and Dickens, J.C. (1999) Odorant binding protein diversity and distribution among the insect orders, as indicated by LAP, an OBP-related protein of the true bug Lygus lineolaris (Hemiptera, Heteroptera). *Chem Senses* **24:** 481-95.

Vosshall, L.B., Amrein, H., Morozov, P.S., Rzhetsky, A. and Axel, R. (1999) A spatial map of olfactory receptor expression in the *Drosophila* antenna. *Cell* **96**: 725-736.

Vosshall, L.B., Wong, A.M. and Axel, R. (2000) An olfactory sensory map in the fly brain. *Cell* **102**: 147-159.

Vosshall, L.B. and Stocker, R.F. (2007) Molecular architecture of smell and taste in *Drosophila*. *Annu Rev Neurosci* **30**: 505-533.

Wang, Y., Wright, N.J., Guo, H., Xie, Z., Svoboda, K., Malinow, R., Smith, D.P. and Zhong, Y. (2001) Genetic manipulation of the odor-evoked distributed neural activity in the Drosophila mushroom body. *Neuron* **29**: 267-276.

Wogulis, M., Morgan, T., Ishida, Y., Leal, W.S. and Wilson, D.K. (2006) The crystal structure of an odorant binding protein from *Anopheles gambiae*: Evidence for a common ligand release mechanism. *Biochem Biophysics Res Commun* **339**: 157-164.

Wojtasek, H., Hansson, B.S. and Leal, W.S. (1998) Attracted or repelled?--a matter of two neurons, one pheromone binding protein, and a chiral center. *Biochem Biophys Res Commun* **250**: 217-222.

Wojtasek, H. and Leal, W.S. (1999) Degradation of an alkaloid pheromone from the pale-brown chafer, Phyllopertha diversa (Coleoptera: Scarabaeidae), by an insect olfactory cytochrome P450. *FEBS Lett* **458**: 333-336.

Wong, A.M., Wang, J.W. and Axel, R. (2002) Spatial representation of the glomerular map in the *Drosophila* protocerebrum. *Cell* **109**: 229-241.

Xu, P.X., Zwiebel, L.J. and Smith, D.P. (2003) Identification of a distinct family of genes encoding atypical odorant-binding proteins in the malaria vector mosquito, *Anopheles gambiae*. *Insect Mol Biol* **12:** 549-560.

Xu, P., Atkinson, R., Jones, D.N. and Smith, D.P. (2005) *Drosophila* OBP LUSH is required for activity of pheromone-sensitive neurons. *Neuron* **45**: 193-200.

Zahiri, N. (1997) *Aedes aegypti* (Diptera: Culicidae), oviposition attraction/repellency. Ph. D thesis in *Natural Resource Sciences*. McGill University, Canada.

Zhou, J.J., Zhang, G.A., Huang, W., Birkett, M.A., Field, L.M., Pickett, J.A. and Pelosi, P. (2004) Revisiting the odorant-binding protein LUSH of *Drosophila melanogaster*: evidence for odour recognition and discrimination. *FEBS Lett* **558**: 23-26.

Zhu, J., Chen, L. and Raikhel, A.S. (2007) Distinct roles of Broad isoforms in regulation of the 20-hydroxyecdysone effector gene, Vitellogenin, in the mosquito *Aedes aegypti*. *Mol Cell Endocrinol* **267**: 97-105.

Ziegelberger, G., van den Berg, M.J., Kaissling, K.E., Klumpp, S. and Schultz, J.E. (1990) Cyclic GMP levels and guanylate cyclase activity in pheromone-sensitive antennae of the silkmoths Antheraea polyphemus and Bombyx mori. *J Neurosci* **10**: 1217-1225.

Ziegelberger, G. (1995) Redox-shift of the pheromone-binding protein in the silkmoth *Antheraea polyphemus*. *Eur J Biochem* **232**: 706-711.

Ziegelberger G. (1996) The multiple role of the pheromone-binding protein in olfactory transduction. *Ciba Found Symp* **200:** 267-75; discussion 275-280.

Zubkov, S., Gronenborn, A.M., Byeon, I.L., and Mohanty, S. (2005) Structural

consequences of the pH-induced conformational switch in *A. polyphemus* pheromone-binding protein: Mechanisms of ligand release. *J Mol Biol* **354**: 1081-1090.